Title
Cell-Extrinsic and Cell-Intrinsic Regulation of Natural Killer Cell Behavior in Mice

Author
Millan Hernandez, Alberto Jovani

Publication Date
2020

Peer reviewed|Thesis/dissertation

UNIVERSITY OF CALIFORNIA, MERCED

Cell-Extrinsic and Cell-Intrinsic Regulation of Natural Killer Cell Behavior in Mice

A dissertation submitted in partial satisfaction of the requirements for the degree Doctor of Philosophy

in

Quantitative and Systems Biology

by

Alberto Jovani Millan Hernandez

Committee in charge:

Professor Marcos E. García-Ojeda, Chair

Professor Anna E. Beaudin

Professor Jennifer O. Manilay

Professor Suzanne S. Sindi

2020

The Dissertation of Alberto Jovani Millan Hernandez is approved, and it is acceptable in quality and form for publication on microfilm and electronically:

_____

Jennifer O. Manilay

_____

Anna E. Beaudin

_____

Suzanne S. Sindi

_____

Marcos E. García-Ojeda, Chair

University of California, Merced

2020

DEDICATION

This entirety of this work, as a culmination of my extensive education journey is dedicated to my entire family, who have always supported by goals and dreams. A special dedication to my wife, Maria D. Aguilar Millan, for all the love and support given throughout the years. Additionally, another special dedication to my father, mother, sister, and brothers:

Alfredo Millan

Martha Hernandez

Monica M. Millan

Daniel A. Totino

David A. Totino

Thank you for all of the support, courage, and strength you have all provided me.

TABLE OF CONTENTS

LIST OF ABBREVIATIONS

ALL: Acute lymphocytic leukemia

BM: Bone marrow

BMD: Bone mineral density

BMP: Bone morphogenetic protein

β_2m: beta-2-microglobulin

$\beta_2m^{-/-}$: beta-2 microglobulin knockout

$\beta_2m^{+/+}$: beta-2 microglobulin sufficient

C: cluster

CAR: Chimeric antigen receptor

CAR cell: CXCL12-abundant reticular cell

CD: Cluster of differentiation

CLP: Common lymphoid progenitor

CXCR4: C-X-C motif chemokine receptor 4

DC: Dendritic cell

DKK1: Dickkopf WNT signaling pathway inhibitor I

Eomes: Eomesodermin

FCM: Flow cytometry

GM-CSF: Granulocyte-macrophage colony-stimulating factor

GSK3β: Glycogen synthase kinase3β

HSCs: Hematopoietic stem cells

IFNγ: Interferon-gamma

IL: Interleukin

iNK: immature natural killer

i.p: Intraperitoneal

KIR: Killer cell immunoglobulin-like receptors

KO: Knockout

Lef1: Lymphoid enhancer-binding factor 1

Lin: Lineage

LLNL: Lawrence Livermore National Laboratories

LN: Lymph node

LRP: Low-density lipoprotein receptor-family

MFI: Mean fluorescence intensity

MHC-I: Major histocompatibility complex class I

μCT: Micro-computed tomography

mNK: most mature natural killer

MSCs : Mesenchymal stem cells

NK: Natural killer

NKPs: NK progenitor cell

PBS: Phosphate buffered saline

PCA: Principal component analysis

PMA: Phorbol 12-myristate 13-acetate

Poly(I:C): Polyinosinic-polycytidylic acid

qPCR: Quantitative PCR

rNKPs: ‘Refined’ NKPs

SH2: Src homology region 2

Sost: Sclerostin

Sostdc1: Sclerostin domain–containing-1

SA: Streptavidin

Tbx21: T-box protein 21

TCF: T cell factor

T_{FH}: T Follicular helper

T_{FR}: T Follicular regulatory

TGF- β: Transforming growth factor-β

TNF-α: Tumor necrosis factor-alpha

tNK: transitional natural killer

tSNE: T-stochastic neighbor embedding

UC: University of California

WT: Wild-type

LIST OF SYMBOLS

α, alpha

β, beta

°, degree

ε, epsilon

γ, gamma

μ, micro

+, positive expression

-, negative expression

LIST OF TABLES

LIST OF FIGURES

ACKNOWLEDGEMENTS

This thesis/dissertation work presented here was only made possible by the contributions of many. I would first like to express my appreciation to my advisor, Professor Jennifer O. Manilay, who has pushed me and properly guided me throughout the entirety of my graduate studies. Jennifer (Jen) continually conveyed a tremendous amount of research techniques, scholarship, and enthusiasm in regard to my academic and research learning structure. I would have never developed into the scientist that I am today without her. I look forward to future natural killer (NK) cell collaborations and a forever friendship with Jen.

I would like to acknowledge my thesis committee members, who have provided essential feedback and support in guiding me in the right direction. First, my committee chair, Professor Marcos E. García-Ojeda, who has challenged me and directed me in the NK cell field. Next, Professor Anna E. Beaudin, who has always challenged my science and public speaking through journal club and joint lab meetings. Finally, Professor Suzanne S. Sindi, who allowed me to venture into the world of mathematics. Suzanne has supported and motivation in mathematics and pushed me to learn programing and modeling during graduate school, which I plan to utilize during my future studies. Together, my committee members have made me the well-rounded and independent scientist that I am today.

Next, I would like to acknowledge the technical support and guidance provided by the UC Merced core facilities. In particular, Dr. David M. Gravano from the UCM Stem Cell Instrumentation Foundry, for the training and guidance for the use of the flow cytometer and sorter. Additionally, UCM Department of Animal Research Services (DARS) staff for the training, maintenance, facility support. In particular, I would like to acknowledge Mrs. Emily Slocum, Mr. Vatthana Vongphakham, and Mr. Roy Hoglund.

Finally, I would like to acknowledge my colleagues, past and present labmates, mentees for their support and friendship throughout my education. In particular, Cristine Donham (Cristie) and Betsabel Chicana for the research support and friendship you continue to provide. Additionally, the labor and friendship provided by the “wondergrads” (undergraduate assistance), including: Sonny R. Elizaldi, Jeffrey O. Aceves, Eric M. Lee, Jeremy Libang, Bryan Hom, Hanna Taglinao, Shawn Ignacio, Asmaa Mohamed, Julia Beale, William Pratcher, Brian Freeman, Michael Chi, Sarkis Koseyan, Jared Camillo, and Vivi.

Chapter 1: Introduction

This work was supported by University of California (UC) Merced faculty research funding and UC graduate student fellowships.

Chapter 2: Sostdc1 Regulates NK Cell Maturation and Cytotoxicity

Originally published in *The Journal of Immunology*. The text found in this section of the thesis/dissertation is a reprint of the material as it appears in *The Journal of Immunology*. Alberto J. Millan, Sonny R. Elizaldi, Eric M. Lee, Jeffrey O. Aceves, Deepa Murugesh, Gabriela G. Loots and Jennifer O. Manilay. Sostdc1 Regulates NK Cell Maturation and Cytotoxicity. *J. Immunol.* 202: 2296-2306. doi: 10.4049/jimmunol.1801157. This work was supported by University of California (UC) Merced faculty research funding, a UC Cancer Research Coordinating Committee grant, a Halcyon-Dixon Trust awarded to Dr. Jennifer Manilay, and UC graduate student fellowships awarded to Alberto J. Millan.

Chapter 3: Evidence for progressive NK cell Ly49 developmental pathways in mice

Originally published in bioRxiv, a preprint server for biology. Alberto J. Millan, Bryan A. Hom, Jeremy B. Libang, Suzanne Sindi, Jennifer O. Manilay. Evidence for prescribed NK cell Ly49 developmental pathways in mice. doi: https://doi.org/10.1101/2020.05.23.112391. This work was supported by UC Merced faculty research funding and UC graduate student fellowships.

CURRICULUM VITA

A. EDUCATION

Doctor of Philosophy: Quantitative and Systems Biology
08/22/15 – 07/13/20
Advisor: Jennifer O. Manilay, Ph.D.
University of California, Merced

BS: Concentration in Molecular and Cell Biology
08/28/10 – 05/27/15
Minor: Chemistry
California State University, Sacramento

High School Graduate: General Education
08/13/06 – 05/13/10
Livingston High School
Livingston C.A, 95334

B. RESEARCH EXPERIENCE

Peer-Assisted Learning Facilitator
08/23/12 – 05/23/14
Sacramento, CA
Supervisor: Jennifer Lundmark, Ph.D.

The objective of this research was to find a new pedagogical method for teaching students chemistry concepts while at home.

- Developed YouTube videos and worksheets for students on struggles observed during chemistry lecture.
- The results showed that students who used the interactive learning videos at home scored higher on their test when compared to the students that did not see the videos at all.

Undergraduate Laboratory Research Assistant
12/10/12 – 05/23/15
Sacramento, CA
Supervisor: John Chapman, Ph.D.

- Research an efficient method for extracting human adipose mesenchymal stem cells for experimentation.
- Experimented with cell culture, tissue digestion, isolation, purification, and differentiation of cells.
- Applied my diverse scientific background to employ an integrated analytic approach for solving complex situations.

McNair Scholar
08/20/14 – 05/20/15
Sacramento, CA
Supervisor: Thomas Landerholm, Ph.D.

- Joined a cohort of students to establish great leadership, community service, and networking skills.
- Researched with separation and isolation of mesenchymal stem cells from human adipose tissue.
- Built a close relationship with my mentor though the constructing of my research project, writing, editing and refining, my journal article for accuracy.

Undergraduate Laboratory Research Assistant
08/23/14 – 05/20/15
Sacramento, CA
Supervisor: Nicholas Ewing, Ph.D.
Investigated growth regulation, cell development, and environmental response in *Arabidopsis*.

- Study focused on auxin regulation on the plasma membrane transporter, H^+-ATPases.
- Utilized a GUS reporter gene attached to our gene of interest to locate its expression within cells.

Graduate Research
08/22/15 – 07/13/20
Merced, CA
Advisor: Jennifer Manilay, Ph.D.

- My graduate work is described in the entirety of this thesis/dissertation.

C. CONTRIBUTIONS TO SCIENCE

Contribution #1: Studying a non-enzymatic method for human adipose mesenchymal stem cell separation.

Traditional collagenase adipose digestion for mesenchymal stem cell (MSC) separation contains toxins that are harmful for regenerative medicine applications. An alternative method such as StromaCell, a mechanical dissociation device, was developed by MicroAire Aesthethics to employ a non-toxic method for MSC separation. In our study, we compared StromaCell to collagenase digestion for the four main contributing factors for MSC separation, including processing time, total numbers of cells recovered and the ability to characterize MSC in extraction. Total number of cells were measured by live-dead fluorescent detection on the NC-3000 Image Cytometer and MSC characterization was measured by CD panel labeling on the BD Accuri flow cytometer. We hypothesize that StromaCell mechanical dissociation of adipose tissue for mesenchymal stem cell separation will give a better alternative when compared to the collagenase adipose digestion method. Our results showed that StromaCell could extract cells at a faster rate, with high viability, and was MSC positive. Although the cells we recovered were lower in MSC cell count then the traditional collagenase method, the non-enzymatic method will further be studied to achieve optimum conditions. A future study would include separating MSC at a fast, abundant, and viable amount of MSC for analogous medical applications.

- **Millan Hernandez, A J**. Landerholm, T. Chapman, J. (2014). Comparison Between Collagenase Adipose Digestion and StromalCell Mechanical Dissociation for Mesenchymal Stem Cell Separation. *McNair Scholars Journal*.15:86-101.

Contribution #2: Studying the role of Sostdc1 in the development and maturation of NK cells.

Natural killer (NK) cells are specialized lymphocytes with the innate ability to eliminate virally infected and cancerous cells, but the mechanisms that control NK cell development and cytotoxicity are incompletely understood. My graduate studies are focused on natural killer (NK) development and function in the absence of Sclerostin domain containing protein 1 (*Sostdc1*). *Sostdc1*-knockout (*Sostdc1*$^{-/-}$) mice display a progressive accumulation of transitional NK cells (CD27^{+}CD11b^{+}, tNK) with age, indicating a partial developmental block. The Ly49 repertoire on NK cells in *Sostdc1*$^{-/-}$ mice is also changed. Lower frequencies of *Sostdc1*$^{-/-}$ splenic tNKs express inhibitory Ly49G2 receptors, but higher frequencies express activating Ly49H and Ly49D receptors. However, the frequencies of Ly49I^{+}, G2^{+}, H^{+} and D^{+} populations were universally decreased at the most mature (CD27^{-} CD11b^{+}, mNK) stage. We hypothesized that the Ly49 repertoire in *Sostdc1*$^{-/-}$ mice would correlate with NK killing ability and observed that *Sostdc1*$^{-/-}$ NK cells are hyporesponsive against MHC-I-deficient cell targets *in vitro* and *in vivo*, despite

higher CD107a surface levels and similar IFNγ expression to controls. Consistent with Sostdc1's known role in the regulation of Wnt signaling, high levels of Wnt coactivators *Tcf7* and *Lef1* were observed in *Sostdc1*$^{-/-}$ NK cells. Expression of the NK development gene *Id2* was decreased in *Sostdc1*$^{-/-}$ iNK and tNK cells, but we observed no changes in *Eomes* and *Tbx21* expression. Reciprocal bone marrow transplant experiments showed that *Sostdc1* regulates NK cell maturation and expression of Ly49 receptors in a cell- extrinsic fashion from both non-hematopoietic and hematopoietic sources. Taken together, these data support a role for *Sostdc1* in the regulation of NK cell maturation, and NK cell cytotoxicity, and identify potential NK cell niches. Future studies involve RNA-Sequencing, bioinformatics and mathematical modeling to understand the transcriptional regulatory mechanism of Sostdc1 in NK cells.

- **Millan, A. J.,** Elizaldi, S. R., Lee, E. M., Aceves, J. O., Loots, G. G., & Manilay, J. O. (2019). Sostdc1 regulates natural killer cell maturation and cytotoxicity. *Journal of Immunology*; 202:2296-2306. PMID: 30814306

Contribution #3: Review on Wnt antagonists in hematopoietic and immune cell fate: Implications for osteoporosis therapies.

We reviewed the current literature on the roles of the Wnt antagonists, sclerostin (Sost) and sclerostin-containing domain protein 1 (Sostdc-1) on bone homeostasis, the relationship of the hypoxia-inducible factor (HIF) and von Hippel Landau (VHL) pathways on Sost expression, and how changes in bone induced by depletion of Sost, Sostdc1 and VHL affect hematopoietic cells. Depletion of Sost and Sostdc1 have effects on immune cell function that warrants investigation in patients receiving Wnt antagonist depleting therapies for treatment of bone diseases. Additional clinical applications for manipulation of Wnt antagonists include cancer immunotherapies, stem cell transplantation, and directed differentiation to immune lineages.

- *Chicana B, *Donham C, ***Millan A. J,** Manilay JO. Wnt antagonists in hematopoietic and immune cell fate: Implications for osteoporosis therapies (2019). *Current Osteoporosis Reports.* PMID: 30835038 * These individuals contributed equally to the writing of this article.

Contribution #4: Study on the progressive NK cell Ly49 developmental pathways in mice.

Previous studies of NK cell inhibitory Ly49 receptors suggested their expression is stochastic. However, relatively few studies have examined this stochasticity in conjunction with activating Ly49 receptors and NK cell maturation. We hypothesized that the expression of activating Ly49 receptors is not stochastic and

is influenced by inhibitory Ly49 receptors. We analyzed NK cell "clusters" defined by combinatorial expression of activating (Ly49H, Ly49D) and inhibitory (Ly49I, Ly49G2) receptors in C57BL/6 mice. Using the product rule to evaluate the interdependencies of the Ly49 receptors, we found evidence for a tightly regulated expression at the immature NK cell stage, with the highest interdependencies between clusters that express at least one activating receptor. Further analysis demonstrated that certain NK clusters predominated at the immature (CD27+CD11b-), transitional (CD27+CD11b+) and mature (CD27-CD11b-) NK cell stages. Using parallel in vitro culture and in vivo transplantation of sorted NK clusters, we discovered non-random upregulation of Ly49 receptors, suggesting that progressive pathways of NK cluster differentiation exist. Our data infer that upregulation of Ly49I is an important step in NK cell maturation. Ki-67 expression and cell counts confirmed that immature NK cells proliferate more than mature NK cells. We found that MHC-I is particularly important for regulation of Ly49D and Ly49G2, even though no known MHC-I ligand for these receptors is present in B6 mice. Our data indicate that the regulatory systems controlling the expression of both activating and inhibitory Ly49 receptors are non-stochastic and support the idea that NK cell clusters develop in a non-random process correlated to their maturation stage.

- **Millan A. J**, Hom A. B, Libang B. J, Sindi S, Manilay J. O. Evidence for prescribed NK cell Ly49 developmental pathways in mice. bioRxiv preprint doi: https://doi.org/10.1101/2020.05.23.112391

D. POSITIONS AND HONORS

Positions and Employment

2010 – 2014 PAL Facilitator, Department of Chemistry, Sacramento State, CA.
2011 – 2015 Undergraduate Laboratory Researcher, Sacramento State, CA.
2012 – 2014 President of McNair Scholar Cohort, Sacramento, CA.
2014 – 2015 Physics Tutor, Athletic Department, Sacramento State, CA.
2015 – 2020 Graduate Student Teaching Fellow, UC Merced
Spring 2020 Graduate Student Teaching Fellow – Instructor of Record, UCM
2020-Present Postdoctoral Scholar-Employee, UCSF

Professional Memberships

2013 – Present Member, McNair Scholars Program.
2015 – Present Member, American Association of Immunologists.

Honors and Awards

2010 Full NCAA I Athletic Scholarship, Sacramento, CA.
2011 Dean's Honor List, Sacramento, CA.
2013 McNair Research Symposium Participant, Sacramento, CA.
2014 Dean's Honor List, Sacramento, CA
2014 Instructionally Related Activities (IRA) Grant Award, Sacramento, CA.
2014 Provost's Student Research Showcase, Sacramento, CA.
2015 Dean's Honor List, Sacramento, CA.
2016 AAI Summer Course in Immunology, Long Beach, CA
2016 QSB Summer Recruitment Fellowship, Merced, CA
2017 AAI Trainee Abstract Awardee, Washington, DC
2017 AAI Lab Travel Award, Washington, DC
2017 Fall Graduate Student Researcher, Merced, CA
2017 Spring Graduate Student Researcher, Merced, CA
2017 QSB Summer Recruitment Fellowship, Merced, CA
2018 AAI Lab Travel Award, Austin, TX
2018 ECI 2018 Poster Award (Top 50), Amsterdam, Netherlands
2018 AAI Travel Grant for ECI 2018, Amsterdam, Netherlands
2018 QSB Summer Recruitment Fellowship, Merced, CA
2019 AAI Minority Scientist Travel Award, San Diego, CA
2019 AAI Trainee Abstract Award, San Diego, CA
2020 AAI Minority Scientist Travel Award, Honolulu, Hawaii
2020 AAI Trainee Abstract Award, Honolulu, Hawaii

E. PRESENTATIONS

McNair Research Symposium
04/14/2014
Comparison Between Collagenase Enzyme Digestion and StromaCell for Mesenchymal Stem Cell Separation
Oral & Poster presentation – CSUS, Redwood Room, Sacramento, CA

Peer Assistant Learning (PAL) Research
05/20/2014
Integrating YouTube Videos for Introductory Chemistry Learning
Authors: **Alberto J Millan Hernandez**, Magda Rahardja, Ashley Pearl, Dr. Stuart Hay, Dr. Jennifer Lundmark
Poster presentation – CSUS, Redwood Room, Sacramento, CA

University of Buffalo McNair Undergraduate Research Conference
07/26/2014
Comparison Between Collagenase Adipose Digestion and StromaCell Mechanical Dissociation for Mesenchymal Stem Cell Separation
Oral presentation – The Conference Center, Niagara Falls, Niagara Falls, NY

McNair Heartland Research Conference
09/20/2014
Comparison Between Collagenase Adipose Digestion and StromaCell Mechanical Dissociation for Mesenchymal Stem Cell Separation
Poster presentation – Kansas City, MO

STEM Undergraduate Research Reception
10/07/2014
Comparison Between Collagenase Adipose Digestion and StromaCell Mechanical Dissociation for Mesenchymal Stem Cell Separation
Poster and Oral Presentation – CSUS, CA

Provost's Student Research Showcase
10/30/2014
Comparison Between Collagenase Adipose Digestion and StromaCell Mechanical Dissociation for Mesenchymal Stem Cell Separation
Poster Presentation - Sacramento State University, Sacramento, CA

MCB Seminar
01/24/2017
Natural Killer Cell Development and Maturation is Regulated by Sostdc1
Oral Presentation – University of California, Merced

AAI Annual Meeting - Immunology 2017
05/13/2017
Natural Killer Cell Development and Maturation is Regulated by Sostdc1
Oral & Poster presentation – Walter E. Washington Convention Center, Washington, DC

AAI Annual Meeting - Immunology 2018
05/04/2018
Sostdc1 regulates natural killer cell maturation and cytotoxicity
Poster presentation – Austin Convention Center, Austin, TX

5th European Congress of Immunology – ECI 2018
09/02/2018
Predicating NK cell behavior with mathematical models
Poster presentation – Amsterdam RAI Exhibition and Convention Centre, Amsterdam, Netherlands

AAI Annual Meeting - Immunology 2019
05/09/2019
Predicting Natural Killer Cell Behavior with Mathematical Models
Oral & Poster presentation – San Diego Convention Center, San Diego, CA

UC San Francisco Seminar Talk
02/03/2020
Understanding Natural Killer Cell Behavior: Evidence for Prescribed NK cell Ly49 Cluster Pathways in Mice
Oral presentation – San Francisco, CA

St. Jude Seminar Talk
03/12/2020
Understanding Natural Killer Cell Behavior: Evidence for Prescribed NK cell Ly49 Cluster Pathways in Mice
Oral presentation – San Francisco, CA

AAI Annual Meeting - Immunology 2020 (Meeting canceled due to COVID)
05/08/2020
Evidence for a prescribed NK cell Ly49 developmental pathway in mice
Oral & Poster presentation – Honolulu, Hawaii

Cell-Extrinsic and Cell-Intrinsic Regulation of Natural Killer Cell Behavior in Mice

by

Alberto Jovani Millan Hernandez

Doctor of Philosophy in Quantitative and Systems Biology

University of California, Merced, 2020

Professor Jennifer O. Manilay

Natural killer (NK) cells play a fundamental role in protecting the host against cancerous and virally infected cells, however the mechanisms that control NK cell maturation and Ly49 receptor expression are incompletely understood. We have identified a novel role for sclerostin domain-containing-1 (Sostdc1) in the regulation of NK maturation and cytotoxicity. Sostdc1-knockout (KO) mice display a partial NK maturation block of transitional ($CD27^+CD11b^-$) NK cells and display decreased frequencies of inhibitory Ly49G2 and increased frequencies of activating Ly49H, Ly49D receptors. We hypothesized that Ly49 receptors in Sostdc1-KO mice would correlate with high NK cell killing. Inversely, we observed Sostdc1-KO NK cells to be hyporesponsive towards β_2m-KO targets in vitro and in vivo. Consistent with Sostdc1's known role in Wnt signaling, we observed increased *Tcf7* and *Lef1* levels in Sostdc1-KO NK cells. Reciprocal bone marrow transplants show that Sostdc1 can regulate NK cells distinctly by nonhematopoietic stromal cells and hematopoietic cells. These data suggest niche cell involvement in NK cell behavior. Furthermore, we show evidence for progressive NK cell Ly49 developmental pathways in C57BL/6 (WT) mice that are not entirely stochastic. We analyzed NK cell "clusters" defined by combinatorial expression of activating Ly49H, Ly49D, and inhibitory Ly49G2, Ly49I receptors. Using the product rule to evaluate Ly49 receptor interdependencies, we found NK cells to tightly regulate Ly49 receptors at the iNK cell stage. We discovered non-random cluster development of Ly49I receptor by transplantation of sorted clusters. Comparing MHC-I-KO and WT mice, we found that MHC-I is a partial regulator of Ly49D and Ly49G2, even though no known MHC-I ligand is present in WT mice. Altogether, these data support a novel role for Sostdc1 in the regulation of NK cell maturation and cytotoxicity and a regulatory mechanism for a non-stochastic expression for Ly49 receptors. These data provide important information for potential NK cell guidance for future NK cell immunotherapies.

CHAPTER 1

BACKGROUND AND HISTORICAL CONTEXT

CHAPTER 1: BACKGROUND AND HISTORICAL CONTEXT

INTRODUCTION

Natural killer (NK) cells are the third most abundant lymphocyte in the immune system and play an integral part in protecting the host against cancerous and virally infected cells by rapidly secreting perforin and granzymes, and secrete pro-inflammatory cytokines such as interferon-gamma (IFN-γ) and tumor necrosis factor-alpha (TNF-α) to alert surrounding cells. NK cells are required to mature and interact with the surrounding microenvironment to govern "self" vs. "non-self" tolerance through the lack of recognition from self-major histocompatibility complex class I (MHC-I), and the expression of "stressed" and transformed molecules on target cells (1, 2). Furthermore, the direct interactions between NK cells and target cells promote NK cytotoxicity via the binding of Ly49 activating and inhibitory receptors (3). NK cells have recently been observed to secrete regulatory cytokine, such as IL-10, and possess features of the adaptive immune system, including antigen specificity, clonal proliferation, and long-lived memory (4, 5). NK cells play an important role in mediating multiple immune functions and respond by eliminating cancers and virally infected cells.

NK cell maturation and Ly49 expression are two main concepts described in this thesis. It is unclear how the microenvironmental factors play a role in NK cell behavior. We hypothesized that the bone defects found in Sostdc1-knockout (KO) mice contribute to altered immune cell behavior. Thus, in the first half of my thesis work, we uncovered a novel role for Sostdc1 in NK cell maturation and function through two distinct regulator mechanism, which are described in Chapter 2 of this thesis. Sostdc1-KO mice show a partial NK cell maturation block, decreased cytotoxicity, and altered Ly49 receptor expression. Thus, these results naturally led us to hypothesize if NK Ly49 receptors are regulated by maturation. Our results show evidence of a progressive pathway for splenic NK cell Ly49 clusters development and regulation via the expression of self-inhibitory Ly49I receptor, proliferation, and MHC-I, which are described in Chapter 3 of this thesis. Together, my thesis work expands on the current literature on the understanding of NK cell microenvironmental influences and Ly49 receptor expression which can be further be applied for future NK cell immunotherapies (6).

REVIEW OF LITERATURE

Part I: NK cell development and maturation

Conventional NK cells develop in the bone marrow (BM) from hematopoietic stem cells (HSCs) (7, 8). The bone marrow niche supports hematopoietic development in which HSCs in adult mice give rise to the common lymphoid progenitor (CLP) (9). Further CLP differentiation leads to the production of the first committed NK progenitor, or the pre-pro NK progenitor cell (pre-pro NKPs) (10). These pre-pro NKPs upregulate CD27, CD127 (IL-7Rα), and CD244 (2B4) receptors and develop into pre-NKPs (11). The next committed progenitor, 'refined' NKPs (rNKPs), arise from pre-NKPs by upregulating CD122 (IL-2Rγ_c), the IL-15 β-chain receptor. IL-15 signaling in rNKPs from the BM becomes essential for NK cell development into immature NK cells (iNK), which express the pan-NK cell marker NK1.1 (C57BL/6 mice and other stains only), NKp46, CD127, CD117 (cKit), and CD27 (8). NK cell maturation from the iNK stage can be tracked in the BM and peripheral tissues by CD27 and CD11b surface expression and transcriptional factors (Figure 1-1) (12, 13). iNKs display the highest proliferation potential, and generate transitional NK cells (CD27+CD11b+; tNK) by upregulating surface receptors CD11b, CD49b, CD43, KLRG1, and Ly6C. tNKs further downregulate CD27 to generate mature NK cells (CD27-CD11b+), which display low proliferation potential, but the greatest effector function (12).

Tissue specific regulation of NK cell maturation

NK cells account for 5 to 20% of mononucleated cells in mice and can be characterized by specific tissue location, which may suggest a tissue-specific microenvironment that regulates NK cell maturation. NK cells predominantly express the CD11b mature marker in the blood circulation and multiple tissue sites including lung, spleen, liver, while NK cells with a more immature phenotype ($CD27^+CD11b^-$) are most prominent in BM and thymus (13, 14). The lymph node express equal parts of iNK and tNKs, while low frequencies of mNKs (13) (Figure 1-2). It is now clear that human NK cell maturation stages are distinguishable at each tissue location (13, 15). Dogra et al. have recently mapped out the human tissue specific NK cells distribution. The authors found most differentiated and cytotoxic NK cells ($CD56^{dim}CD16^+$) were localized in the spleen, blood, and bone marrow, whereas the precursor and immature ($CD56^{high}CD16^-$) NK cells were found in the lymph nodes, tonsils, and intestines and reduced effector function (15). NK cell tissue-specific microenvironment can be an important factor in regulating NK cell maturation and function.

The bone marrow microenvironment provides developmental support for NK cells. BM-derived NK cells are conventional NK cells, which can egress into

the circulation to further mature and gain functional competence (Figure 1-3) (16). Under homeostatic conditions, NK cell migration is governed by the chemoattractant receptors CXCR4 and $S1P_5$, such that CXCR4 is highly expressed on NKPs and iNK cells (17, 18). Osteoblasts in the endosteal region of the bone and CXCL12-abundant reticular (CAR) cells secrete CXCL12, which may act as a retention mechanism for NKPs and iNK cells in the BM (19). Furthermore, BM stromal cells, including CAR, Mesenchymal Stem Cells (MSCs), and fibroblast reticular cells, secrete the cytokine IL-15, which is an essential cytokine for NK cells development and function (20, 21). Thus, it can be suggested that the BM microenvironment can play an essential role in retaining NKPs and iNK cells via CXCR4-dependent mechanisms and then further supported by IL-15 produced by stromal cells.

The thymus in particular, promotes an alternative NK cell developmental pathway which is GATA3-dependent relative to BM-derived conventional NK cells. Thymic-derived NK cells are identified by high expression of the zinc-finger transcription factor GATA-3, surface receptor CD127 (IL-7Rα), express few Ly49 receptors, and lack CD11b (22, 23). Furthermore, thymic NK cells function with low cytotoxicity potential while able to produce high amounts of cytokines, such as IFN-γ, granulocyte-macrophage colony-stimulating factor (GM-CSF), and TNF, relative to splenic or BM NK cells (23). Thymic NK cells require microenvironmental IL-7, whereas the cytokine is not essential for BM derived NK cells (24). Thus, thymic NK cells provided more evidence for tissue specific NK cell maturation and function.

Sostdc1's role in NK cell maturation and effector function

Sclerostin domain-containing-1 (Sostdc1), paralog to sclerostin (Sost), has aliases Ectodin, USAG1 and Wise (25-28), and has been well studied in the context of tooth development, early digit formation, vibrissae, hair, feathers, mammary glands, kidneys, and cancers (29-31). Sostdc1 is first expressed during the 17 embryonic days in mice (28). Moreover, Sostdc1's role has only been recently identified in bone fracture repair and we show, in this thesis, its regulation in NK cell maturation and function (Thesis Chapter 2) (32, 33). Micro-computed tomography (μCT) measurements of Sostdc1-knockout ($Sostdc1^{-/-}$) mice femurs show the bone mineral density (BMD) of the cortical bone and the total cortical bone area to increase by about 16 percent (%) relative to WT femurs. The bone marrow area is also enlarged by 21% compared to WT mice (32). Furthermore, Sostdc1 expression was observed in the periosteum, fibroblast, and mesenchymal stem cells (MSCs) (32). Upon bone fracture, $Sostdc1^{-/-}$ mice had enhanced bone

formation and remodeling of the callus. Elevated Sostdc1 expression was also found in MSCs after fracture, suggesting a role for Sostdc1 in regulating MSC function in bone remodeling. As will be described further in Chapter 2, we found Sostdc1 expressing in hematopoietic $CD4^+$ and $CD8^+$ cells T cell which may regulate NK cell surface receptor Ly49 profile in the spleen (33). Previously, T cell subsets were identified to express Sostdc1, such as memory PD-1^+CD4^+ T cell (34), and T follicular helper (T_{FH}) cells found in the Peyer's patches and peripheral lymph nodes (35). These results suggest a magnitude of roles for Sostdc1 in bone development and immune cell regulation.

BMP/Smad-dependent role in NK cells

Mechanistically, Sostdc1 can antagonize the bone morphogenetic protein (BMP) signaling and regulate cellular outcomes (28). Sostdc1 acts as an extracellular BMP inhibitor by binding BMP-2, -4, and -7 and decreasing canonical BMP/Smad-dependent signaling (Figure 1-4) (27, 36). BMPs are a group of signaling molecules that belong to the Transforming growth factor-β (TGF-β) superfamily of proteins (37). BMPs have various roles in different cell types during organ and tissue development, such as in apoptosis, growth, and differentiation (37). The cell surface BMP signaling cascade is transduced when BMP ligands bind to the cell surface serine/threonine type II receptors, in which phosphorylation of the Type I receptors and forming a heterotetrametric complex. The phosphorylated Type I receptor can further activating Smad-1, -5, and -8 (38). The active forms of the Smad-1/5/8 complex recruits co-Smad (Smad4) and translocate into the nucleus for gene transcription (39). When Sostdc1 binds BMP ligands, the canonical BMP/Smad-dependent pathway is halted and gene transcription in decreased.

BMPs were originally identified by their ability to induce ectopic bone formation (38). Most recently, studies of BMP signaling in hematopoiesis suggest a crucial role for HSC number and function (39-41). Goldman et al. have shown that BMP4-deficient mice have reduced numbers of Lineage-negative c-kit^+Sca-1^+ progenitor cells. When serially transplanted, these cells reduce the repopulating activity of WT HSCs in BMP4-deficient host (40). Thus, BMP regulated signaling may be essential for adult hematopoiesis. Furthermore, studies which analyze the effects of BMP signaling on NK cells are very limited. However, Robson et al. have demonstrated a possible role for BMP/Smad-dependent signaling in human blood NK cells (42). The authors identified human blood-circulating NK cells to express type I and type II BMP receptors and phosphorylated isoforms of Smad-1, -5, -8. Furthermore, when human NK cells were treated with a BMP receptor inhibitor,

Compound C/dorsomorphin, and then stimulated with IL-2, IL-12, and poly I:C, the NK cells reduced expression of IFN-γ and decreased capacity to kill K562 target cells (42). Similar results were observed when human NK cells were treated with Noggin, which inhibits extracellular BMP ligands in the same fashion as Sostdc1 (42). To my knowledge, Sostdc1, one of the known BMP signaling antagonists, has yet to be studied in the regulation of NK cell development and function.

Sostdc1/Wnt/β-catenin/TCF-1 and LEF-1 role in NK cells

Sostdc1 is a known antagonist to canonical Wnt/β-catenin signaling (25). Wnt signaling is initiated at the surface membrane of the cell after binding of the Wnt ligand to the Frizzled receptor and recruiting the co-receptors, low-density lipoprotein receptor-family (LRP) 5 or LRP6 (Figure 1-5) (43, 44). The binding of the Wnt ligand inactivates the glycogen synthase kinase3β (GSK3β), which normally prevents the accumulations of β-catenin in the cytoplasm. In the process of Wnt activation, GSK3β and Axin2 degrade and allows β-catenin to translocate into the nucleus and where is bind the transcription co-activators lymphoid enhancer-binding factor 1 (Lef1) and T cell factor (TCF) for gene transcription (45, 46). When Sostdc1 binds to the Wnt co-receptors LRP4 and LRP5/6, Wnt signaling is diminished by degrading cytosolic β-catenin, thus decreasing targeted gene transcription (26, 47). Similarly, dickkopf WNT signaling pathway inhibitor I (DKK1) show similar characteristics to Sostdc1 and also binds LRP5/6 and antagonizes Wnt/ β-catenin signaling (48, 49).

Wnt signaling has been well studied in the framework of HSCs to help promote proliferation, differentiation, and homeostasis (50). It is now evident that canonical Wnt signaling plays a crucial role in the regulation of many immune cells (51). Interestedly, overactive *Lrp5* gene in mice lead to high bone mass, while loss-of-function mutation in *Lrp5* causes osteoporosis (52). Sostdc1$^{-/-}$ mice show increased bone mass, which may indicate that Sostdc1 may be responsible for phenotypic bone growth via a binding of *Lrp5* in Wnt signaling (32). In my thesis work, I found that Sostdc1$^{-/-}$ mice NK cells show a maturation blockade at the tNK cells stage of maturation and dysregulation of Ly49 frequencies in the BM and spleen. We further observed one of the co-activators to canonical Wnt signaling, TCF-1, was significantly upregulated in tNK and mNK cells, but normal at the iNK stage. Additionally, the secondary coactivator, LEF-1, was only significantly upregulated in the mNK cell stage. Our analysis strongly implies that canonical signaling by Wnt/β-catenin/TCF-1 and LEF-1 signaling is required specifically at the tNK stage of maturation. Previously, TCF-1 and LEF-1 have shown redundant role in NK cell development, whereas TCF-1 contributes significantly more to NK

cell development than LEF-1 (53). Furthermore, TCF-1 alone has been shown to regulate the Ly49 receptor in mice NK cells by directly binding to the *Klra1* (Ly49A) gene and promoting its expression (54).

Part II: NK cell regulation of Ly49 activating and inhibitory receptor expression

NK cells, unlike T and B cells, acquire germline encoded Ly49 receptors which recognize and eliminate cancerous and virally infected cells. NK cell Ly49 receptors are one of the distinct families of surface receptors involved in NK cell recognition of polymorphic MHC-I molecules (Table 1-1) (3, 55). It is currently understood that expression of *Klra* (Ly49) genes, located on mouse chromosome 6, are regulated in a random manner by gene expression mechanisms (55, 56). Therefore, each NK cell outcome has a probability of expressing a unique set of activating and inhibitory receptors on the cell surface. Nonetheless, studies have shown that MHC-I expression and the bidirectional transcriptional regulation of Pro1 and Pro2 may account for tightly regulated, non-random, expression of Ly49 activating and inhibitory receptors (57). This process may reflect an evolutionary process which ensures host immunity while maintaining self-tolerance (58). A common pathway of inhibitory Ly49 signaling is provided by Immunoreceptor tyrosine-based inhibition motifs (ITIM) sequences in the cytoplasmic domains of these otherwise structurally diverse receptors. Upon ligand binding and activation, the inhibitory NK cell receptors become tyrosine phosphorylated and recruit tyrosine phosphatases, Src homology region 2 (SH2) domain-containing protein phosphatase SHP-1, resulting in inhibition of NK cell-mediated cytotoxicity and cytokine expression (3, 59). In contrast to inhibitory receptors, the activating Ly49 receptors transduce signals through associated adaptor proteins, such as DAP12, and with the associated immunoreceptor tyrosine-based activation motif (ITAM) (3, 60, 61).

Ly49 receptor role in NK cell mediated cytotoxicity

Ly49 receptors play an important role in NK cell education and recognition of transformed cells. Kärre et al. first showed that NK cells are geared to detect decreased or deleted expression of self-MHC-I and coined this process the “missing-self hypothesis” (1). Cancerous or infected cells often down-regulate self-MHC-I expression on their surface to avoid detection and killing by cytotoxic T cells, thus according to the hypothesis, NK cells constantly survey the microenvironment for altered expression of self-MHC-I on neighboring cells for Ly49-mediated killing (2, 3). In addition, NK cells in β2m-deficient mice show

diminished ability to lyse target cells when compared to mice WT NK cells (62). This discovery led to a new hypothesis which incorporates the expression of self-MHC-I for NK cell effector function. The hypothesis was later identified as NK cell "licensing", a process in which self-Ly49 inhibitory receptors require binding to self-MHC-I to produce optimal killing function. Conversely, "unlicensed" NK cells are those that do not express self-Ly49 inhibitory receptor and lack killing function (63-65). Most recently, NK cells have been shown to quantitatively tune killing function by the number of self-MHC-I ligands expressed and stimulatory integrations encountered in the microenvironment. Thus, the "rheostat" model ensures self-tolerance and yet optimized for adaptations in the microenvironment (66).

Ly49 receptors' role in NK cell memory

NK cells have been recently shown to share features of adaptive immunity similar to T and B cells, including antigen specificity, clonal proliferation, and long-lived memory (4, 5). It has been shown that after cytomegalovirus (CMV) infection in mice, a subset of NK cells expressing the activating Ly49H receptor expand into long-lived NK cells and acquire robust recall responses (67). Furthermore, the murine CMV-encoded MHC-I-like protein (m157) was shown to bind Ly49H activating receptor and provided direct pathogen recognition by NK cells (68). Additionally, NK cells expressing Ly49C/I inhibitory receptors were found to persist and respond up to 4 weeks after mice were sensitized with hapten (69). In humans, infection with CMV show similar NK cell memory phenotypes. For example, after CMV infection, a long-lasting NK cell subset expressing NKG2C or activating KIR persists (70, 71). Together, NK cells utilize surface activating and inhibitory Ly49 receptors to recognize and produce killing function, while showing features of NK cell memory.

Ly49 stochastic gene expression

NK cells express a diverse set of surface activating and inhibitory receptors that recognize host cells and cellular targets. The Ly49 gene in mice or the KIR gene expression in humans are believed to be stochastic, however, growing amount of evidence are now uncovering tightly regulated mechanisms which can control Ly49 gene expression. Mathematically, the product rule can determine the frequencies of Ly49 gene expression with a significant degree of independence. The independence is consistent with a stochastic initiation of the Ly49 receptor gene expression. Nonetheless, examination between the inhibitory Ly49 receptors and NKG2A show an underrepresentation of frequencies provided by the product rule, suggesting that NKG2A may not significantly associate with inhibitory Ly49

receptor gene expression in mice (56, 72). Furthermore, Forbes et al. provide support of interdependencies between Ly49H and Ly49D surface expression which are distinctly influenced by the co-expression of inhibitory receptor Ly49C (73). Transcriptionally, Held et al. show that TCF-1 transcription factor controls the expression of Ly49A and Ly49D (74), while more groups have shown that the bidirectional regulation of Pro1 in immature NK cells and Pro2 in mature NK cells control Ly49 gene expression (57, 75). Notably, Rouhi et al. have shown differences between activating and inhibiting Ly49 DNA methylation patterns, which may add additional complexly to the stochastic nature of the Ly49 expression in mice (76).

NK cell surface Ly49 receptor expression during development

Studies suggest that NK cell Ly49 receptor expression is regulated in an orderly manner. This concept was originally developed when a fraction of sorted mice NK cells expressing Ly49A or Ly49G2 were transferred in vivo and later expressed other Ly49 receptors while maintaining the initial Ly49 expression (77). Moreover, $Ly49A^{+}C/I^{-}G2^{-}$ sorted NK cells after 10 days expressed Ly49G2 and less frequent the Ly49C/I receptor. The $Ly49A^{-}C/I^{-}G2^{+}$ sorted NK cells then expressed the inhibitory Ly49C/I receptors (72). Thus, these results suggest a sequential progression of NK cell Ly49 receptor expression in a manner that may be initiated by Ly49A, then Ly49G2, and finally Ly49C/I. Furthermore, RT-PCR analysis of the Ly49 RNA clones at different time points support the sequential model, such as the Ly49G2 gene was expressed first, followed by Ly49C/I, and finally Ly49A gene (78). Moreover, NK cell Ly49 expression has shown to increase gradually throughout ontogeny in mice over the first several weeks after birth (77, 79). Smith et al. show that the activating Ly49H and Ly49D are expressed during the same time points during mouse development and lag behind in the expression of the inhibitory Ly49 receptors (72). Together, these studies suggest that Ly49 receptors can be expressed sequentially in a cumulative fashion during NK cell development.

NK cell surface Ly49 receptor expression during maturation

In Chapter 3 of this thesis, we provided direct evidence for a progressive pathway of NK “cluster transitions” in vitro and in vivo, which suggest that Ly49 inhibitory receptors acquisition is directly associated with NK cell maturation. Thus, our data support the idea that NK cell clusters develop in a non-random manner and provide additional evidence that the regulatory system that controls the

expression of both Ly49 activating and inhibitory receptors can be regulated in a variegated and sequential manner.

REFERENCES

1. Karre, K., H. G. Ljunggren, G. Piontek, and R. Kiessling. 1986. Selective rejection of H-2-deficient lymphoma variants suggests alternative immune defence strategy. *Nature* 319.
2. Orr, M. T., and L. L. Lanier. 2010. Natural killer cell education and tolerance. *Cell* 142: 847-856.
3. Rahim, M. M., M. M. Tu, A. B. Mahmoud, A. Wight, E. Abou-Samra, P. D. Lima, and A. P. Makrigiannis. 2014. Ly49 receptors: innate and adaptive immune paradigms. *Front Immunol* 5: 145.
4. Sun, J. C., and L. L. Lanier. 2011. NK cell development, homeostasis and function: parallels with CD8(+) T cells. *Nat Rev Immunol* 11: 645-657.
5. Vivier, E., D. H. Raulet, A. Moretta, M. A. Caligiuri, L. Zitvogel, L. L. Lanier, W. M. Yokoyama, and S. Ugolini. 2011. Innate or adaptive immunity? The example of natural killer cells. *Science* 331: 44-49.
6. Shimasaki, N., A. Jain, and D. Campana. 2020. NK cells for cancer immunotherapy. *Nat Rev Drug Discov* 19: 200-218.
7. Brillantes, M., and A. M. Beaulieu. 2019. Transcriptional control of natural killer cell differentiation. *Immunology* 156: 111-119.
8. Goh, W., and N. D. Huntington. 2017. Regulation of Murine Natural Killer Cell Development. *Front Immunol* 8: 130.
9. Kondo, M., I. L. Weissman, and K. Akashi. 1997. Identification of Clonogenic Common Lymphoid Progenitors in Mouse Bone Marrow. *Cell* 91: 661-672.
10. Rosmaraki, E. E., L. Douagi, C. Roth, F. Colucci, A. Cumano, and J. P. Di Santo. 2001. Identification of committed NK cell progenitors in adult murine bone marrow. *Eur J Immunol* 31.
11. Carotta, S., S. H. Pang, S. L. Nutt, and G. T. Belz. 2011. Identification of the earliest NK-cell precursor in the mouse BM. *Blood* 117: 5449-5452.
12. Chiossone, L., J. Chaix, N. Fuseri, C. Roth, E. Vivier, and T. Walzer. 2009. Maturation of mouse NK cells is a 4-stage developmental program. *Blood* 113: 5488-5496.
13. Hayakawa, Y., and M. J. Smyth. 2006. CD27 dissects mature NK cells into two subsets with distinct responsiveness and migratory capacity. *J Immunol* 176: 1517-1524.
14. Takeda, K., E. Cretney, Y. Hayakawa, T. Ota, H. Akiba, K. Ogasawara, H. Yagita, K. Kinoshita, K. Okumura, and M. J. Smyth. 2005. TRAIL identifies immature natural killer cells in newborn mice and adult mouse liver. *Blood* 105: 2082-2089.
15. Dogra, P., C. Rancan, W. Ma, M. Toth, T. Senda, D. J. Carpenter, M. Kubota, R. Matsumoto, P. Thapa, P. A. Szabo, M. M. Li Poon, J. Li, J. Arakawa-Hoyt, Y. Shen, L. Fong, L. L. Lanier, and D. L. Farber. 2020. Tissue Determinants of Human NK Cell Development, Function, and Residence. *Cell* 180: 749-763 e713.

16. Bernardini, G., G. Sciume, and A. Santoni. 2013. Differential chemotactic receptor requirements for NK cell subset trafficking into bone marrow. *Front Immunol* 4: 12.
17. Abel, A. M., C. Yang, M. S. Thakar, and S. Malarkannan. 2018. Natural Killer Cells: Development, Maturation, and Clinical Utilization. *Front Immunol* 9: 1869.
18. Bernardini, G., G. Sciume, D. Bosisio, S. Morrone, S. Sozzani, and A. Santoni. 2008. CCL3 and CXCL12 regulate trafficking of mouse bone marrow NK cell subsets. *Blood* 111: 3626-3634.
19. Petit, I., M. Szyper-Kravitz, A. Nagler, M. Lahav, A. Peled, L. Habler, T. Ponomaryov, R. S. Taichman, F. Arenzana-Seisdedos, N. Fujii, J. Sandbank, D. Zipori, and T. Lapidot. 2002. G-CSF induces stem cell mobilization by decreasing bone marrow SDF-1 and up-regulating CXCR4. *Nat Immunol* 3: 687-694.
20. Di Santo, J. P. 2006. Natural killer cell developmental pathways: a question of balance. *Annu Rev Immunol* 24: 257-286.
21. Noda, M., Y. Omatsu, T. Sugiyama, S. Oishi, N. Fujii, and T. Nagasawa. 2011. CXCL12-CXCR4 chemokine signaling is essential for NK-cell development in adult mice. *Blood* 117: 451-458.
22. Ribeiro, V. S., M. Hasan, A. Wilson, L. Boucontet, P. Pereira, S. Lesjean-Pottier, N. Satoh-Takayama, J. P. Di Santo, and C. A. Vosshenrich. 2010. Cutting edge: Thymic NK cells develop independently from T cell precursors. *J Immunol* 185: 4993-4997.
23. Vosshenrich, C. A., M. E. Garcia-Ojeda, S. I. Samson-Villeger, V. Pasqualetto, L. Enault, O. Richard-Le Goff, E. Corcuff, D. Guy-Grand, B. Rocha, A. Cumano, L. Rogge, S. Ezine, and J. P. Di Santo. 2006. A thymic pathway of mouse natural killer cell development characterized by expression of GATA-3 and CD127. *Nat Immunol* 7: 1217-1224.
24. Vosshenrich, C. A., T. Ranson, S. I. Samson, E. Corcuff, F. Colucci, E. E. Rosmaraki, and J. P. Di Santo. 2005. Roles for common cytokine receptor gamma-chain-dependent cytokines in the generation, differentiation, and maturation of NK cell precursors and peripheral NK cells in vivo. *J Immunol* 174: 1213-1221.
25. Collette, N. M., C. S. Yee, D. Murugesh, A. Sebastian, L. Taher, N. W. Gale, A. N. Economides, R. M. Harland, and G. G. Loots. 2013. Sost and its paralog Sostdc1 coordinate digit number in a Gli3-dependent manner. *Dev Biol* 383: 90-105.
26. Itasaki, N., C. M. Jones, S. Mercurio, A. Rowe, P. M. Domingos, J. C. Smith, and R. Krumlauf. 2003. Wise, a context-dependent activator and inhibitor of Wnt signalling. *Development* 130: 4295-4305.
27. Laurikkala, J., Y. Kassai, L. Pakkasjarvi, I. Thesleff, and N. Itoh. 2003. Identification of a secreted BMP antagonist, ectodin, integrating BMP, FGF, and SHH signals from the tooth enamel knot. *Dev Biol* 264.
28. Yanagita, M., M. Oka, T. Watabe, H. Iguchi, A. Niida, S. Takahashi, T. Akiyama, K. Miyazono, M. Yanagisawa, and T. Sakurai. 2004. USAG-1: a

bone morphogenetic protein antagonist abundantly expressed in the kidney. *Biochem Biophys Res Commun* 316: 490-500.
29. Chen, G., H. Gong, T. Wang, J. Wang, Z. Han, G. Bai, S. Han, X. Yang, W. Zhou, T. Liu, and J. Xiao. 2018. SOSTDC1 inhibits bone metastasis in non-small cell lung cancer and may serve as a clinical therapeutic target. *INTERNATIONAL JOURNAL OF MOLEcULAR MEdIcINE* 42.
30. Laurikkala, J., M. L. Mikkola, M. James, M. Tummers, A. A. Mills, and I. Thesleff. 2006. p63 regulates multiple signalling pathways required for ectodermal organogenesis and differentiation. *Development* 133: 1553-1563.
31. Shigetani, Y., and N. Itasaki. 2007. Expression of Wise in chick embryos. *Dev Dyn* 236: 2277-2284.
32. Collette, N. M., C. S. Yee, N. R. Hum, D. K. Murugesh, B. A. Christiansen, L. Xie, A. N. Economides, J. O. Manilay, A. G. Robling, and G. G. Loots. 2016. Sostdc1 deficiency accelerates fracture healing by promoting the expansion of periosteal mesenchymal stem cells. *Bone* 88: 20-30.
33. Millan, A. J., S. R. Elizaldi, E. M. Lee, J. O. Aceves, D. Murugesh, G. G. Loots, and J. O. Manilay. 2019. Sostdc1 Regulates NK Cell Maturation and Cytotoxicity. *J Immunol* 202: 2296-2306.
34. Shimatani, K., Y. Nakashima, M. Hattori, Y. Hamazaki, and N. Minato. 2009. PD-1+ memory phenotype CD4+ T cells expressing C/EBPalpha underlie T cell immunodepression in senescence and leukemia. *Proc Natl Acad Sci U S A* 106: 15807-15812.
35. Georgiev, H., I. Ravens, G. Papadogianni, S. Halle, B. Malissen, G. G. Loots, R. Forster, and G. Bernhardt. 2018. Shared and Unique Features Distinguishing Follicular T Helper and Regulatory Cells of Peripheral Lymph Node and Peyer's Patches. *Front Immunol* 9: 714.
36. Yanagita, M., T. Okuda, S. Endo, M. Tanaka, K. Takahashi, F. Sugiyama, S. Kunita, S. Takahashi, A. Fukatsu, M. Yanagisawa, T. Kita, and T. Sakurai. 2006. Uterine sensitization-associated gene-1 (USAG-1), a novel BMP antagonist expressed in the kidney, accelerates tubular injury. *J Clin Invest* 116: 70-79.
37. Wang, R. N., J. Green, Z. Wang, Y. Deng, M. Qiao, M. Peabody, Q. Zhang, J. Ye, Z. Yan, S. Denduluri, O. Idowu, M. Li, C. Shen, A. Hu, R. C. Haydon, R. Kang, J. Mok, M. J. Lee, H. L. Luu, and L. L. Shi. 2014. Bone Morphogenetic Protein (BMP) signaling in development and human diseases. *Genes Dis* 1: 87-105.
38. Mishina, Y. 2003. FUNCTION OF BONE MORPHOGENETIC PROTEIN SIGNALING DURING MOUSE DEVELOPMENT. *Frontiers in Bioscience* 8.
39. Zhang, J., and L. Li. 2005. BMP signaling and stem cell regulation. *Dev Biol* 284: 1-11.
40. Goldman, D. C., A. S. Bailey, D. L. Pfaffle, A. Al Masri, J. L. Christian, and W. H. Fleming. 2009. BMP4 regulates the hematopoietic stem cell niche. *Blood* 114: 4393-4401.

41. Lefort, S., and V. Maguer-Satta. 2020. Targeting BMP signaling in the bone marrow microenvironment of myeloid leukemia. *Biochem Soc Trans* 48: 411-418.
42. Robson, N. C., L. Hidalgo, T. Mc Alpine, H. Wei, V. G. Martinez, A. Entrena, G. J. Melen, A. S. MacDonald, A. Phythian-Adams, R. Sacedon, E. Maraskovsky, J. Cebon, M. Ramirez, A. Vicente, and A. Varas. 2014. Optimal effector functions in human natural killer cells rely upon autocrine bone morphogenetic protein signaling. *Cancer Res* 74: 5019-5031.
43. Pinson, K. I., J. Brennan, S. Monkley, B. J. Avery, and W. C. Skarnes. 2000. An LDL-receptor-related protein mediates Wnt signalling in mice. *Nature* 407.
44. Tamai, K., M. Semenov, Y. Kato, R. Spokony, C. Liu, Y. Katsuyama, F. Hess, J. Saint-Jeannet, and X. He. 2000. LDL-receptor-related proteins in Wnt signal transduction. *Nature* 407.
45. Behrens, J., J. P. von Kries, M. Kuhl, L. Bruhn, D. Wedlich, R. Grosschedl, and W. Birchmeier. 1996. Functional interaction of p-catenin with the transcription factor LEF-1. *Nature* 382.
46. Cox, R. T., L. Pai, J. R. Miller, S. Orsulic, J. Stein, C. A. McCormick, Y. Audeh, W. Wang, R. T. Moon, and M. Peifer. 1999. Membrane-tethered Drosophila Armadillo cannot transduce Wingless signal on its own. *Development*.
47. Ohazama, A., E. B. Johnson, M. S. Ota, H. Y. Choi, T. Porntaveetus, S. Oommen, N. Itoh, K. Eto, A. Gritli-Linde, J. Herz, and P. T. Sharpe. 2008. Lrp4 modulates extracellular integration of cell signaling pathways in development. *PLoS One* 3: e4092.
48. Andl, T., S. T. Reddy, T. Gaddapara, and S. Millar. 2002. WNT Signals Are Required for the Initiation of Hair Follicle Development. *Developmental Cell* 2: 643-653.
49. Glinka, A., W. Wu, H. Delius, P. Monaghan, C. Blumenstock, and C. Niehrs. 1998. Dickkopf-1 is a member of a new family of secreted proteins and functions in head induction. *Nature*.
50. Richter, J., D. Traver, and K. Willert. 2017. The role of Wnt signaling in hematopoietic stem cell development. *Crit Rev Biochem Mol Biol* 52: 414-424.
51. Undi, R. B., U. Gutti, I. Sahu, S. Sarvothaman, S. R. Pasupuleti, R. Kandi, and R. K. Gutti. 2016. Wnt Signaling: Role in Regulation of Haematopoiesis. *Indian J Hematol Blood Transfus* 32: 123-134.
52. Zhang, M., Y. Yan, Y. B. Lim, D. Tang, R. Xie, A. Chen, P. Tai, S. E. Harris, L. Xing, Y. X. Qin, and D. Chen. 2009. BMP-2 modulates beta-catenin signaling through stimulation of Lrp5 expression and inhibition of beta-TrCP expression in osteoblasts. *J Cell Biochem* 108: 896-905.
53. Held, W., H. Clevers, and R. Grosschedl. 2003. Redundant functions of TCF-1 and LEF-1 during T and NK cell development, but unique role of TCF-1 for Ly49 NK cell receptor acquisition. *Eur J Immunol* 33: 1393-1398.

54. Kunz, B., and W. Held. 2001. Positive and negative roles of the trans-acting T cell factor-1 for the acquisition of distinct Ly-49 MHC class I receptors by NK cells. *J Immunol* 166: 6181-6187.
55. Schenkel, A. R., L. C. Kingry, and R. A. Slayden. 2013. The ly49 gene family. A brief guide to the nomenclature, genetics, and role in intracellular infection. *Front Immunol* 4: 90.
56. Sternberg-Simon, M., P. Brodin, Y. Pickman, B. Onfelt, K. Karre, K. J. Malmberg, P. Hoglund, and R. Mehr. 2013. Natural killer cell inhibitory receptor expression in humans and mice: a closer look. *Front Immunol* 4: 65.
57. McCullen, M. V., H. Li, M. Cam, S. K. Sen, D. W. McVicar, and S. K. Anderson. 2016. Analysis of Ly49 gene transcripts in mature NK cells supports a role for the Pro1 element in gene activation, not gene expression. *Genes Immun* 17: 349-357.
58. Jaeger, B. N., and E. Vivier. 2012. Natural killer cell tolerance: control by self or self-control? *Cold Spring Harb Perspect Biol* 4.
59. Makrigiannis, A. P., P. Gosselin, L. H. Mason, L. S. Taylor, D. W. McVicar, R. J. Ortaldo, and S. K. Anderson. 1999. Cloning and Characterization of a Novel Activating Ly49 Closely Related to Ly49A. *J Immunol* 163: 4931-4938.
60. Gosselin, P., L. H. Mason, J. Willette-Brown, R. J. Ortaldo, D. W. McVicar, and S. K. Anderson. 1999. Induction of DAP12 phosphorylation, calcium mobilization, and cytokine secretion by Ly49H. *Journal of Leukocyte Biology* 66.
61. Smith, K. M., J. Wu, A. B. H. Bakker, J. H. Phillips, and L. L. Lanier. 1998. Cutting Edge: Ly-49D and Ly-49H Associate with Mouse DAP12 and Form Activating Receptors. *J Immunol*: 7-10.
62. Liao, N., M. Bix, M. Zijlstra, R. Jaenisch, and D. H. Raulet. 1991. MHC ClassIDeficiency:SusceptibilitytoNatural Killer(NK)CellsandImpairedNK Activity. *Science*.
63. Belanger, S., M. M. Tu, M. M. Rahim, A. B. Mahmoud, R. Patel, L. H. Tai, A. D. Troke, B. T. Wilhelm, J. R. Landry, Q. Zhu, K. S. Tung, D. H. Raulet, and A. P. Makrigiannis. 2012. Impaired natural killer cell self-education and "missing-self" responses in Ly49-deficient mice. *Blood* 120: 592-602.
64. Brodin, P., K. Karre, and P. Hoglund. 2009. NK cell education: not an on-off switch but a tunable rheostat. *Trends Immunol* 30: 143-149.
65. Kim, S., J. Poursine-Laurent, S. M. Truscott, L. Lybarger, Y. J. Song, L. Yang, A. R. French, J. B. Sunwoo, S. Lemieux, T. H. Hansen, and W. M. Yokoyama. 2005. Licensing of natural killer cells by host major histocompatibility complex class I molecules. *Nature* 436: 709-713.
66. Joncker, N. T., N. C. Fernandez, E. Treiner, E. Vivier, and D. H. Raulet. 2009. NK cell responsiveness is tuned commensurate with the number of inhibitory receptors for self-MHC class I: the rheostat model. *J Immunol* 182: 4572-4580.

67. Sun, J. C., J. N. Beilke, and L. L. Lanier. 2009. Adaptive immune features of natural killer cells. *Nature* 457: 557-561.
68. Arase, H., E. S. Mocarski, A. E. Campbell, A. B. Hill, and L. L. Lanier. 2002. Direct Recognition of Cytomegalovirus by Activating and Inhibitory NK Cell Receptors. *Science* 296.
69. O'Leary, J. G., M. Goodarzi, D. L. Drayton, and U. H. von Andrian. 2006. T cell- and B cell-independent adaptive immunity mediated by natural killer cells. *Nat Immunol* 7: 507-516.
70. Beziat, V., L. L. Liu, J. A. Malmberg, M. A. Ivarsson, E. Sohlberg, A. T. Bjorklund, C. Retiere, E. Sverremark-Ekstrom, J. Traherne, P. Ljungman, M. Schaffer, D. A. Price, J. Trowsdale, J. Michaelsson, H. G. Ljunggren, and K. J. Malmberg. 2013. NK cell responses to cytomegalovirus infection lead to stable imprints in the human KIR repertoire and involve activating KIRs. *Blood* 121: 2678-2688.
71. Guma, M., A. Angulo, C. Vilches, N. Gomez-Lozano, N. Malats, and M. Lopez-Botet. 2004. Imprint of human cytomegalovirus infection on the NK cell receptor repertoire. *Blood* 104: 3664-3671.
72. Smith, H. R. C., H. H. Chuang, L. L. Wang, M. Salcedo, J. Heusel, and W. M. Yokoyama. 2000. Nonstochastic Coexpression of Activating Receptors on Murine Natural Killer Cells. *J. Exp. Med* 191: 1341-1354.
73. Forbes, C. A., A. Scalzo, A. M. Degli-Esposti, and J. D. Coudery. 2016. Ly49C Impairs NK Cell Memory in Mouse Cytomegalovirus Infection. *J Immunol* 197: 128-140.
74. Held, W., B. Kunz, B. Lowin-Kropf, M. Van de Wetering, and H. Clevers. 1999. Clonal Acquisition of the Ly49 NK Cell Receptor is Dependent on the trans-Acting Factor TCF-1. *Immunity* 11: 433-442.
75. Freund, L. R., M. May, E. Yand, H. Li, M. V. McCullen, B. Zhang, T. Lenvik, S. Cichocki, S. K. Anderson, and T. Kambayashi. 2016. Activating Receptor Signals Drive Receptor Diversity in Developing Natural Killer Cells. *PLoS Biol* 14.
76. Rouhi, A., C. B. Lai, T. P. Cheng, F. Takei, W. M. Yokoyama, and D. L. Mager. 2009. Evidence for high bi-allelic expression of activating Ly49 receptors. *Nucleic Acids Res* 37: 5331-5342.
77. Dorfman, R. J., and D. H. Raulet. 1998. Acquisition of Ly49 Receptor Expression by Developing Natural Killer Cells. *J. Exp. Med* 187: 609-618.
78. Williams, N. S., A. Kubota, M. Bennett, V. Kumar, and F. Takei. 2000. Clonal analysis of NK cell development from bone marrow progenitors in vitro: orderly acquisition of receptor gene expression. *Eur J Immunol* 30: 2074-2082.
79. Kubota, A., S. Kubota, S. Lohwasser, D. L. Mager, and F. Takei. 1999. Diversity of NK Cell Receptor Repertoire in Adult and Neonatal Mice. *The Journal of Immunology* 163: 212-216.

TABLES

Table 1-1: Ly49 receptors and known ligand binding. NK cell Ly49 receptors in B6 (C57BL/6) mice and known binding ligands. Information was adapted from Schenkel et al. 2013 (55).

B6: H2-D^b, H2-K^b (C57BL/6)	**Ligands**	**Function**
Ly49D	H2-D^d	Activating
Ly49H	MCMV m157	
Ly49A	H2-D^d, H2-D^K, H2-D^p	Inhibitory
Ly49B	Unknown	
Ly49C	H2-K^b, H2-K^d, H2-D^d, H2-D^K	
Ly49F	H2-K^d	
Ly49G2	H2-D^d	
Ly49I	H2-K^b, H2-D^d, H2-K^d, H2-K^K	
Ly49J	Unknown	
Ly49Q	H2-K^b	

FIGURES AND FIGURE LEGENDS

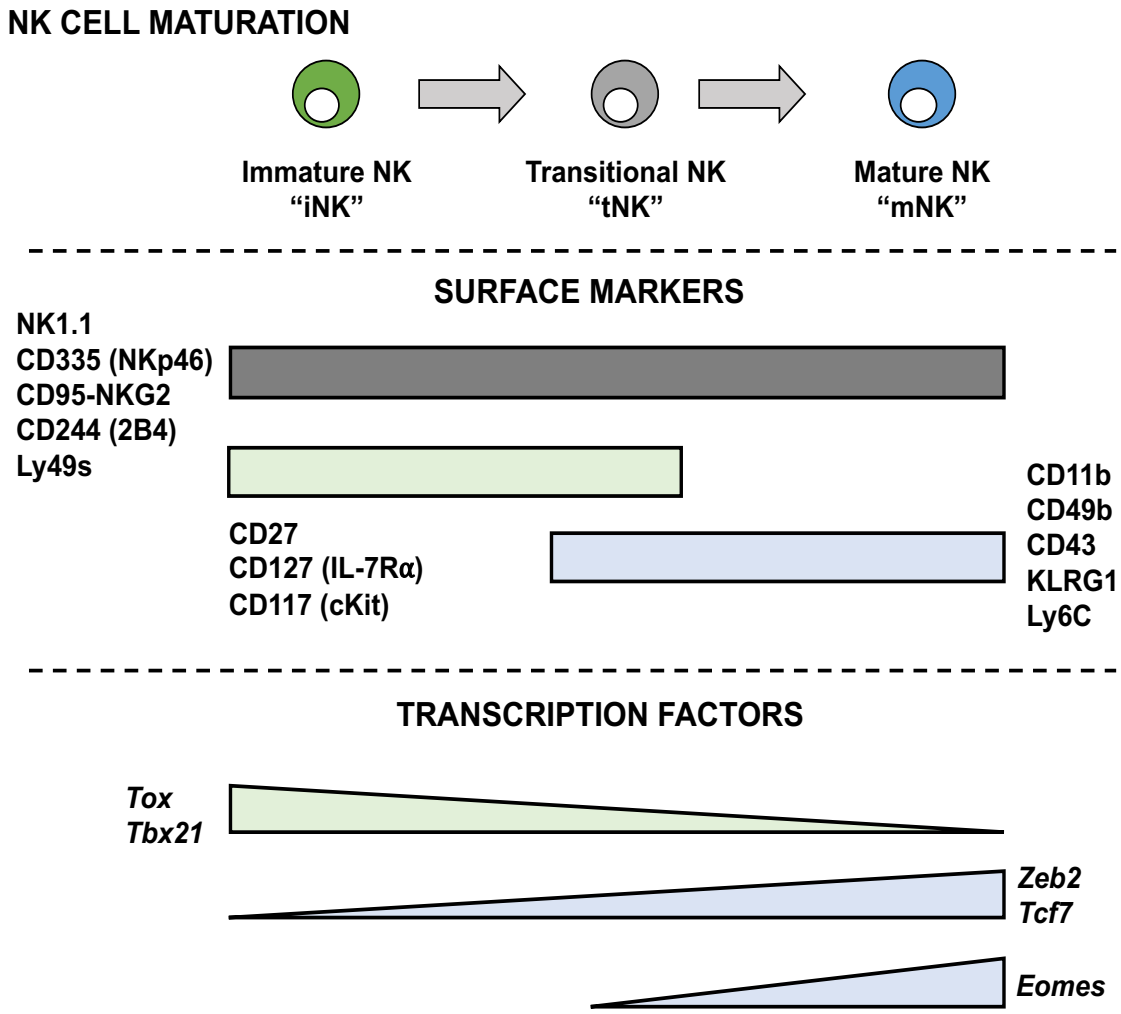

Figure 1-1: Phenotypic NK cell maturation surface markers and transcriptional factors in mice. Immature NK cells (iNKs) are distinctly characterized with surface expression CD27, CD127, CD117, and transcription factors (TF) *Tox* and *Tbx21*. iNKs start to upregulate CD11b, DX5, CD43, KLRG1, and Ly6C surface receptor to become transitional NK cells (tNKs), while beginning to upregulate TF *Eomes, Zeb2,* and *Tcf7*. tNKs downregulate CD27 and become mature NK cells (mNKs). NK1.1, CD335, CD94-NKG2, CD244, and Ly49s are surface markers found on NK cells throughout maturation.

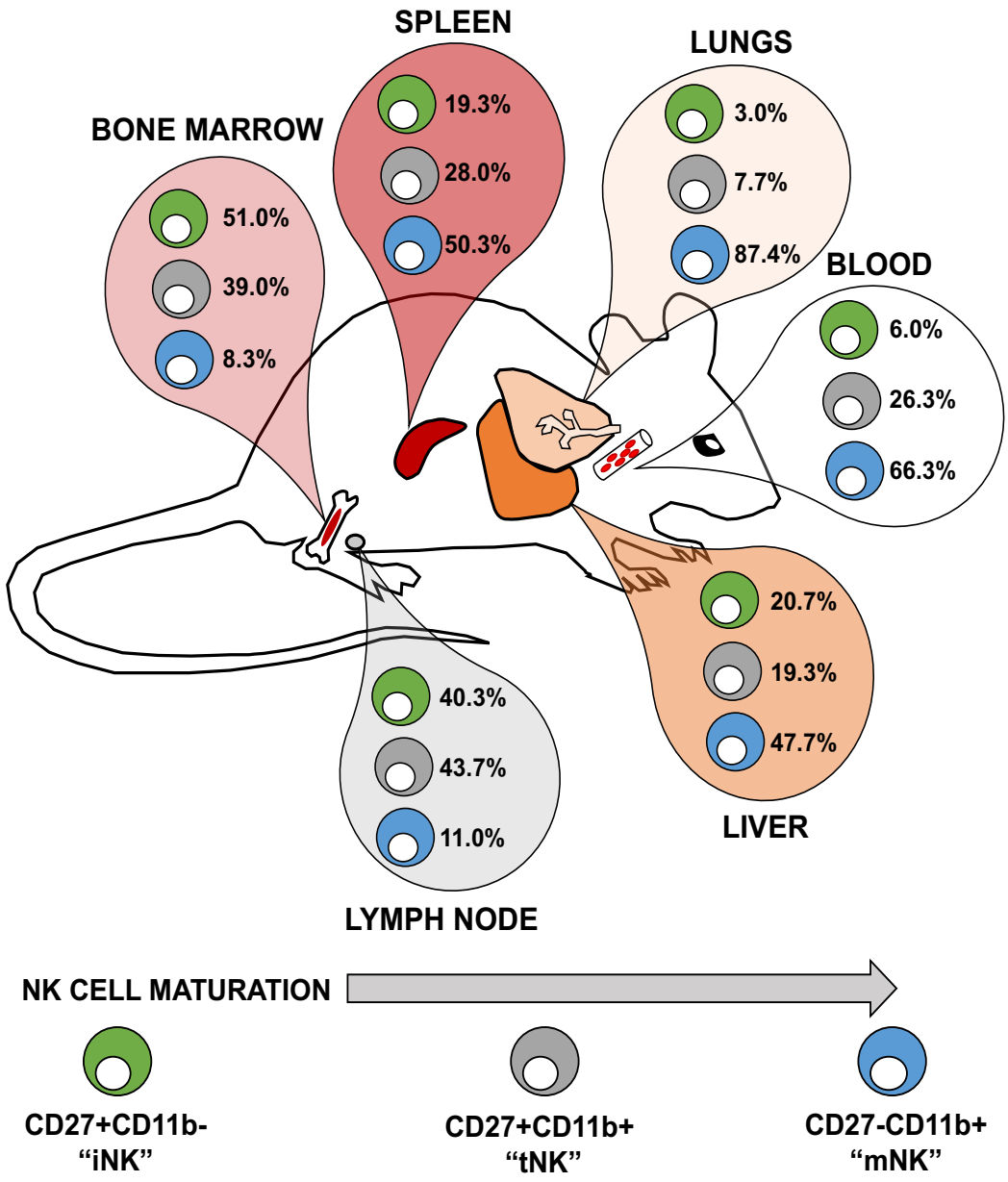

Figure 1-2: Tissue specific NK cell maturation in mice. The bone marrow shows predominant frequencies of immature NK cells (iNK), while the lymph nodes show equal parts of iNKs and transitional NK cells (tNKs). The spleen, lungs, blood, and liver show predominant frequencies of mature NK cells (mNKs). The mean frequencies (%) data for each NK cell maturation stage were adopted from Hayakawa et al. 2006 (13).

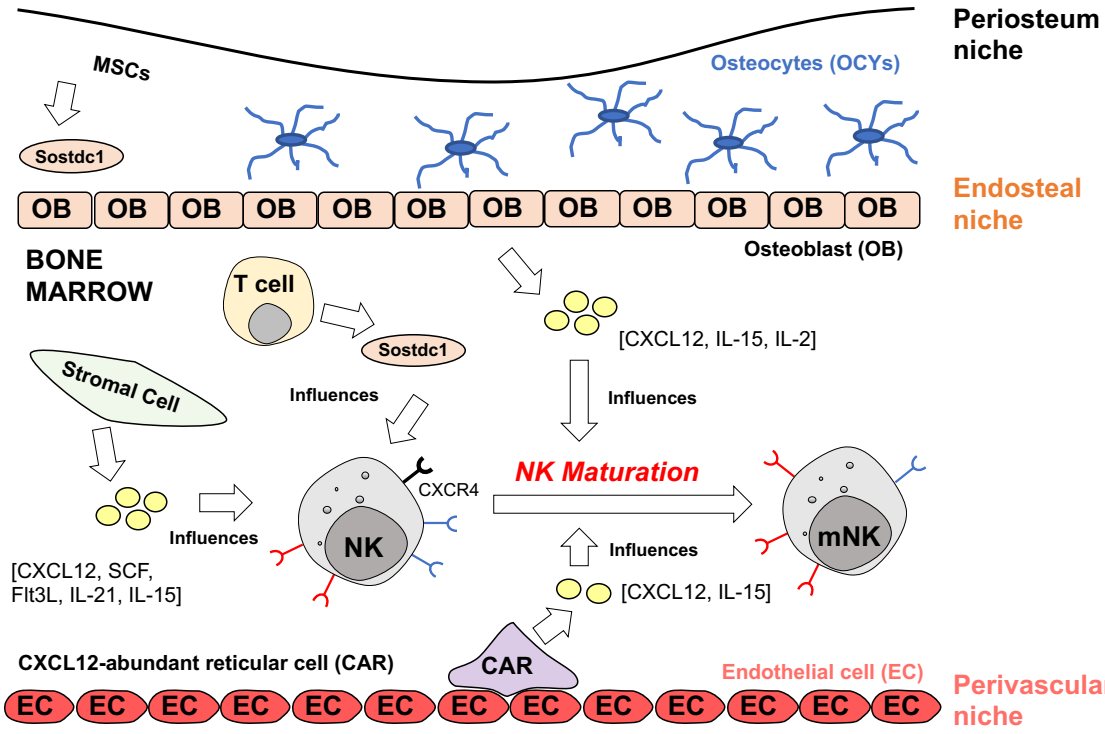

Figure 1-3: NK cell bone marrow niche. The periosteum primarily consists of osteocytes and mesenchymal stem cells (MSCs), and a source for the production of Sostdc1. The endosteal niche consists of osteoblast which can secrete known NK regulatory molecules such as, CXCL12, IL-15, and IL-2. In the bone marrow cavity, T cells produce Sostdc1, stromal cells can also secrete CXCL12, SCF, Flt3L, IL-21, and IL-15. The perivascular niche supports CXCL12-abundant reticular cell (CAR) which secrete CXCL12 and IL-15. Together, these bone marrow niches have been shown to influence NK cell behavior.

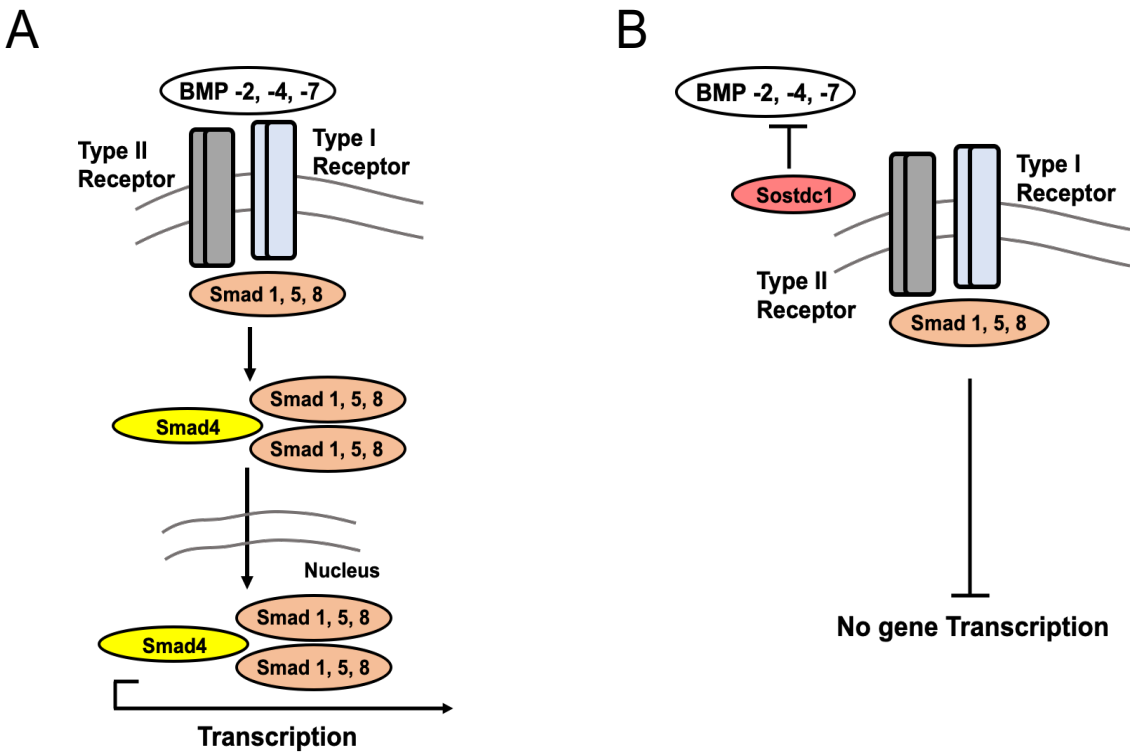

Figure 1-4: Sostdc1's role in Bone Morphogenetic Protein (BMP) signaling. (A) BMP signaling occurs when BMP-2, -4, -7 ligands bind the cell surface type II receptor and phosphorylates type I receptor. Phosphorylation of type I receptor activates intracellular R-Smad molecules (Smad-1, -5, -8). Smad4 forms a complex with two R-Smad molecules and translocate into the nucleus for gene transcription. (B) Sostdc1 has been shown to bind BMP-2, -4, -7 ligands and decreases BMP signaling.

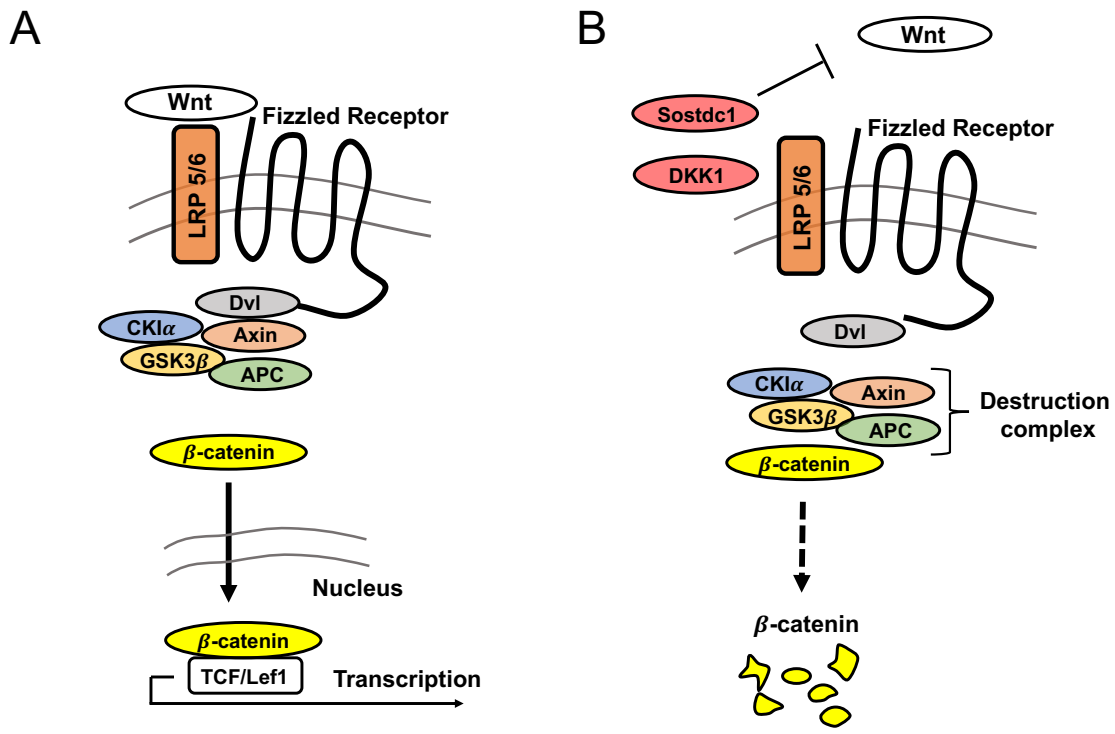

Figure 1-5: Sostdc1's role in canonical Wnt signaling. (A) The binding of Wnt ligand to the Frizzled receptor and the Wnt co-receptor Lrp5/6 will active the adaptor protein Disheveled (Dvl) and recruit the destruction complex (CKIα, Axin, GSK3β, APC) to the LRPs. The decreased proteasomal degradation of β-catenin leads to the accumulation and translocation of β-catenin into the nucleus. β-catenin forms a complex with TCF-1/LEF-1 for gene transcription. (B) Sostdc1 and DKK1 are known to bind LRP 5/6 and block Wnt ligand from binding the Frizzled receptor. The destruction complex then degrades intracellular β-catenin and reduces overall gene transcription.

CHAPTER 2

SOSTDC1 REGULATES NK CELL MATURATION AND CYTOTOXICITY

The Journal of Immunology

Sostdc1 Regulates NK Cell Maturation and Cytotoxicity

Alberto J. Millan, Sonny R. Elizaldi, Eric M. Lee, Jeffrey O. Aceves, Deepa Murugesh, Gabriela G. Loots and Jennifer O. Manilay

J Immunol 2019; 202:2296-2306; Prepublished online 27 February 2019;
doi: 10.4049/jimmunol.1801157
http://www.jimmunol.org/content/202/8/2296

Supplementary Material http://www.jimmunol.org/content/suppl/2019/02/26/jimmunol.1801157.DCSupplemental

References This article **cites 57 articles**, 16 of which you can access for free at:
http://www.jimmunol.org/content/202/8/2296.full#ref-list-1

The Journal of Immunology is published twice each month by
The American Association of Immunologists, Inc.,
1451 Rockville Pike, Suite 650, Rockville, MD 20852

Print ISSN: 0022-1767 Online ISSN: 1550-6606.

Sostdc1 Regulates NK Cell Maturation and Cytotoxicity

Alberto J. Millan,* Sonny R. Elizaldi,* Eric M. Lee,* Jeffrey O. Aceves,* Deepa Murugesh,* Gabriela G. Loots,*,† and Jennifer O. Manilay*

NK cells are innate-like lymphocytes that eliminate virally infected and cancerous cells, but the mechanisms that control NK cell development and cytotoxicity are incompletely understood. We identified roles for sclerostin domain–containing-1 (*Sostdc1*) in NK cell development and function. *Sostdc1*-knockout (*Sostdc1*$^{-/-}$) mice display a progressive accumulation of transitional NK cells (tNKs) (CD27^{+}CD11b^{+}) with age, indicating a partial developmental block. The NK cell Ly49 repertoire in *Sostdc1*$^{-/-}$ mice is also changed. Lower frequencies of *Sostdc1*$^{-/-}$ splenic tNKs express inhibitory Ly49G2 receptors, but higher frequencies express activating Ly49H and Ly49D receptors. However, the frequencies of Ly49I^{+}, G2^{+}, H^{+}, and D^{+} populations were universally decreased at the most mature (CD27^{-}CD11b^{+}) stage. We hypothesized that the Ly49 repertoire in *Sostdc1*$^{-/-}$ mice would correlate with NK killing ability and observed that *Sostdc1*$^{-/-}$ NK cells are hyporesponsive against MHC class I–deficient cell targets in vitro and in vivo, despite higher CD107a surface levels and similar IFN-γ expression to controls. Consistent with Sostdc1's known role in Wnt signaling regulation, *Tcf7* and *Lef1* levels were higher in *Sostdc1*$^{-/-}$ NK cells. Expression of the NK development gene *Id2* was decreased in *Sostdc1*$^{-/-}$ immature NK and tNK cells, but *Eomes* and *Tbx21* expression was unaffected. Reciprocal bone marrow transplant experiments showed that *Sostdc1* regulates NK cell maturation and expression of Ly49 receptors in a cell-extrinsic fashion from both nonhematopoietic and hematopoietic sources. Taken together, these data support a role for *Sostdc1* in the regulation of NK cell maturation and cytotoxicity, and identify potential NK cell niches. *The Journal of Immunology*, 2019, 202: 2296–2306.

Natural killer cells are innate lymphocytes that are important for early immune defense against tumors and virally infected cells. Since the initial discovery of NK cells in 1975, studies from many groups have identified NK cell receptors that are involved in self/nonself recognition, NK cell precursors and stages of maturation, cytokines and transcription factors that are critical for NK cell development and function, and evidence for NK cell immune memory (1–9). Despite over 40 years of NK cell history, the molecular and cellular mechanisms that drive and integrate these processes is still unclear. In particular, how the microenvironment regulates NK cell maturation and function is still an area of ongoing investigation.

Conventional NK cells develop in the bone marrow (BM) from hematopoietic stem cells following a well-established sequence of maturational stages, and egress to the peripheral organs to fully mature and function (10–12). NK cell maturation (Fig. 1A) originates with the immature NK (iNK) (CD27^{+}CD11b^{-}) cells, which progresses to the transitional NK (tNK) cell stage (CD27^{+}CD11b^{+}, also known as DP [13], and not to be confused with tissue resident NK cells [14]), then to the final mature NK (mNK) cell stage (CD27^{-}CD11b^{+}) (13, 15–17). As NK cells progress through these stages, they lose proliferative and cytokine-producing capability but gain cytotoxic ability against target cells (12, 18, 19). Although the BM microenvironment is critical for NK cell development, how the peripheral microenvironment regulates NK cell maturation and cytotoxicity is incompletely understood and requires further investigation.

Sclerostin domain–containing-1 (*Sostdc1*), also known as Wise, Ectodin, Usag-1, and Sost-like, has been studied in the context of tooth development, kidney disease, hair follicle formation, and bone fracture (20–26). Sostdc1 can function as an antagonist of both bone morphogenetic protein and canonical Wnt signaling pathways (21, 22, 24). Sostdc1 expression is highly expressed in skin, brain, and intestine as well as in skeletal muscles, kidney, lungs, and vasculature (21, 23, 24). Most recently, we found it also to be expressed in the bone periosteum and mesenchymal stem cells to support bone formation and fracture remodeling (27). In this study, we reveal *Sostdc1*'s cell-extrinsic roles in the regulation of NK cell maturation, Ly49 receptor expression, and cytotoxic function in the BM and spleen.

Materials and Methods

Mice

Sostdc1$^{-/-}$ mice have been described (23, 27) and were both bred and transferred from Lawrence Livermore National Laboratories (LLNL) to

*Department of Molecular Cell Biology, School of Natural Sciences, University of California, Merced, Merced, CA 95343; and †Physical and Life Sciences Directorate, Lawrence Livermore National Laboratories, Livermore, CA 94550

ORCIDs: 0000-0002-0958-2399 (E.M.L.); 0000-0002-1431-5295 (J.O.M.).

Received for publication August 23, 2018. Accepted for publication February 6, 2019.

This work was supported by University of California (UC) Merced faculty research funding, a UC Cancer Research Coordinating Committee grant, a Halcyon-Dixon Trust award (to J.O.M.), and UC graduate student fellowships (to A.J.M.). G.G.L. works under the auspices of the U.S. Department of Energy through the Lawrence Livermore National Laboratory under Contract DE-AC52-07NA27344.

G.G.L. and D.M. provided the *Sostdc1*$^{-/-}$ mice. Study design: A.J.M. and J.O.M. Study conduct: A.J.M., S.R.E., E.M.L., J.O.A., and J.O.M. Data collection: A.J.M., S.R.E., E.M.L., and J.O.A. Data analysis: A.J.M., S.R.E., E.M.L., J.O.A., and J.O.M. Data interpretation: A.J.M. and J.O.M. Drafting manuscript: A.J.M. and J.O.M. Revising manuscript content: A.J.M. and J.O.M. Approving final version of manuscript: J.O.M. J.O.M. takes responsibility for the integrity of the data analysis.

Address correspondence and reprint requests to Dr. Jennifer O. Manilay, University of California, Merced, School of Natural Sciences, 5200 North Lake Road, Merced, CA 95343. E-mail address: jmanilay@ucmerced.edu

The online version of this article contains supplemental material.

Abbreviations used in this article: BM, bone marrow; DC, dendritic cell; Eomes, Eomesodermin; FCM, flow cytometry; iNK, immature NK; KO, knockout; LLNL, Lawrence Livermore National Laboratories; $\beta_2m^{-/-}$, β-2 microglobulin knockout; $\beta_2m^{+/+}$, β-2 microglobulin sufficient; MHC-I, MHC class I; mNK, mature NK; poly(I:C), polyinosinic-polycytidylic acid; qPCR, quantitative PCR; *Sostdc1*, sclerostin domain–containing-1; Tbx21, T-box protein 21; tNK, transitional NK; UC, University of California; WT, wild-type.

www.jimmunol.org/cgi/doi/10.4049/jimmunol.1801157

University of California (UC) Merced to begin an independent breeding colony. C57B6/J (CD45.2$^+$/5.2$^+$) and B6.SJL-Ptprca Pepcb/BoyJ (CD45.1$^+$/5.1$^+$) and B6.129P2-B2mtm1Unc/J β-2 microglobulin knockout (KO) ($\beta_2m^{-/-}$) mice were obtained from The Jackson Laboratory. Mice of 28–38 wk of age and of both sexes were used. No differences between sexes nor mice from LLNL and UC Merced colonies have been observed. All mice were housed in conventional housing with autoclaved feed. Mice were euthanized by carbon dioxide asphyxiation followed by cervical dislocation. All animal procedures were approved by the UC Merced and LLNL Institutional Animal Care and Use Committees.

Flow cytometry

Isolation of spleen and BM cells were performed and stained for flow cytometry (FCM) as described (27). Abs against CD161 (also known as NK1.1, PK136), CD11b (M1/70), CD27 (LG.3A10), CD19 (6D5), CD3 (2C11), Gr1-Ly6C/G (Gr1), Ly49G2 (4D11), Ly49I (YL1-90), Ly49H (3D10), Ly49D (eBio4E5), CD45.2 (104), CD45.1 (A20), CD45 (30-F11), CD4 (GK1.5), CD8 (2.43), Ter119 (TER119), CD107a (1D4B), rat IgG2a κ isotype control (RTK2758), IFN-γ (XMG1.2), rat IgG1 κ isotype control (RTK2071), GM-CSF (MP1-22E9), granzyme B (GB11), perforin (eBioOMAK-D) IL-12/IL-23 p40 (C15.6), TNF-α (TN3-19.12), and BUV395 streptavidin, eFluor 780 fixable viability dye, eFluor 506 fixable viability dye were purchased from eBioscience, BioLegend, Miltenyi Biotec, and BD Biosciences. Staining of all cells included a preincubation step with unconjugated anti-CD16/32 (clone 2.4G2 or clone 93) mAb to prevent nonspecific binding of mAbs to FcγR. For extracellular staining, the cells were washed and incubated with a panel of mAbs for 15–20 min at 4°C or on ice and then washed again. Intracellular staining was performed using the BD Cytofix/Cytoperm Fixation/Permeabilization Kit (BD Biosciences) per the manufacturer's instructions. To purify NK cells and NK cell subsets, enrichment of NK cells was first achieved by staining with biotinylated anti-"lineage" mixture (anti-CD3, -CD4, -CD8, -CD19, -Gr1, and -Ter119) followed by magnetic separation using EasySep Positive Selection Kit (STEMCELL Technologies), After enrichment, cells were stained with streptavidin-FITC, anti-CD27, and additional anti-CD3, -CD19, -Gr1, -CD45, -NK1.1, and -CD11b. Lineage-negative CD45$^+$ NK1.1$^+$ iNKs, tNKs, and mNKs were sorted on the FACSAria II (Becton Dickinson). Single-color stains were used for setting compensations, and gates were determined by historical data in addition to fluorescent-minus-one control stains. Flow cytometric data were acquired on the BD LSR II or FACSAria II cell sorter (Becton Dickinson). The data were analyzed using FlowJo version 7.6 or 10 (Tree Star).

In vivo NK cell killing assay

Sostdc1$^{-/-}$ and B6 control mice received 200 μg of polyinosinic-polycytidylic acid (poly[I:C]) (Sigma-Aldrich) via injection into the i.p. cavity. Thirty-six hours later, splenic cells from age- and sex-matched $\beta_2m^{-/-}$ and β-2 microglobulin sufficient ($\beta_2m^{+/+}$) (wild-type [WT] or *Sostdc1*$^{-/-}$) mice were harvested and processed to a single-cell suspension in media (medium 199, 2% FCS, 2mM L-glutamine, 100 U/ml penicillin, 100 μg/ml streptomycin, 25 mM HEPES) and counted using a hemocytometer. $\beta_2m^{+/+}$ (WT or *Sostdc1*$^{-/-}$) and $\beta_2m^{-/-}$ control target cells were stained with anti-CD45 conjugated to either allophycocyanin or PE in media for 20 min on ice. A total of 5×10^6 $\beta_2m^{-/-}$ stained splenic cells were mixed with 5×10^6 $\beta_2m^{+/+}$ stained control cells at a 50:50 ratio, thus providing a method to track each target cell type by FCM. Stained cell target cell mixtures were injected i.v. by retro-orbital injection. Fourteen hours later, spleens from *Sostdc1*$^{-/-}$ and WT recipients were then harvested and processed for FCM. NK cell lysis of targets was determined by FCM and calculated by the ratio of live $\beta_2m^{+/+}$ (WT), $\beta_2m^{+/+}$ (*Sostdc1*$^{-/-}$), and $\beta_2m^{-/-}$ targets over WT control cells in the same mouse.

In vitro NK cell killing assay

NK cells were enriched by magnetic bead sorting as described above. NK cell stimulation with IL-2 and feeder cells was performed as described (9). On day 4, spleen cells from $\beta_2m^{+/+}$ (WT) and $\beta_2m^{-/-}$ mice were harvested and labeled with anti-CD45 allophycocyanin and used as targets in separate wells. NK cells and targets were cocultured at specific E:T ratios with a minimum of 1×10^5 NK cells and 1×10^5 targets per culture well. NK cell lysis of targets was determined by FCM and quantified using the ratio of live $\beta_2m^{-/-}$ CD45-allophycocyanin–positive targets to WT control CD45-allophycocyanin–positive cells in the cocultures.

NK cell stimulation assay

Splenic cells from *Sostdc1*$^{-/-}$ and B6 mice were isolated, and 2×10^6 cells were transferred to a flat-bottom plate in the presence of anti-CD107a or isotype control mAb. Cells were stimulated with PMA and ionomycin at a final concentration of 100 ng/ml and 1000 ng/ml and incubated at 37°C and 5% CO_2 conditions for 4 h (28). Protein transport inhibitors brefeldin A (BioLegend) and monensin (BioLegend) were added 1 h poststimulation at a final concentration of 1×. Cells were washed and cell surface stained for CD27, CD3, CD19, Gr1, NK1.1, CD11b, fixable viability dye, and Fc block. Cells were then fixed and stained intracellularly with anti–IFN-γ or isotype mAb control using the BD Cytofix/Cytoperm Kit (BD Biosciences) according to the manufacturer's suggested protocol. Cells were analyzed using FCM on the LSR II (Becton Dickinson).

NK cell proinflammatory cytokine assay

Age- and sex-matched Sostdc1$^{-/-}$ and B6 control mice received 200 μg of poly(I:C) (Sigma-Aldrich) via injection into the i.p. cavity. Sixteen hours later, splenic cells were harvested, processed to a single-cell suspension in RPMI1640 media supplemented with 10% FBS 3, 0.09 mM nonessential amino acids, 2 mM L-glutamine, 1 mM sodium pyruvate, 100 U/ml penicillin, 100 μg of streptomycin, 0.025 mM BME, and 0.01 M HEPES buffer, and RBCs were lysed with ammonium-chloride-potassium buffer. A total of 5×10^6 splenic cells were additionally stimulated in 96-well flat-bottom plates with 100 ng/ml of PMA and 1000 ng/ml of ionomycin and incubated at 37°C and 5% CO_2 conditions for 5 h. Brefeldin A (BioLegend) was added 1 h poststimulation at a final concentration of 1×. Cells were washed and stained with Abs against CD3, CD19, Gr1, NK1.1, fixable viability dye, and Fc block. Cells were then fixed and stained intracellularly with anti–GM-CSF, –TNF-α, –IFN-γ, –granzyme B, -perforin, or –isotype mAb control according to the BD Cytofix/Cytoperm Kit (BD Biosciences) manufacturer's suggested protocol.

IL-12 cytokine expression assay

Five million splenic cells from Sostdc1$^{-/-}$ and B6 control mice were stimulated in 96-well flat-bottom plates with 100 ng/ml LPS (Sigma-Aldrich) and incubated at 37°C with 5% CO_2 for 3 h with brefeldin A (BioLegend) at a final concentration of 1×. Cells were washed and stained with Abs specific for CD8α, CD11c, CD45, fixable viability dye, and Fc block. Cells were then fixed and stained intracellularly with anti–IL-12 or isotype mAb control according to the BD Cytofix/Cytoperm Kit (BD Biosciences) manufacturer's suggested protocol.

Gene expression analysis by quantitative PCR

Cells were pelleted and resuspended in RNeasy Lysis Buffer with 2-ME (Qiagen). Total RNA was purified using Qiagen RNeasy Mini Kit (Qiagen) according to manufacturer's protocol. RNA concentration and purity was analyzed using a NanoDrop ND-1000 Spectrophotometer (Thermo Fisher Scientific). iScript cDNA Synthesis Kit was used (Bio-Rad Laboratories) according to the manufacturer's protocol. Real-time quantitative PCR (qPCR) performed using the iTaq Universal SYBR Green Supermix kit (Bio-Rad Laboratories) and ran on a Stratagene Mx3000P thermocycler (Thermo Fisher Scientific) using the following conditions: 1 cycle at 9°C for 30 s, followed by 40 cycles of 95°C for 5 s and 60°C for 30 s, and a final cycle at 95°C for 1 min, 55°C for 30 s, and 95°C for 30 s to end the run. The PCR products were visualized on a 2% agarose gel and imaged under UV light using a ChemiDoc (Bio-Rad Laboratories) with SYBR Safe (Invitrogen) stain. The genes and primer sequences used are as follows: β-galactosidase: forward 5′-ACGGCCAGGACAGTCGTTTG-3′, reverse 5′-CCGCTCATCCGCCACATATC-3′; Sostdc1: forward 5′-CACCCTGAATCAAGCCAGGA-3′, reverse 5′-TAGCCTCCTCCGATCCAGTT-3′; Axin2: forward 5′-ACGCACTGACCGACGATTC-3′, reverse 5′-CCATGCGGTAAGGAGGGAC-3′; Myc: forward 5′-GCTGTTTGAAGGCTGGATTTC-3′, reverse 5′-GA TGAAATAGGGCTGTACGGAG-3′; Tcf7: forward 5′-AAGGTCATTGCTGAGTGCACAC-3′, reverse 5′-TGCATGCCACCTGCGAC-3′; Lef1: forward 5′-AAGGCGATCCCCAGAAG GAG-3′, reverse 5′-AGGGTGTTCTCTGGCCTTGT-3′; Eomesodermin (Eomes): forward 5′-TCCTAACACTGGCTCCCACT-3′, reverse 5′-GTCACTTCCACGATGTGCAG-3′; Id2: forward 5′-GTCC TTGCAGGCATCTGAAT-3′, reverse 5′-TTCAACGTGTTCTCCTGGTG-3′; Tbx12: forward 5′-CAACCAGCACCAGACAGAGA-3′, reverse 5′-ACAAACATCCTGTAATGGCTTG-3′; and GAPDH: forward 5′-TCACCACCATGGAGAAGGC-3′, reverse 5′-GCTAAGCAGTTGGTGGTGCA-3′.

BM chimeras

Whole BM cells were aseptically isolated from B6 (CD45.1 or CD45.2), WT, or *Sostdc1*$^{-/-}$ (CD45.2) mice, and 5×10^6 cells were transferred via retro-orbital injection into lethally (10 Gy) irradiated recipients 4 h after irradiation using a cesium irradiator. Mice were given neomycin-containing drinking water for 2 wk posttransfer. Chimeras were analyzed 14 wk posttransplant.

Statistical analysis

Student *t* test with a two-tailed distribution and with two-sample equal variance (homoscedastic test) was used to determine differences in means between groups using GraphPad Prism software. A p value < 0.05 was considered to be statistically significant.

Results

Sostdc1$^{-/-}$ mice display a partial block at the tNK stage

Our previous studies demonstrated that femurs of *Sostdc1$^{-/-}$* mice display a 21% increase in BM cavity volume compared with WT controls (27). Consistent with this, the total BM cellularity of *Sostdc1$^{-/-}$* bones was increased (Fig. 1B). *Sostdc1$^{-/-}$* mice also displayed higher total splenic cell numbers (Fig. 1C). The increased cellularity suggested that the *Sostdc1$^{-/-}$* BM and spleen microenvironments may be altered and that immune cell development may also be affected by the loss of *Sostdc1*. To test this, we performed FCM and observed no differences in frequencies or absolute numbers of CD19$^+$ B lymphocytes, CD3$^+$ T lymphocytes, and CD11b$^+$ Gr1$^+$ granulocytes (data not shown). However, the frequency of CD11b$^+$ Gr1$^-$ cells in the *Sostdc1$^{-/-}$* spleen was reduced. To determine if the CD11b$^+$ Gr1$^-$ cells were monocytes or NK cells, we performed more detailed analysis with anti-NK1.1. Total NK (live, CD3$^-$, CD19$^-$, Gr1$^-$, NK1.1$^+$) frequencies were not affected, but total NK cell numbers were increased only in the BM of *Sostdc1$^{-/-}$* mice (Fig. 1D–G). We then investigated if lack of *Sostdc1* affected NK cell maturation (Fig. 1A) and discovered that *Sostdc1$^{-/-}$* mice exhibit a partial block between the tNK (NK1.1$^+$ CD11b$^+$ CD27$^+$) and mNK (NK1.1$^+$ CD11b$^+$ CD27$^-$) cell stages in both the BM and spleen, as demonstrated by the increase in frequency and number of tNK cells in the BM (Fig. 1H, 1I) and spleen (Fig. 1J, 1K) and the decreased frequency of mNKs in the spleen. These data indicated that *Sostdc1* is required for full developmental progression from the tNK to the mNK cell stages.

Absence of Sostdc1 alters the Ly49 receptor repertoire on NK cells

We also examined if NK cells in *Sostdc1$^{-/-}$* mice expressed different levels and distributions of inhibitory (Ly49I and Ly49G2) and activating (Ly49D and Ly49H) Ly49 receptors. FCM analysis of the Ly49 repertoire on iNKs, tNKs, and mNKs in *Sostdc1$^{-/-}$* mice revealed decreased frequencies of Ly49G2$^+$ cells at all NK cell stages in the BM (Supplemental Fig. 1A–C) and spleen (Fig. 1L–N). In contrast, frequencies of Ly49H$^+$ iNK and tNK cells in the *Sostdc1$^{-/-}$* BM and spleen were higher than controls, but the frequencies of Ly49H$^+$ mNK cells were reduced in both tissues (although only statistically significant in the spleen). Similarly, frequencies of Ly49D$^+$ in iNK and tNK cells were increased and reduced among the mNKs in the *Sostdc1$^{-/-}$* BM and spleen (Fig. 1L–N, Supplemental Fig. 1A–C). The frequencies of Ly49I$^+$ in iNK and tNK cells were similar to controls, but frequencies of Ly49I$^+$ mNK cells were decreased in *Sostdc1$^{-/-}$* mice (Fig. 1N, Supplemental Fig. 1C). The median fluorescent intensity of staining for Ly49G2 and Ly49H was reduced on *Sostdc1$^{-/-}$* BM mNK cells only, indicating a relatively minor effect of Sostdc1 on cell surface Ly49 receptor expression levels (Supplemental Fig. 1D–K).

Because it is theorized that NK cell activity is governed by the combined set of Ly49 receptors expressed on a given NK cell, we further compared the frequencies of WT and *Sostdc1$^{-/-}$* NK cells that express different combinations of Ly49 receptors (29) (Supplemental Fig. 2). Higher frequencies of iNK and tNK cells expressing more activating than inhibitory receptors (i.e., "activating repertoires") were observed in *Sostdc1$^{-/-}$* mice (Supplemental Fig. 2D, 2E). However, lower frequencies of mNK cells with activating repertoires were observed (Supplemental Fig. 2F). Taken together, these data show the lack of *Sostdc1* influences the Ly49 receptor repertoire.

NK cells in Sostdc1$^{-/-}$ mice are impaired in their ability to kill β_2m-deficient targets

The reduced frequency of splenic mNK with activating repertoires suggested that NK cell cytotoxicity in *Sostdc1$^{-/-}$* mice would be impaired. To determine if the alterations in NK Ly49 repertoire correlated with NK cell killing ability, we analyzed *Sostdc1$^{-/-}$* NK cell cytotoxicity with FCM-based in vivo and in vitro killing assays (Fig. 2, Supplemental Fig. 3A–E). $\beta_2m^{-/-}$ cells express little to no cell surface MHC class I (MHC-I) molecules and therefore are sensitive targets for NK cell killing (30). To test NK cell killing in vivo, we preactivated NK cells in *Sostdc1$^{-/-}$* and WT control mice with poly(I:C) (31) (Fig. 2A) and challenged them with equal numbers of $\beta_2m^{-/-}$ and β-2 microglobulin-sufficient ($\beta_2m^{+/+}$) target cells, each labeled with two different fluorochromes (Fig. 2B). $\beta_2m^{+/+}$ target cells from WT and *Sostdc1$^{-/-}$* mice were both included as negative "self" controls (Fig. 2C–E and data not shown). After 14 h of target cell challenge, we quantified the remaining $\beta_2m^{-/-}$, WT ($\beta_2m^{+/+}$), and *Sostdc1$^{-/-}$* ($\beta_2m^{+/+}$) targets by FCM to determine the frequency of live cells in each target population (Fig. 2A, 2C, 2D) and calculated the ratio of WT ($\beta_2m^{+/+}$), *Sostdc1$^{-/-}$* ($\beta_2m^{+/+}$), and $\beta_2m^{-/-}$ targets in each setting (Fig. 2E). An increased proportion of $\beta_2m^{-/-}$ targets remained in the *Sostdc1$^{-/-}$* mice compared with WT controls (Fig. 2E). We confirmed that there was no effect on fluorophore labeling on $\beta_2m^{-/-}$ cell target killing with reciprocal labeling of targets of opposite fluorophore (Fig. 2C, 2D).

This result was confirmed using an in vitro NK cell killing assay (Supplemental Fig. 3) using enriched NK cells from *Sostdc1$^{-/-}$* and WT mice (32) challenged with fluorescently labeled $\beta_2m^{-/-}$ or $\beta_2m^{+/+}$ targets for 4 h in E:T ratios of 1:1, 2:1, and 4:1 (Supplemental Fig. 3A–C). As expected, WT NK and *Sostdc1$^{-/-}$* NK cells did not lyse $\beta_2m^{+/+}$ targets at any E:T ratio (Supplemental Fig. 3D). However, as shown in Supplemental Fig. 3E, *Sostdc1$^{-/-}$* NK cells have reduced capacity to lyse $\beta_2m^{-/-}$ targets, even at the highest 4:1 E:T ratio, indicating their hyporesponsiveness to $\beta_2m^{-/-}$ targets. FCM analysis of *Sostdc1$^{-/-}$* NK cells to measure the cytokine IFN-γ after stimulation revealed comparable levels to WT controls (Supplemental Fig. 3F, 3G). Surprisingly, activated *Sostdc1$^{-/-}$* NK cells at all developmental stages expressed significantly increased levels of the degranulation marker CD107a (Supplemental Fig. 3H, 3I). Furthermore, the impaired killing ability of NK cells in *Sostdc1$^{-/-}$* mice is independent of the expression of NK cell proinflammatory and cytotoxic cytokines GM-CSF, TNF-α, and IFN-γ as well as granzyme B and perforin expression, as we confirmed their levels are similar between *Sostdc1$^{-/-}$* and WT NK cells (Fig. 2F–H). We further investigated if *Sostdc1$^{-/-}$* mice display decreased IL-12 expression in the spleen (33–35) and found no significant difference in expression between WT and *Sostdc1$^{-/-}$* IL-12–producing CD8-CD11c$^{(hi)}$ and CD8$^+$CD11c$^+$ dendritic cells (DCs) (Supplemental Fig. 3J, 3K). Taken together, these results suggest that *Sostdc1$^{-/-}$* NK cell cytotoxicity is impaired despite their ability to produce comparable levels of IFN-γ, similar levels of inflammatory cytokine production, and evidence of elevated accumulation of cytotoxic granules at the cell surface and similar levels of IL-12 production in the microenvironment.

Sostdc1-KO NK cell subsets upregulate Wnt genes Tcf7 and Lef1

Given that Sostdc1 is a known antagonist to canonical Wnt signaling, we hypothesized that expression of canonical Wnt pathway transcription factors would be increased in *Sostdc1$^{-/-}$* NK cell

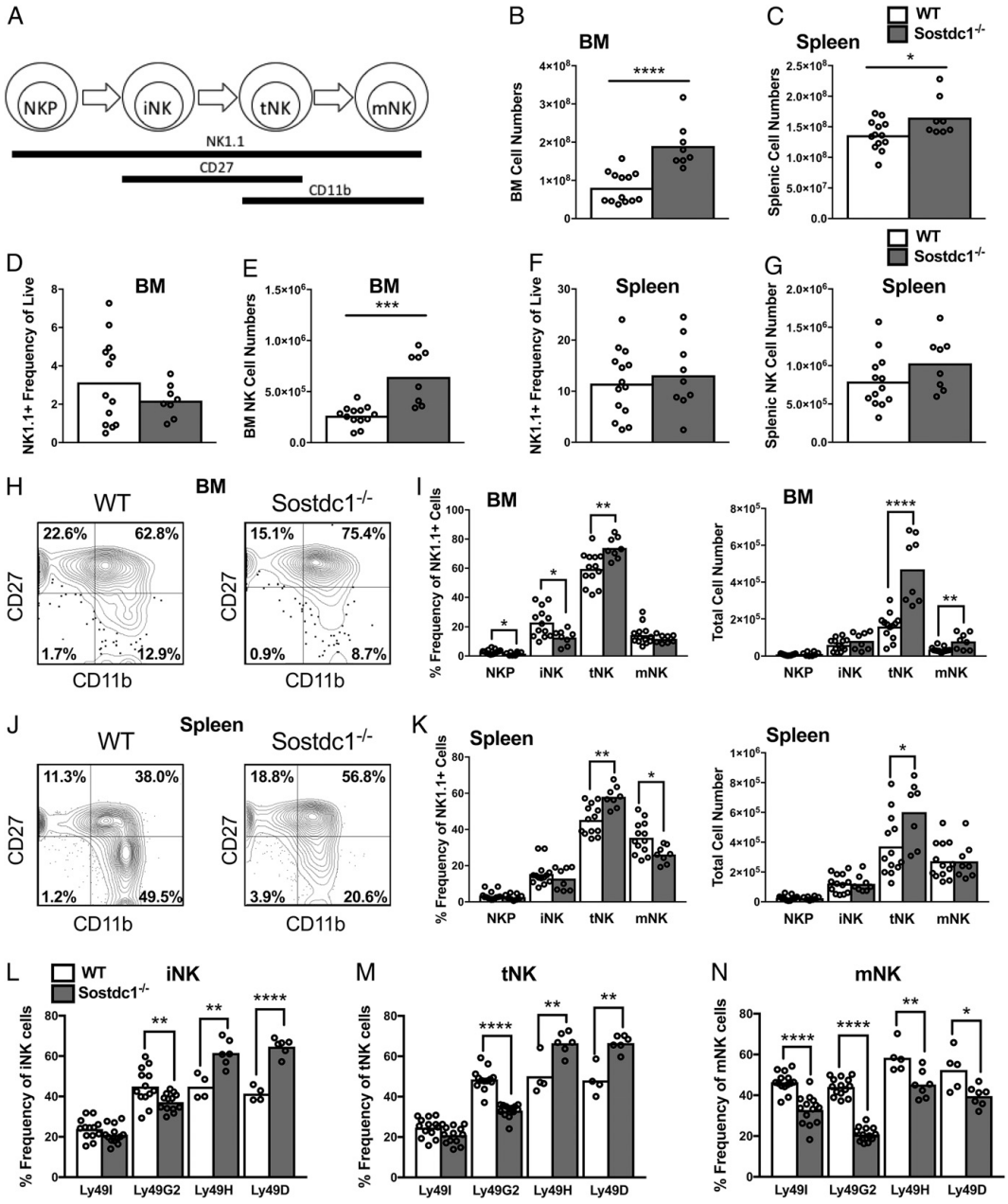

FIGURE 1. Delayed NK cell development and altered Ly49 repertoire in *Sostdc1*$^{-/-}$ mice. (**A**) Schematic diagram of NK cell development. (**B**) Total cellularity of BM in the femurs and tibiae and (**C**) spleen of WT and *Sostdc1*$^{-/-}$ (KO) mice; (**D** and **F**) frequencies; and (**E** and **G**) absolute numbers of NK1.1^{+} cells in BM and spleen; (**H**) Representative FCM plots showing NK cell stages in BM; (**I**) Summary of frequencies and absolute numbers of NKP, iNK, tNK, and mNK cells in BM; (**J**) Representative FCM plots showing NK cell stages in spleen; (**K**) Summary of frequencies and absolute numbers of NKP, iNK, tNK, and mNK cells in spleen; (**L**–**N**) distribution of splenic NK cells expressing Ly49I, Ly49G2, Ly49H, and Ly49D on iNK, tNK, and mNK cells. Asterisks indicate statistically significant differences between means as determined by Student *t* test. Each point represents a single mouse. $*p < 0.05$, $**p < 0.01$, $****p < 0.0001$. NKP, NK progenitor (CD27^{-}CD11b^{-}).

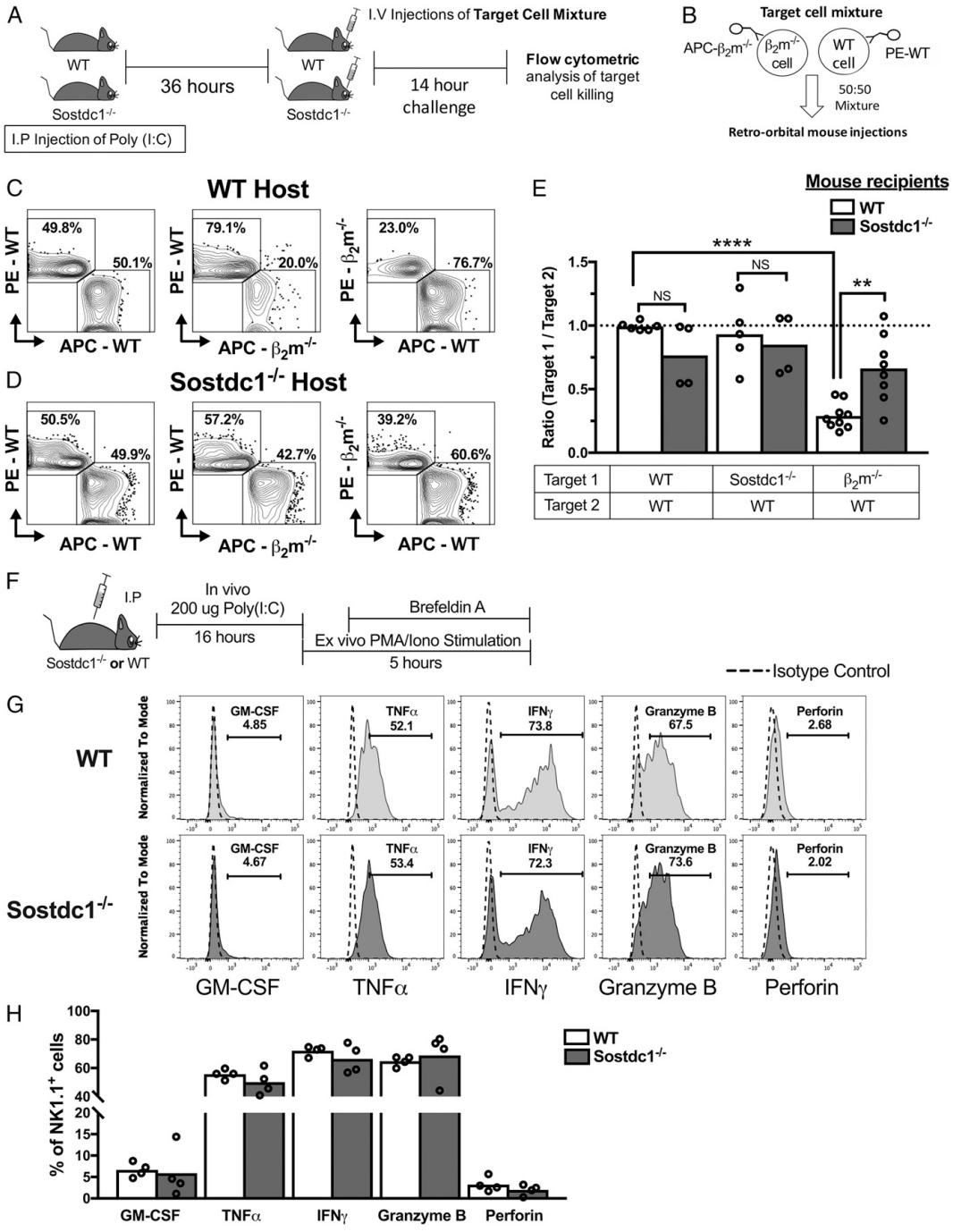

FIGURE 2. *Sostdc1* deficiency results in impaired NK cell killing, independent of NK inflammatory and cytotoxic cytokines. (**A**) Scheme of in vivo NK cell killing assay. (**B**) Cartoon depicting how WT and $\beta_2m^{-/-}$ target cells were labeled for detection by FCM. (**C** and **D**) Representative FCM plots showing distinct populations of live WT and $\beta_2m^{-/-}$ target in poly(I:C)–treated WT and *Sostdc1*$^{-/-}$ mice. The left column shows representative FCM plots enumerating the frequencies of WT targets in WT and *Sostdc1*$^{-/-}$ mice. The middle and right column show representative FCM plots enumerating the frequencies of reciprocally labeled $\beta_2m^{-/-}$ and WT targets. (**E**) Ratio of targets to show their distribution after 14 h in vivo *(Figure legend continues)*

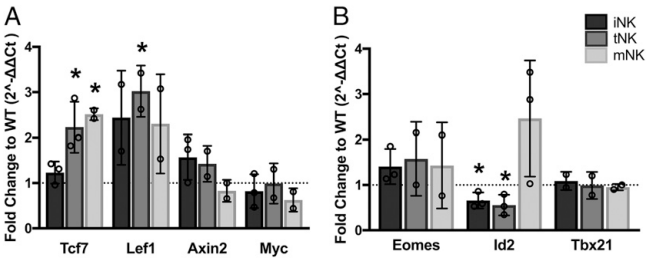

FIGURE 3. Expression of Wnt pathway and NK cell development genes in *Sostdc1*$^{-/-}$ NK cell subsets. (**A**) Gene expression of Wnt pathway genes *Tcf7*, *Lef1*, *Axin2*, and *Myc* by qPCR; (**B**) Gene expression of NK cell development genes *Eomes*, *Id2*, and *Tbx21*. Data in (A) and (B) are shown relative to WT controls. *$p < 0.05$, Student *t* test.

subsets. We purified iNK, tNK, and mNK cells by FCM and analyzed expression of Wnt pathway genes *Tcf7* (3, 36), *Lef1* (37), *Axin2* (38), and *Myc* (39) by real-time qPCR. Our results showed that relative to WT subsets, *Sostdc1*$^{-/-}$ splenic tNK and mNK cells express significantly higher levels of *Tcf7*, and tNK cells also show significantly increased expression of *Lef1* (Fig. 3A), consistent with our hypothesis. We did not observe any remarkable difference in *Axin2* and *Myc* expression in any *Sostdc1*$^{-/-}$ NK cell subset (Fig. 3A). Together, these results support a role for Wnt signaling by *Tcf7* and *Lef1* in NK cells of *Sostdc1*$^{-/-}$ mice.

We also analyzed expression of transcription factors that govern NK cell maturation. T-box family members Eomes and T-box protein 21 (Tbx21) have been shown to play a crucial role in early iNK and mNK cell maturation (40, 41). Additionally, Eomes-deficient NK cells have reduced Ly49A, Ly49D, Ly49G2, and Ly49H frequencies (40). Inhibitor of DNA-binding 2 (Id2) is an early transcription factorinvolved in NK and innate lymphoid cell lineage commitment (41–43). *Id2*-deficient mice have fewer mNK cells and impaired cell killing in vitro (44). Because *Sostdc1*$^{-/-}$ mice display a partial maturation block at the tNK cell stage and altered Ly49 receptor frequencies (Fig. 1), we hypothesized that we would observe decreased expression of *Eomes, Tbx21*, and *Id2* at distinct NK cell stages (40–47). We found *Id2* expression was decreased in iNK and tNK cells in *Sostdc1*$^{-/-}$ mice (Fig. 3B). These results suggest a strong regulation of *Id2* by *Sostdc1* at early NK cell stages, whereas *Eomes* and *Tbx21* are not regulated by *Sostdc1*.

Sostdc1 in nonhematopoietic stromal cells regulate the maturation of NK cells

To determine if and how *Sostdc1* within specific microenvironmental cell types contributes to the partial block in NK cell maturation and changes in Ly49 repertoires, we performed whole BM transplantation experiments. To investigate if *Sostdc1* in nonhematopoietic cells influenced NK cell development, we first transplanted whole BM cells from WT (CD45.1$^+$/5.1$^+$) donors into lethally irradiated *Sostdc1*$^{-/-}$(CD45.2$^+$/5.2$^+$) recipients to create WT→KO chimeras. WT(CD45.1$^+$/5.1$^+$)→WT(CD45.2$^+$/5.2$^+$) control chimeras were also prepared (Fig. 4A). Fourteen weeks post–BM transplantation, we analyzed donor-derived NK cell subsets and Ly49 receptor frequencies by FCM. Splenic NK cell numbers were increased (Fig. 4B), and WT→KO chimeras displayed a partial block between tNK and mNK cell stages in the spleen (Fig. 4C–E) and BM (Supplemental Fig. 4C–E), similar to the phenotype that was observed in the nontransplanted *Sostdc1*$^{-/-}$ mice (Fig. 1H–K). Ly49H$^+$ mNK cells were decreased in WT→KO, similar to nontransplanted *Sostdc1*$^{-/-}$ mice in the spleen (Figs. 1N, 4F). In contrast, WT→KO chimeras contained decreased frequencies of splenic Ly49H$^+$ iNK and tNK cells compared with WT→WT controls, a result that was the opposite of the increased frequencies of Ly49H$^+$ cells within these NK subsets of nontransplanted *Sostdc1*$^{-/-}$ mice (Figs. 1L, 1M, 4F). In addition, no differences in Ly49G2 and Ly49D subsets were observed between the WT→KO and control chimeras, a result that also differed from the nontransplanted *Sostdc1*$^{-/-}$ mice in the spleen (Figs. 1L–N, 4F) and BM (Supplemental Fig. 4F). Taken together, these results suggested that *Sostdc1* in nonhematopoietic cells controls progression from tNK to mNK stages and NK cellularity, but plays a smaller role in shaping the Ly49 receptor repertoire.

Sostdc1 in a hematopoietic cell lineage other than NK cells regulates the Ly49 receptor repertoire

We next prepared reciprocal KO→WT chimeras (whole BM cells from *Sostdc1*$^{-/-}$ (CD45.2$^+$/5.2$^+$) donors transplanted into lethally irradiated WT (CD45.1$^+$/5.1$^+$) recipient mice to determine how *Sostdc1*$^{-/-}$ NK cells mature and if their Ly49 receptor frequency was changed in a *Sostdc1*-sufficient microenvironment (Fig. 5A). Remarkably, splenic NK cell numbers (Fig. 5B) and maturation (Fig. 5C–E) were not affected in KO→WT chimeras, in contrast to the nontransplanted *Sostdc1*$^{-/-}$ mice and the WT→KO chimeras (Figs. 1H, 1I, 4B–E, respectively). However, the BM analysis showed an increase in NK cell numbers (Supplemental Fig. 4H) and a similar tNK cell accumulation as observed in the nontransplanted *Sostdc1*$^{-/-}$ mice (Fig. 1H–K, Supplemental Fig. 4K). Furthermore, analysis of donor-derived Ly49-expressing NK cell subsets in the spleens in KO→WT chimeras demonstrated some similar patterns as nontransplanted *Sostdc1*$^{-/-}$ mice, such as the increase in frequencies of Ly49H$^+$ and Ly49D$^+$ tNK cells and a decrease in the frequencies of Ly49G2$^+$ iNK cells and decreased frequencies of Ly49G2$^+$ and Ly49I$^+$ mNK cells (Figs. 1L–N, 5F). However, higher frequencies of mNK cells expressing Ly49H and Ly49D were observed in the KO→WT spleens, whereas these populations were decreased in nontransplanted *Sostdc1*$^{-/-}$ mice (Figs. 1L–N, 5F).

The Ly49 frequency patterns observed in the KO→WT chimeras strongly suggested that *Sostdc1* in NK cells regulated the Ly49 repertoire in a cell-intrinsic fashion. To confirm this, we examined *Sostdc1* expression in sorted WT iNK, tNK, and mNK

(target 1 and target 2 identified in table below the graph). (**F**) Experimental scheme of Sostdc1$^{-/-}$ or WT mice stimulated in vivo with 200 μg of poly(I:C) for 16 h; splenic cells were stimulated ex vivo with PMA and ionomycin for 5 h with the addition of brefeldin A for the last 4 h. (**G**) Representative histograms normalized to mode for WT (top row) and KO (bottom row) NK cells expressing GM-CSF, TNF-α, IFN-γ, granzyme B, and perforin. (**H**) Quantification of cytokine expression frequencies of NK1.1$^+$ cells. Quantification of specific staining were determined by subtracting nonspecific background signal from specific Ab signal. Each point represents an independent biological replicate. **$p < 0.01$, ****$p < 0.0001$, Student *t* test.

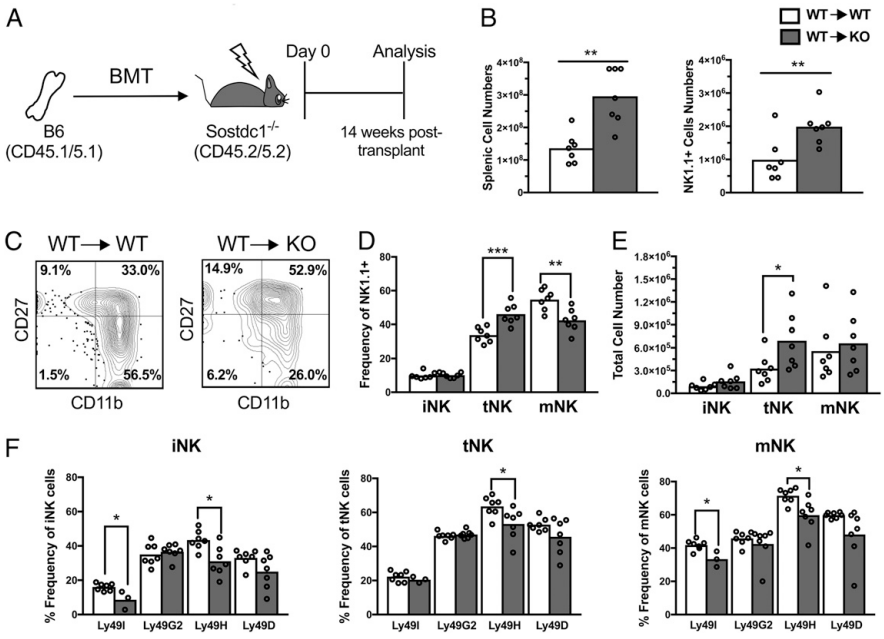

FIGURE 4. Nonhematopoietic stromal cells regulate the maturation of NK cells. (**A**) Experimental scheme to create WT→*Sostdc1*$^{-/-}$ (WT→KO) BM chimeras. (**B**) Total spleen cellularity (left) and total splenic NK cell numbers in chimeras (right); (**C**) representative FCM plots of NK cell maturation in donor (CD45.1$^+$)-derived NK cells in WT→WT and WT→KO chimeras; (**D**) quantification of donor-derived NK cell subset frequencies and (**E**) NK subset cellularity; (**F**) analysis of Ly49 repertoire on donor-derived iNK (left), tNK (center), and mNK (right) cells in WT→WT and WT→KO chimeras. $*p < 0.05$, $**p < 0.01$, $***p < 0.001$, Student *t* test.

cells by qPCR. Surprisingly, iNK, tNK, and mNK cells do not express *Sostdc1* (Fig. 5G). To determine alternative possible hematopoietic sources of *Sostdc1*, we examined other populations, such as lineage$^-$Sca1$^+$Kit$^+$ (LSK), lineage$^-$Kit$^+$Sca1$^-$ (LK), and common lymphoid progenitors, NKT cells, macrophages, B cells, and granulocytes, which were all negative for *Sostdc1* (Fig. 5G). Only CD4$^+$ and CD8$^+$ T cells displayed high levels of *Sostdc1* expression (Fig. 5G). This expression pattern was confirmed in CD4 and CD8 T cells from *Sostdc1*$^{-/-}$ mice using PCR for LacZ (27) (data not shown). Collectively, these results indicate that *Sostdc1* does not regulate splenic NK cell development in a NK cell–intrinsic manner and identifies *Sostdc1*-positive T cells as putative NK "niche cells" that may contribute to shaping of the Ly49 repertoire (Fig. 6).

Discussion

To our knowledge, we have uncovered novel roles of the *Sostdc1* gene in NK cell maturation and function through two distinct mechanisms. Our working model is illustrated in Fig. 6. Our data support that Sostdc1 from two distinct sources, nonhematopoietic stromal cells and hematopoietic cells (in particular, CD4$^+$ and CD8$^+$ T lymphocytes), regulate NK cell maturation versus Ly49 receptor expression and frequencies, respectively, in somewhat independent manners, and that this occurs through the control of Wnt signaling activation. Our developmental and functional NK cytotoxicity assay results lead us to conclude that several NK niche cell populations exist that require Sostdc1 expression to produce a healthy NK cell repertoire that can distinguish between self and nonself.

The microenvironmental cytokines may influence the development and functions of NK cells in relation to the niche, stromal, and T cells. In the spleen, the abundance of microenvironment cytokines, such as IL-2, IL-12, IL-15, IL-18, and IL-21, maintain NK cells in a steady-state and promote cytotoxic function (48). IL-15 supports NK cell development and function and is secreted by hematopoietic cells such as DCs, macrophages, and monocytes as well as nonhematopoietic stromal cells (49, 50). Alternatively, in an inflammatory microenvironment, activated T cells and DCs secrete abundant sources of cytokines that enhance NK cell cytotoxic function, such as IL-2, IL-12, IL-18, and IL-21 (35, 48, 51). We show that the hyporesponsiveness of *Sostdc1*$^{-/-}$ NK cells toward $\beta_2m^{-/-}$ cell targets is not mediated by an inability of DCs to produce IL-12 in the spleen (Supplemental Fig. 3). We have also concluded that production of inflammatory cytokines IFN-γ, GM-CSF, and TNF-α by NK cells is not affected by loss of *Sostdc1*. Detailed investigation of other cytokines such as IL-2, IL-7, IL-15, and IL-21 in the microenvironment are necessary to fully determine how *Sostdc1* by hematopoietic and nonhematopoietic cells influence NK cytotoxicity and development.

Perhaps the most surprising finding from our studies is that *Sostdc1* is not expressed in NK cells themselves and that Ly49 receptor expression in the spleen is possibly controlled in a cell-extrinsic manner by CD4$^+$ and CD8$^+$ T cells. Evidence that T cells shape the NK Ly49 receptor profile exist, but the mechanisms underlying this are still unclear. Jeannet et al. (2006) show that TCRβδ$^{-/-}$ mice have increased frequencies of Ly49G$^+$ and Ly49I$^+$ NK cells, but frequencies of Ly49D$^+$ NK cells are similar to controls. RAG-1$^{-/-}$ mice also have increased NK cell Ly49I$^+$ frequencies but no changes in Ly49G$^+$ or Ly49I$^+$ populations (52). In *Sostdc1*$^{-/-}$→WT chimeras, in which *Sostdc1* is absent from T cells, we have observed decreased frequencies of Ly49G and

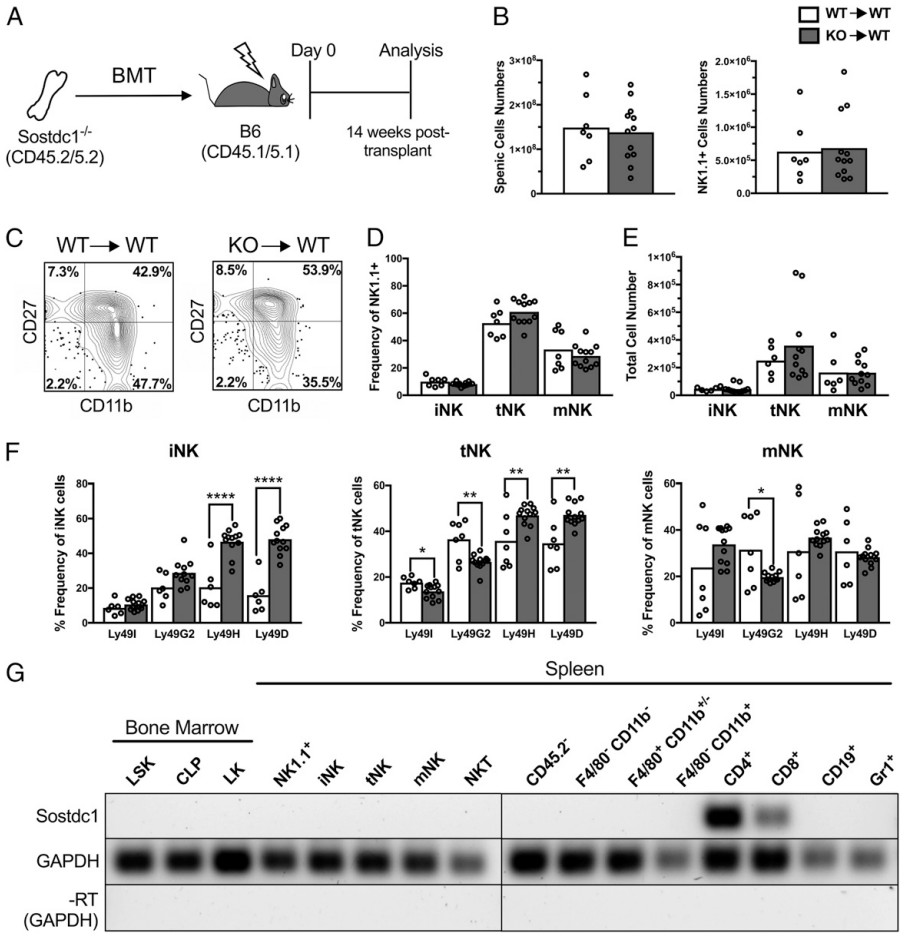

FIGURE 5. Sostdc1 in hematopoietic non–NK cells regulates the Ly49 NK receptor repertoire. (**A**) Experimental scheme to create *Sostdc1*$^{-/-}$→WT (KO→WT) BM chimeras. (**B**) Total cellularity in spleen (left) and total donor (CD45.2$^+$)-derived NK cell numbers (right) in chimeras; (**C**) representative FCM plots of splenic NK cell maturation of donor-derived NK cells in WT→WT and KO→WT chimeras; (**D**) quantification of donor NK cell subset frequencies and (**E**) NK cellularity in the spleen of chimeras; (**F**) analysis of Ly49 repertoire on donor-derived iNK (left), tNK (center), and mNK (right) cells in WT→WT and KO→WT spleens. (**G**) *Sostdc1* expression in hematopoietic cell lineages by RT-PCR. The black lines indicate where parts of the image were joined. *$p < 0.05$, **$p < 0.01$, ****$p < 0.0001$, Student t test.

Ly49I and increased frequencies of Ly49D$^+$ mNK cells (Fig. 5F), opposite and distinct from the pattern found in TCRβδ$^{-/-}$ and RAG-1$^{-/-}$ mice. Taken together, our data and the literature show that complete lack of T cells is not essential for NK cell development and suggest that a specific subset of T cells may regulate the NK cell repertoire. Recent studies have defined *Sostdc1* as a marker of relatively rare memory PD-1$^+$ CD4$^+$ T cells (53, 54) and T follicular helper cells found in the Peyer's Patches and peripheral lymph nodes (10) but only cite *Sostdc1*'s role on humoral immunity. We observed high expression of *Sostdc1* in bulk sorted splenic CD4$^+$ and CD8$^+$ cells from the spleen, and we assume that most of the *Sostdc1* expression is coming from PD1$^+$ CD4$^+$ T cells and T follicular helper cell subsets based on these published studies. We have not observed any obvious block in T cell development in the *Sostdc1*$^{-/-}$ mice (data not shown). Undeniably, further experimentation is required to definitively connect the role of these T cell subsets in NK cell regulation and to determine whether the T cells are regulating Ly49 receptor expression via directly binding to NK cells or mediating their effects indirectly by secreting Sostdc1 in a paracrine fashion.

Wnt signaling has been well studied in the framework of hematopoietic stem cells to help promote proliferation, differentiation, and homeostasis (55, 56). It is now evident that canonical Wnt signaling plays a crucial role in the regulation of many immune cells (55). Based on the antagonist role of Sostdc1 on Wnt signaling and our discovery of increased *Tcf7* and *Lef1* expression in NK cells from *Sostdc1*$^{-/-}$ mice, we conclude that canonical Wnt signaling plays a crucial role in NK cell development and function, particularly at the tNK cell stage. In the absence of *Sostdc1*, tNK cells are partially blocked in their maturation, express dysregulated Ly49 frequencies in the BM and spleen, and appear to be more reliant on Wnt activation. Our observations that one of the coactivators of canonical Wnt signaling, *Tcf7*, was significantly upregulated in tNK and mNK cells, and

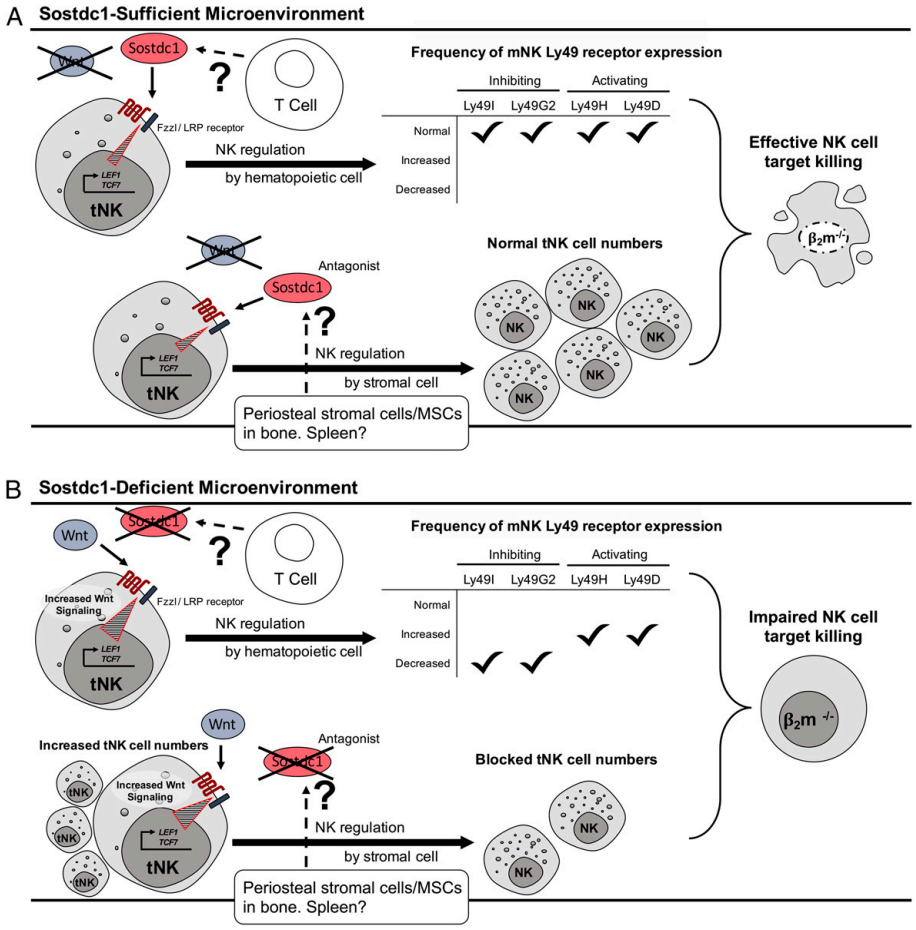

FIGURE 6. Working model of Sostdc1's role in NK cell maturation and cytotoxicity. (**A**) In a *Sostdc1*-sufficient (WT) microenvironment, *Sostdc1* is expressed by nonhematopoietic stromal cells in the bone that antagonizes Wnt signaling in NK cells, resulting in baseline levels of *Tcf7* and *Lef1*, and regulates NK cell numbers. *Sostdc1* expressed by T cells also influences Wnt signaling genes but distinctly controls the distribution of the Ly49 repertoire. Collectively, Sostdc1 is required in the microenvironment for development of NK cells with the ability to effectively recognize, be primed for activation, and lyse MHC-I–deficient targets. (**B**) In the absence of *Sostdc1* in bone stromal cells, splenic stromal cells, or T cells, *Tcf7* and *Lef1* expression is increased as a result of overstimulated Wnt signaling, which adversely affects NK cell numbers. Loss of *Sostdc1* in T cells might also dysregulate the distribution of Ly49s among NK cell subsets. Collectively, loss of *Sostdc1* in stromal cells and T cells acts cell-extrinsically on NK cells, producing NK cells that are hyporesponsive to MHC-I–deficient targets. Our data have ruled out any differences in IL-12, IFN-γ, TNF-α, and GM-CSF expression in *Sostdc1*$^{-/-}$ mice, but changes in other cytokines from stromal or T cells, such as IL-2, IL-15, IL-18, and IL-21, require further investigation.

the secondary coactivator, *Lef1*, was significantly upregulated in the mNK cell stage, suggest that a critical period exists in which tNK cells require downregulation of *Tcf7* and *Lef1* to progress to the mNK cell stage. Our results and interpretation are consistent with a recent study that downregulation of Tcf1 (encoded by *Tcf7*) is required for full NK cell maturation and cytotoxicity (3).

Based on our current findings, we cannot rule out whether the impaired killing of $\beta_2m^{-/-}$ targets by NK cells from *Sostdc1*$^{-/-}$ mice is due to insufficient numbers of mNK cells, inefficient execution of the perforin and granzyme pathways, the dysregulation of Ly49 receptor frequencies among NK cells, or a combination of all of these possible mechanisms. NK cells at tNK and mNK stages express genes involved in cytotoxic function (11–13). It has been shown that Ly49 receptor expression is required for NK cell cytotoxicity (57), which is consistent with our observations that the splenic mNK cells in the *Sostdc1*$^{-/-}$ mice contain decreased frequencies of all Ly49-expressing subsets and the killing ability of *Sostdc1*$^{-/-}$ NK cells toward $\beta_2m^{-/-}$ targets is poor. Because *Sostdc1*$^{-/-}$ mice express increased proportions of tNK cells with an "activating" repertoire (58) and high CD107a levels, we would have expected enhanced target cell killing by the *Sostdc1*$^{-/-}$ NK cells, but we observed them to be hyporesponsive. Taken together, our results suggest that NK cell cytotoxicity is universally disabled in the absence of *Sostdc1* but is caused by distinct mechanisms in tNK and mNK cells. Further experiments, in which the killing ability of purified tNK and mNK cells from *Sostdc1*$^{-/-}$ mice is specifically examined, are necessary to definitely demonstrate this. Additional work is also needed to dissect the specific

roles of nonhematopoietic and hematopoietic cells on NK cell cytotoxicity. Understanding the details of the basic biology underlying the development and regulation of NK cell cytotoxicity and how these processes are quantitatively integrated could be applied to manipulate these processes in a controlled fashion to produce specific numbers of NK cells with enhanced killing ability and perhaps impact the production of NK cell–based cancer immunotherapies (1–6).

Acknowledgments

We thank the staff of the Department of Animal Research Services and the Flow Cytometry Core of the Stem Cell Instrumentation Foundry at University of California Merced for excellent animal care and technical support, and Dr. Anna Beaudin and Dr. Marcos E. García-Ojeda for their comments on the manuscript.

Disclosures

The authors have no financial conflicts of interest.

References

1. Cifaldi, L., F. Locatelli, E. Marasco, L. Moretta, and V. Pistoia. 2017. Boosting natural killer cell-based immunotherapy with anticancer drugs: a perspective. *Trends Mol. Med.* 23: 1156–1175.
2. Geary, C. D., and J. C. Sun. 2017. Memory responses of natural killer cells. *Semin. Immunol.* 31: 11–19.
3. Jeevan-Raj, B., J. Gehrig, M. Charmoy, V. Chennupati, C. Grandclément, P. Angelino, M. Delorenzi, and W. Held. 2017. The transcription factor Tcf1 contributes to normal NK cell development and function by limiting the expression of granzymes. *Cell Reports* 20: 613–626.
4. Kim, S., J. Poursine-Laurent, S. M. Truscott, L. Lybarger, Y. J. Song, L. Yang, A. R. French, J. B. Sunwoo, S. Lemieux, T. H. Hansen, and W. M. Yokoyama. 2005. Licensing of natural killer cells by host major histocompatibility complex class I molecules. *Nature* 436: 709–713.
5. Lin, C., and J. Zhang. 2018. Reformation in chimeric antigen receptor based cancer immunotherapy: Redirecting natural killer cell. *Biochim Biophys Acta Rev Cancer* 1869: 200–215.
6. Mehta, R. S., B. Randolph, M. Daher, and K. Rezvani. 2018. NK cell therapy for hematologic malignancies. *Int. J. Hematol.* 107: 262–270.
7. Manilay, J. O., and M. Sykes. 1998. Natural killer cells and their role in graft rejection. *Curr. Opin. Immunol.* 10: 532–538.
8. Manilay, J. O., G. L. Waneck, and M. Sykes. 1999. Levels of Ly-49 receptor expression are determined by the frequency of interactions with MHC ligands: evidence against receptor calibration to a "useful" level. *J. Immunol.* 163: 2628–2633.
9. Manilay, J. O., G. L. Waneck, and M. Sykes. 1998. Altered expression of Ly-49 receptors on NK cells developing in mixed allogeneic bone marrow chimeras. *Int. Immunol.* 10: 1943–1955.
10. Grégoire, C., L. Chasson, C. Luci, E. Tomasello, F. Geissmann, E. Vivier, and T. Walzer. 2007. The trafficking of natural killer cells. *Immunol. Rev.* 220: 169–182.
11. Yokoyama, W. M., S. Kim, and A. R. French. 2004. The dynamic life of natural killer cells. *Annu. Rev. Immunol.* 22: 405–429.
12. Di Santo, J. P. 2006. Natural killer cell developmental pathways: a question of balance. *Annu. Rev. Immunol.* 24: 257–286.
13. Chiossone, L., J. Chaix, N. Fuseri, C. Roth, E. Vivier, and T. Walzer. 2009. Maturation of mouse NK cells is a 4-stage developmental program. *Blood* 113: 5488–5496.
14. Peng, H., and Z. Tian. 2017. Diversity of tissue-resident NK cells. *Semin. Immunol.* 31: 3–10.
15. Huntington, N. D., H. Tabarias, K. Fairfax, J. Brady, Y. Hayakawa, M. A. Degli-Esposti, M. J. Smyth, D. M. Tarlinton, and S. L. Nutt. 2007. NK cell maturation and peripheral homeostasis is associated with KLRG1 up-regulation. *J. Immunol.* 178: 4764–4770.
16. Hayakawa, Y., and M. J. Smyth. 2006. CD27 dissects mature NK cells into two subsets with distinct responsiveness and migratory capacity. *J. Immunol.* 176: 1517–1524.
17. Kim, S., K. Iizuka, H. S. Kang, A. Dokun, A. R. French, S. Greco, and W. M. Yokoyama. 2002. In vivo developmental stages in murine natural killer cell maturation. *Nat. Immunol.* 3: 523–528.
18. Orr, M. T., and L. L. Lanier. 2010. Natural killer cell education and tolerance. *Cell* 142: 847–856.
19. Sun, J. C. 2010. Re-educating natural killer cells. *J. Exp. Med.* 207: 2049–2052.
20. Togo, Y., K. Takahashi, K. Saito, H. Kiso, H. Tsukamoto, B. Huang, M. Yanagita, M. Sugai, H. Harada, T. Komori, et al. 2016. Antagonistic functions of USAG-1 and RUNX2 during tooth development. *PLoS One* 11: e0161067.
21. Ellies, D. L., A. Economou, B. Viviano, J. P. Rey, S. Paine-Saunders, R. Krumlauf, and S. Saunders. 2014. Wise regulates bone deposition through genetic interactions with Lrp5. [Published erratum appears in 2014 *PLoS One* 9: e104467.] *PLoS One* 9: e96257.
22. Kiso, H., K. Takahashi, K. Saito, Y. Togo, H. Tsukamoto, B. Huang, M. Sugai, A. Shimizu, Y. Tabata, A. N. Economides, et al. 2014. Interactions between BMP-7 and USAG-1 (uterine sensitization-associated gene-1) regulate supernumerary organ formations. *PLoS One* 9: e96938.
23. Collette, N. M., C. S. Yee, D. Murugesh, A. Sebastian, L. Taher, N. W. Gale, A. N. Economides, R. M. Harland, and G. G. Loots. 2013. Sost and its paralog Sostdc1 coordinate digit number in a Gli3-dependent manner. *Dev. Biol.* 383: 90–105.
24. Tanaka, M., S. Endo, T. Okuda, A. N. Economides, D. M. Valenzuela, A. J. Murphy, E. Robertson, T. Sakurai, A. Fukatsu, G. D. Yancopoulos, et al. 2008. Expression of BMP-7 and USAG-1 (a BMP antagonist) in kidney development and injury. *Kidney Int.* 73: 181–191.
25. Saito, K., K. Takahashi, M. Asahara, H. Kiso, Y. Togo, H. Tsukamoto, B. Huang, M. Sugai, A. Shimizu, M. Motokawa, et al. 2016. Effects of Usag-1 and Bmp7 deficiencies on murine tooth morphogenesis. *BMC Dev. Biol.* 16: 14.
26. Collette, N. M., D. C. Genetos, D. Murugesh, R. M. Harland, and G. G. Loots. 2010. Genetic evidence that SOST inhibits WNT signaling in the limb. *Dev. Biol.* 342: 169–179.
27. Collette, N. M., C. S. Yee, N. R. Hum, D. K. Murugesh, B. A. Christiansen, L. Xie, A. N. Economides, J. O. Manilay, A. G. Robling, and G. G. Loots. 2016. Sostdc1 deficiency accelerates fracture healing by promoting the expansion of periosteal mesenchymal stem cells. *Bone* 88: 20–30.
28. Assenmacher, M., J. Schmitz, and A. Radbruch. 1994. Flow cytometric determination of cytokines in activated murine T helper lymphocytes: expression of interleukin-10 in interferon-gamma and in interleukin-4-expressing cells. *Eur. J. Immunol.* 24: 1097–1101.
29. Sternberg-Simon, M., P. Brodin, Y. Pickman, B. Onfelt, K. Kärre, K. J. Malmberg, P. Höglund, and R. Mehr. 2013. Natural killer cell inhibitory receptor expression in humans and mice: a closer look. *Front. Immunol.* 4: 65.
30. Regner, M., L. Pavlinovic, N. Young, and A. Müllbacher. 2011. In vivo elimination of MHC-I-deficient lymphocytes by activated natural killer cells is independent of granzymes A and B. *PLoS One* 6: e23252.
31. Alter, G., J. M. Malenfant, and M. Altfeld. 2004. CD107a as a functional marker for the identification of natural killer cell activity. *J. Immunol. Methods* 294: 15–22.
32. Kehrl, J. H., M. Dukovich, G. Whalen, P. Katz, A. S. Fauci, and W. C. Greene. 1988. Novel interleukin 2 (IL-2) receptor appears to mediate IL-2-induced activation of natural killer cells. *J. Clin. Invest.* 81: 200–205.
33. Fukao, T., S. Matsuda, and S. Koyasu. 2000. Synergistic effects of IL-4 and IL-18 on IL-12-dependent IFN-gamma production by dendritic cells. *J. Immunol.* 164: 64–71.
34. Nguyen, K. B., T. P. Salazar-Mather, M. Y. Dalod, J. B. Van Deusen, X. Q. Wei, F. Y. Liew, M. A. Caligiuri, J. E. Durbin, and C. A. Biron. 2002. Coordinated and distinct roles for IFN-alpha beta, IL-12, and IL-15 regulation of NK cell responses to viral infection. *J. Immunol.* 169: 4279–4287.
35. Parikh, B. A., S. J. Piersma, M. A. Pak-Wittel, L. Yang, R. D. Schreiber, and W. M. Yokoyama. 2015. Dual Requirement of Cytokine and Activation Receptor Triggering for Cytotoxic Control of Murine Cytomegalovirus by NK Cells. *PLoS Pathog.* 11: e1005323.
36. Held, W., H. Clevers, and R. Grosschedl. 2003. Redundant functions of TCF-1 and LEF-1 during T and NK cell development, but unique role of TCF-1 for Ly49 NK cell receptor acquisition. *Eur. J. Immunol.* 33: 1393–1398.
37. van Genderen, C., R. M. Okamura, I. Fariñas, R.-G. Quo, T. G. Parslow, L. Bruhn, and R. Grosschedl. 1994. Development of several organs that require inductive epithelial-mesenchymal interactions is impaired in LEF-1-deficient mice. *Genes Dev.* 8: 2691–2703.
38. Jho, E. H., T. Zhang, C. Domon, C. K. Joo, J. N. Freund, and F. Costantini. 2002. Wnt/beta-catenin/Tcf signaling induces the transcription of Axin2, a negative regulator of the signaling pathway. *Mol. Cell. Biol.* 22: 1172–1183.
39. Nayak, G., Y. Odaka, V. Prasad, A. F. Solano, E. J. Yeo, S. Vemaraju, J. D. Molkentin, A. Trumpp, B. Williams, S. Rao, and R. A. Lang. 2018. Developmental vascular regression is regulated by a Wnt/β-catenin, MYC and CDKN1A pathway that controls cell proliferation and cell death. *Development* 145: dev154898.
40. Gordon, S. M., J. Chaix, L. J. Rupp, J. Wu, S. Madera, J. C. Sun, T. Lindsten, and S. L. Reiner. 2012. The transcription factors T-bet and Eomes control key checkpoints of natural killer cell maturation. *Immunity* 36: 55–67.
41. Daussy, C., F. Faure, K. Mayol, S. Viel, G. Gasteiger, E. Charrier, J. Bienvenu, T. Henry, E. Debien, U. A. Hasan, et al. 2014. T-bet and Eomes instruct the development of two distinct natural killer cell lineages in the liver and in the bone marrow. *J. Exp. Med.* 211: 563–577.
42. van Helden, M. J., S. Goossens, C. Daussy, A. L. Mathieu, F. Faure, A. Marçais, N. Vandamme, N. Farla, K. Mayol, S. Viel, et al. 2015. Terminal NK cell maturation is controlled by concerted actions of T-bet and Zeb2 and is essential for melanoma rejection. *J. Exp. Med.* 212: 2015–2025.
43. Townsend, M. J., A. S. Weinmann, J. L. Matsuda, R. Salomon, P. J. Farnham, C. A. Biron, L. Gapin, and L. H. Glimcher. 2004. T-bet regulates the terminal maturation and homeostasis of NK and Valpha14i NKT cells. *Immunity* 20: 477–494.
44. Robbins, S. H., M. S. Tessmer, L. Van Kaer, and L. Brossay. 2005. Direct effects of T-bet and MHC class I expression, but not STAT1, on peripheral NK cell maturation. *Eur. J. Immunol.* 35: 757–765.
45. Boos, M. D., Y. Yokota, G. Eberl, and B. L. Kee. 2007. Mature natural killer cell and lymphoid tissue-inducing cell development requires Id2-mediated suppression of E protein activity. *J. Exp. Med.* 204: 1119–1130.
46. Delconte, R. B., W. Shi, P. Sathe, T. Ushiki, C. Seillet, M. Minnich, T. B. Kolesnik, L. C. Rankin, L. A. Mielke, J. G. Zhang, et al. 2016. The helix-loop-helix protein

ID2 governs NK cell fate by tuning their sensitivity to interleukin-15. *Immunity* 44: 103–115.
47. Yokota, Y., A. Mansouri, S. Mori, S. Sugawara, S. Adachi, S. Nishikawa, and P. Gruss. 1999. Development of peripheral lymphoid organs and natural killer cells depends on the helix-loop-helix inhibitor Id2. *Nature* 397: 702–706.
48. Wu, Y., Z. Tian, and H. Wei. 2017. Developmental and functional control of natural killer cells by cytokines. *Front. Immunol.* 8: 930.
49. Castillo, E. F., S. W. Stonier, L. Frasca, and K. S. Schluns. 2009. Dendritic cells support the in vivo development and maintenance of NK cells via IL-15 trans-presentation. *J. Immunol.* 183: 4948–4956.
50. Cui, G., T. Hara, S. Simmons, K. Wagatsuma, A. Abe, H. Miyachi, S. Kitano, M. Ishii, S. Tani-ichi, and K. Ikuta. 2014. Characterization of the IL-15 niche in primary and secondary lymphoid organs in vivo. *Proc. Natl. Acad. Sci. USA* 111: 1915–1920.
51. Ma, A., R. Koka, and P. Burkett. 2006. Diverse functions of IL-2, IL-15, and IL-7 in lymphoid homeostasis. *Annu. Rev. Immunol.* 24: 657–679.
52. Jeannet, G., J. D. Coudert, and W. Held. 2006. T and B lymphocytes exert distinct effects on the homeostasis of NK cells. *Eur. J. Immunol.* 36: 2725–2734.
53. Norrie, I. C., E. Ohlsson, O. Nielsen, M. S. Hasemann, and B. T. Porse. 2014. C/EBPα is dispensable for the ontogeny of PD-1+ CD4+ memory T cells but restricts their expansion in an age-dependent manner. *PLoS One* 9: e84728.
54. Shimatani, K., Y. Nakashima, M. Hattori, Y. Hamazaki, and N. Minato. 2009. PD-1+ memory phenotype CD4+ T cells expressing C/EBPalpha underlie T cell immunodepression in senescence and leukemia. *Proc. Natl. Acad. Sci. USA* 106: 15807–15812.
55. Undi, R. B., U. Gutti, I. Sahu, S. Sarvothaman, S. R. Pasupuleti, R. Kandi, and R. K. Gutti. 2016. Wnt signaling: role in regulation of haematopoiesis. *Indian J. Hematol. Blood Transfus.* 32: 123–134.
56. Hoppler, S., and C. L. Kavanagh. 2007. Wnt signalling: variety at the core. *J. Cell Sci.* 120: 385–393.
57. Lindberg, J., A. Martín-Fontecha, and P. Höglund. 1999. Natural killing of MHC class I(-) lymphoblasts by NK cells from long-term bone marrow culture requires effector cell expression of Ly49 receptors. *Int. Immunol.* 11: 1239–1246.
58. Lanier, L. L. 2005. NK cell recognition. *Annu. Rev. Immunol.* 23: 225–274.

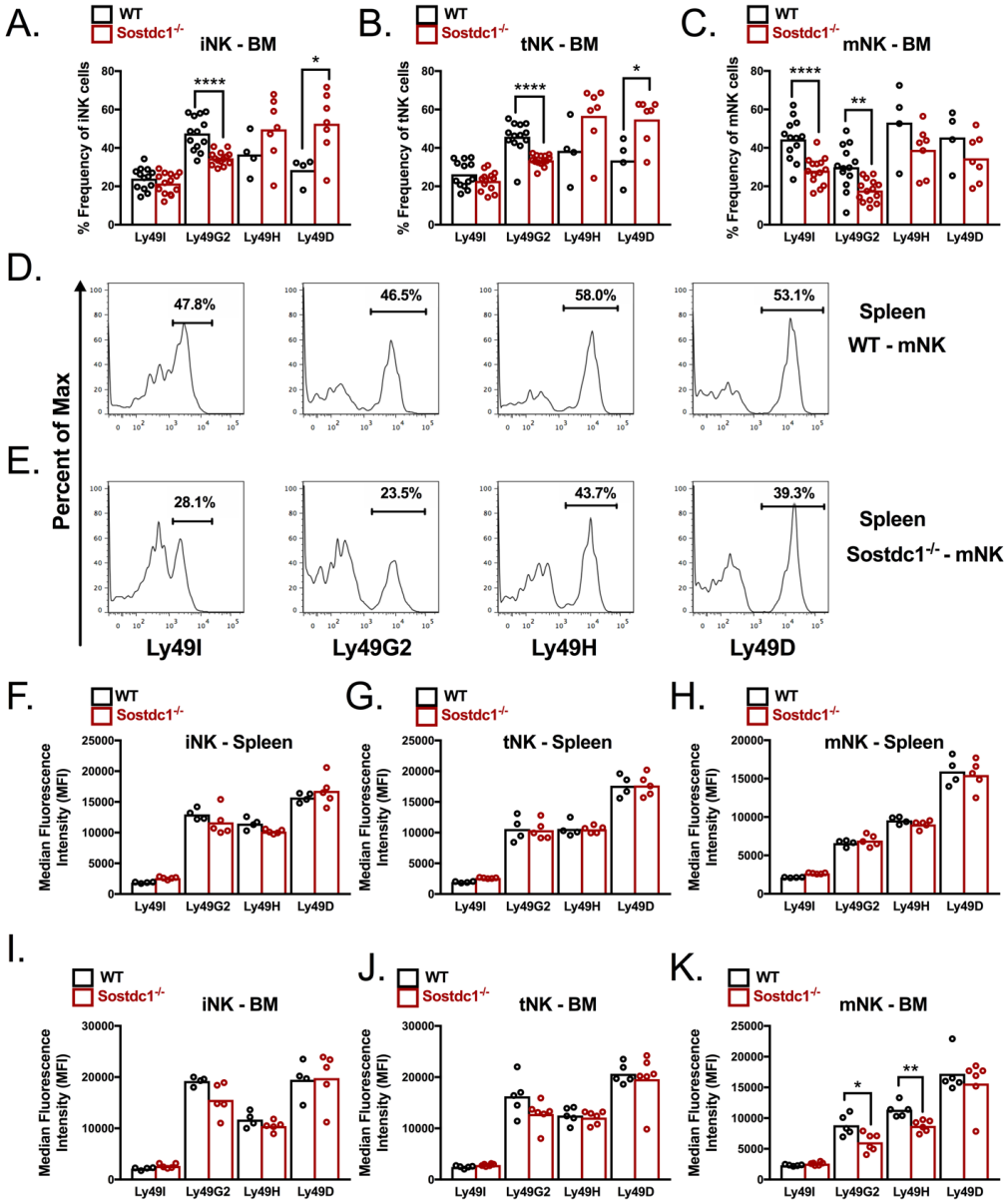

Supplemental Figure 1. Altered Ly49 repertoire frequencies in *Sostdc1*$^{-/-}$ mice. Frequency distribution of bone marrow NK cells expressing Ly49I, Ly49G2, Ly49H and Ly49D on iNK (A), tNK (B), and mNK (C) cells; representative FCM histograms of Ly49 receptor staining on splenic WT (D) and *Sostdc1*$^{-/-}$ mNK cells (E); median fluorescence intensity (MFI) of Ly49I, Ly49G2, Ly49H and Ly49D receptors on splenic iNK (F), tNK (G) and mNK cells (H). MFI quantification of NK cells in BM of Ly49I, Ly49G2, Ly49H and Ly49D on iNK (I), tNK (J) and mNK (K). Asterisks indicate statistically significant differences between means, as determined by Student’s t-test. *p<0.05, **p<0.01, ****p<0.0001. Each point represents a single mouse.

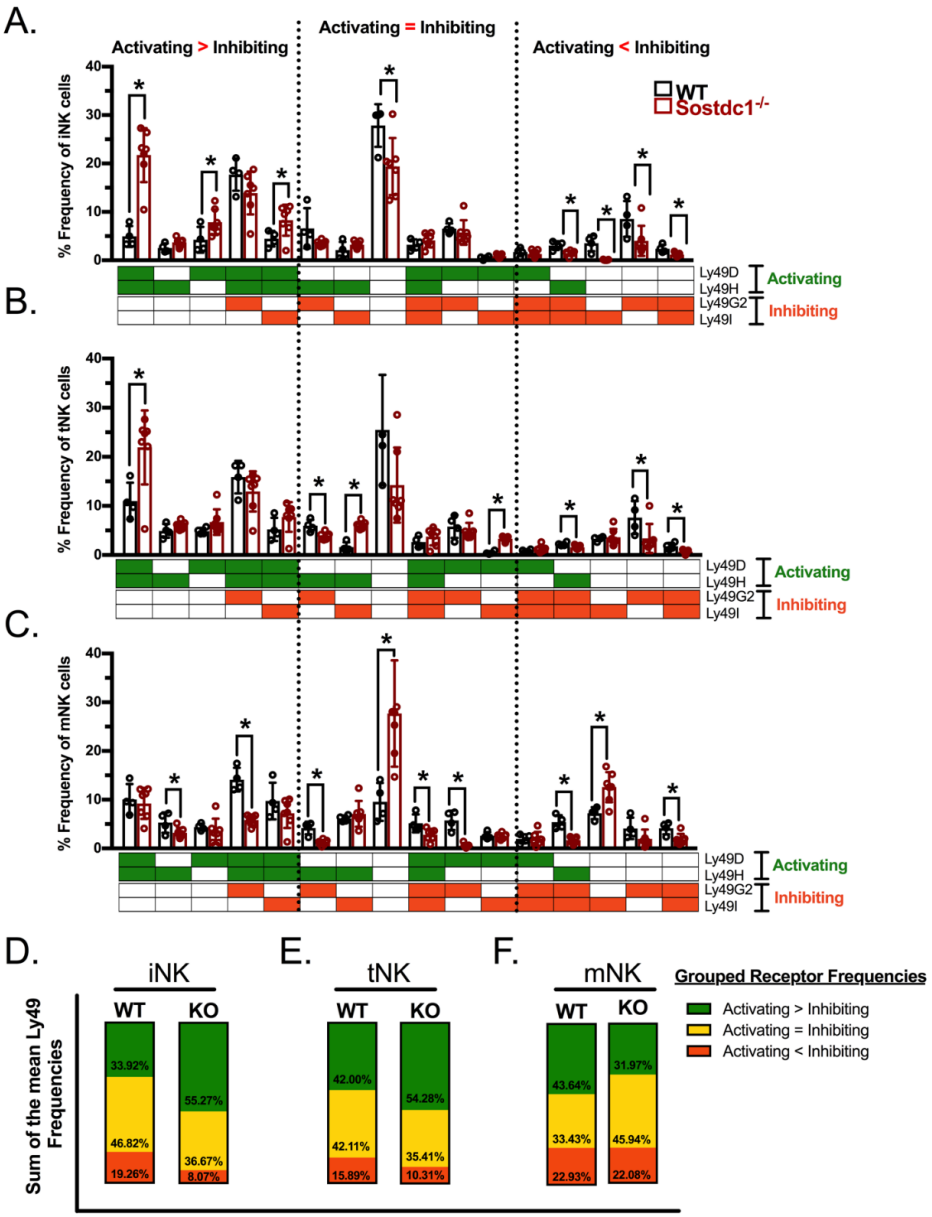

Supplemental Figure 2. Sostdc1-deficiency results in changes in the combinatorial expression of Ly49 receptors on individual NK cells. A-C) frequencies of iNK, tNK and mNK cells expressing 16 different combinations of Ly49I, Ly49G2, Ly49H, and Ly49D. Green or orange boxes indicate expression of the indicated activating or inhibitory Ly49 receptor, respectively, whereas white boxes indicate no expression of that specific Ly49 receptor. D-F) Summary of the NK cell frequencies in WT and *Sostdc1*$^{-/-}$ mice that express two activating and no inhibitory receptors, or one activating and no inhibitory receptors (Activating > Inhibiting), NK cells either expressing only one Ly49 activating and inhibitory receptor, all receptors, or no receptors (Activating = Inhibiting), and NK cells that express two Ly49 inhibitory receptors and no activating Ly49 receptors, or one inhibitory and no activating Ly49 receptors (Activating < Inhibiting). Asterisks indicate statistically significant differences between means, as determined by Student’s t-test. *p<0.05. Each point represents a single mouse.

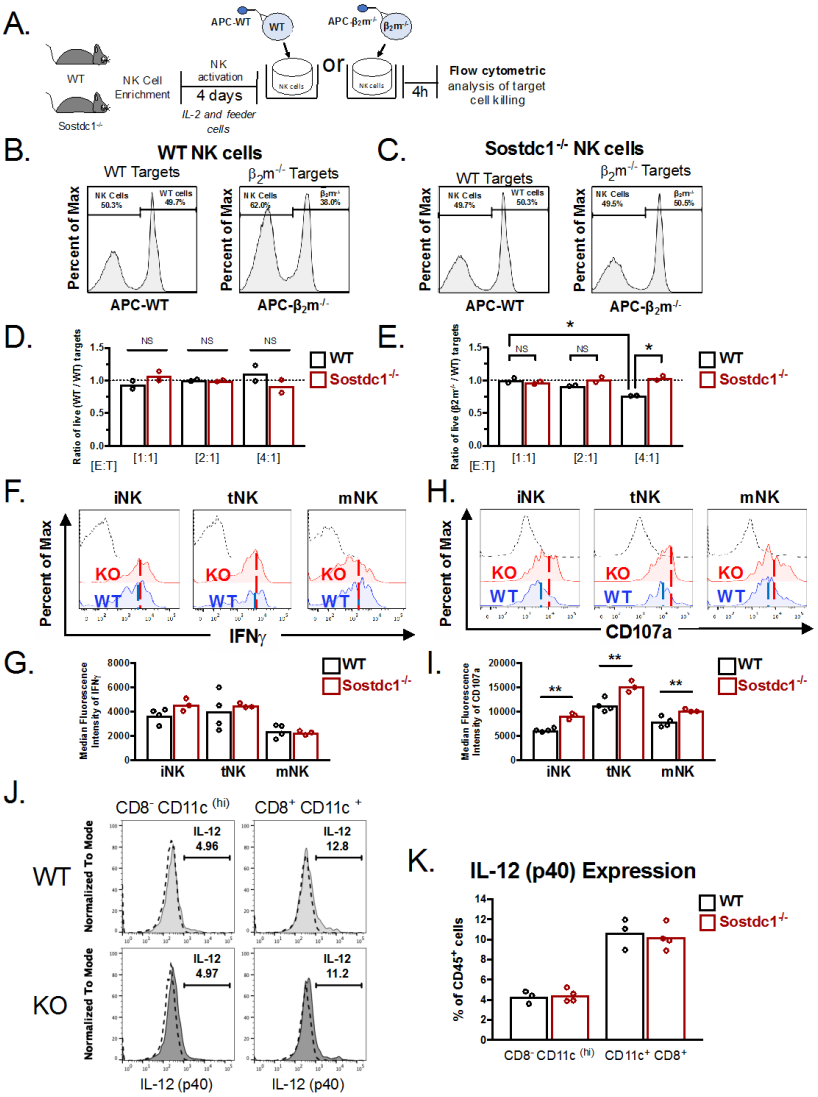

Supplemental Figure 3. *Sostdc1*-deficiency results in impaired in vitro NK cell killing, independent of CD107a expression, IFNγ and IL-12 production. A) Scheme of *in vitro* NK cell killing assay using enriched, pre-activated NK cells. B) Representative FCM plots showing frequencies of anti-CD45-APC labeled WT or $\beta_2m^{-/-}$ targets after 4 hours in culture with NK cells from WT mice or C) *Sostdc1*$^{-/-}$ mice. D) Quantification of control WT target cell lysis within vitro cultures with effector:target ratios of 1:1, 2:1 and 4:1. E) Quantification of $\beta_2m^{-/-}$ target cell lysis within vitro cultures with effector:target ratios of 1:1, 2:1 and 4:1. F) Overlay representative histogram plots of 2x10^6 NK enriched WT (blue line) and *Sostdc1*$^{-/-}$ (red line) cells for intracellular IFNγ, and H) CD107a after 5 hours of PMA and ionomycin stimulation. In F and H, isotype staining control is shown as a black dashed line. Quantification of median fluorescence intensity (MFI) of IFNγ (G) and CD107a (I). Sostdc1$^{-/-}$ or WT splenic cells stimulated in vitro with 100 ng/ml LPS and brefeldin A for 3 hours, then analyzed for intracellular IL-12 (p40) cytokine. J) Representative histograms normalized to mode for WT (top row) and KO (bottom row) of IL-12 (p40) for CD8$^-$CD11c$^{(hi)}$ DCs and CD8$^+$CD11c$^+$ DCs populations. K) Quantification of IL-12 (p40) expression frequencies of Singlets, Live, CD45$^+$ cells. Quantifications of specific staining were determined by subtracting non-specific background signal from specific antibody signal. Asterisks indicate statistically significant differences between means, as determined by Student’s t-test. *p<0.05 **p<0.01, ***p<0.001. Each point represents a single mouse.

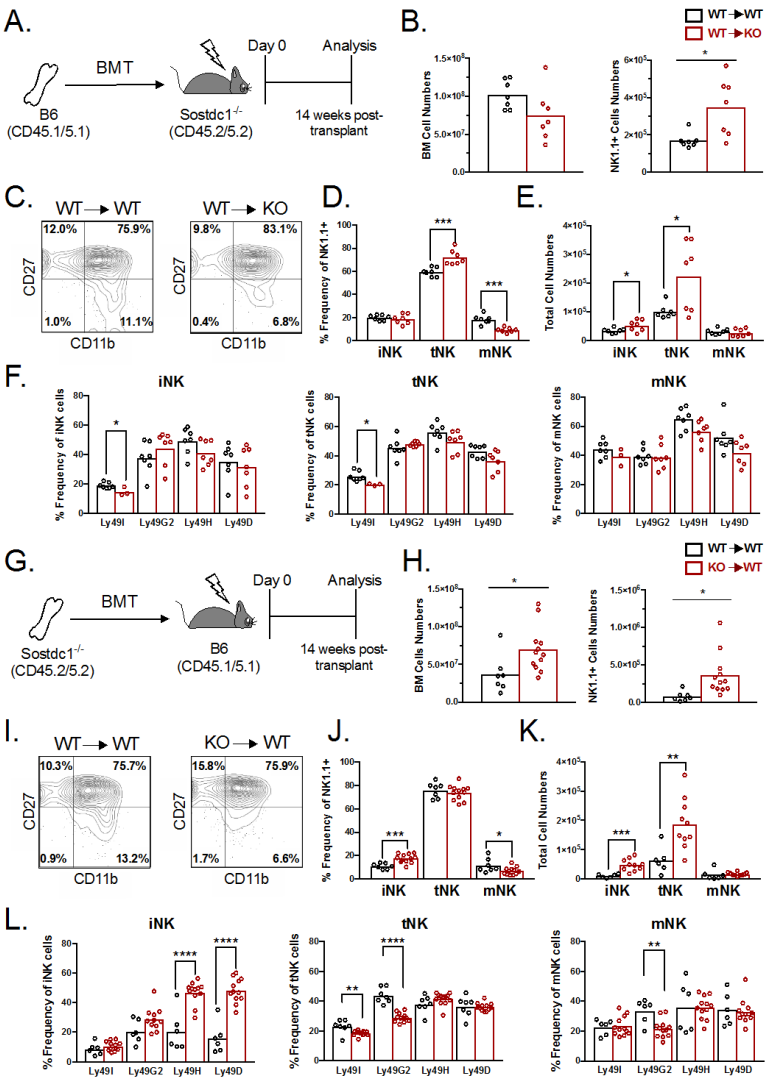

Supplemental Figure 4. Evidence for the influences of Sostdc1 expression in both hematopoietic and non-hematopoietic cells on NK cell development in the bone marrow. A) Experimental scheme to create WT→*Sostdc1*$^{-/-}$ KO (WT→KO) bone marrow chimeras. B) Total cellularity in BM (left) and total donor derived NK cell numbers (right) in chimeras; C) Representative FCM plots of NK cell maturation in donor (CD45.1^{+})-derived NK cells in the bone marrow of WT→WT *and* WT→KO chimeras; D) Quantification of NK cell subsets and E) NK cellularity in bone marrow of chimeras; F) Analysis of Ly49 repertoire on donor-derived iNK (left), tNK (center) and mNK (right) cells in the bone marrow of WT→WT and WT→KO chimeras; G) Experimental scheme to create *Sostdc1*$^{-/-}$→WT (KO→WT) bone marrow chimeras; H) total cellularity in BM (left) and total donor derived NK cell numbers (right) in chimeras; I) representative FCM plots of NK cell maturation in donor (CD45.2^{+})-derived NK cells in the bone marrow of WT→WT and KO→WT chimeras; J) quantification of NK cell subsets and K) NK cellularity in the bone marrow of chimeras; L) analysis of Ly49 repertoire on donor-derived iNK (left), tNK (center) and mNK (right) cells in the bone marrow of WT→WT and KO→WT chimeras. *p<0.05 **p<0.01, ***p<0.001, Student’s t-test.

CHAPTER 3

EVIDENCE FOR PROGRESSIVE NK CELL LY49 DEVELOPMENT PATHWAYS IN MICE

Evidence for progressive NK cell Ly49 developmental pathways in mice

Alberto J. Millan*†, Bryan A. Hom*, Jeremy B. Libang*, Suzanne Sindi†‡ and Jennifer O. Manilay*‡§[1]

*Department of Molecular and Cell Biology, †Department of Applied Mathematics and ‡Quantitative and Systems Biology Graduate Group, University of California - Merced, School of Natural Sciences, 5200 North Lake Road, Merced, CA 95343

Running title: Interdependencies of NK cell clusters within the iNK stage

§Corresponding Author:

Phone: 209-228-4175

Fax: none

Email: jmanilay@ucmerced.edu

[1] This work was supported by University of California (UC) Merced faculty research funding and UC graduate student fellowships (to A.J.M.).

ABSTRACT

Previous studies of NK cell inhibitory Ly49 receptors suggested their expression is stochastic. However, relatively few studies have examined this stochasticity in conjunction with activating Ly49 receptors. We hypothesized that the expression of activating Ly49 receptors is not stochastic and is influenced by inhibitory Ly49 receptors. We analyzed NK cell "clusters" defined by combinatorial expression of activating (Ly49H, Ly49D) and inhibitory (Ly49I, Ly49G2) receptors in C57BL/6 mice. Using the product rule to evaluate the interdependencies of the Ly49 receptors, we found evidence for a tightly regulated expression at the immature NK cell stage, with the highest interdependencies between clusters that express at least one activating receptor. Further analysis demonstrated that certain NK clusters predominated at the immature (CD27+CD11b-), transitional (CD27+CD11b+) and mature (CD27-CD11b-) NK cell stages. Using parallel in vitro culture and in vivo transplantation of sorted NK clusters, we discovered non-random upregulation of Ly49 receptors, suggesting that progressive pathways of NK cluster differentiation exist. Our data infer that upregulation of Ly49I is an important step in NK cell maturation. Ki-67 expression and cell counts confirmed that immature NK cells proliferate more than mature NK cells. We found that MHC-I is particularly important for regulation of Ly49D and Ly49G2, even though no known MHC-I ligand for these receptors is present in B6 mice. Our data indicate that the regulatory systems controlling the expression of both activating and inhibitory Ly49 receptors are non-stochastic and support the idea that NK cell clusters develop in a non-random process correlated to their maturation stage.

INTRODUCTION

Natural killer (NK) cells are innate lymphocytes which function in immune cell surveillance by the recognition and elimination of cellular targets. Unlike their T and B lymphocyte counterparts, which acquire antigen-specific diversity through genetic recombination events, NK cells generate germline-encoded receptors that can recognize and lyse cellular targets by releasing perforin, granzymes, and secrete regulatory and proinflammatory cytokines. Activating and inhibitory Ly49 receptors employ NK cell signaling pathways, which dictate NK cell effector functions through cytoplasmic immunoreceptor tyrosine-based inhibitory motifs (ITIMs) and immunoreceptor tyrosine-based activating motifs (ITAM) (1-4). NK cell subsets are thought to utilize a “rheostat” process in which NK cell subsets are tuned quantitatively by self-MHC class I ligands corresponding to specific Ly49 inhibitory receptors, which in turn provides a diversity of responsiveness towards cellular targets (5, 6). Through this mechanism, NK cells distinguish healthy from unhealthy cells. However, what regulates the acquisition of specific NK cell Ly49 receptors during NK cell development and maturation is still an unanswered and complex question. In addition, how models derived from the biology of Ly49 inhibitory receptors pertain to the acquisition of Ly49 activating receptors is unresolved.

NK cell subsets that express single as well as overlapping Ly49 activating and inhibitory receptors exist, which may reflect the complexity required to ensure host immunity while maintaining self-tolerance (7). Expression of Ly49 receptors, encoded by the polymorphic and polygenic *Klra* genes located on mouse chromosome 6, is often described as stochastic (8, 9). However, Ly49 receptor acquisition may not be entirely stochastic, as it has been shown that inhibitory Ly49 receptors can be regulated by self-MHC class I (MHC-I) expression and controlled by the Ly49 bidirectional transcriptional regulation of Pro1 and Pro2 (10, 11). In contrast, activating Ly49 receptors lack a defined Pro1 region. Mathematical methods to test the interdependence of expression of individual Ly49 inhibitory receptors on the expression of other Ly49 members in MHC-I-deficient and MHC-I-sufficient (wild type) mice support that Ly49 inhibitory receptor expression may not be independently distributed and thus may not be entirely random (8, 12-15). Previous studies provide support that Ly49H and Ly49D are distinctly influenced by co-expression with inhibitory receptor Ly49C (16) and non-stochastic (10, 17) regulation of the expression of Ly49 activating receptors.

In this study, we tested the hypothesis that expression of Ly49 activating receptors is not stochastic and is influenced by Ly49 inhibitory receptors. To test this hypothesis, we utilized a combination of statistical, in vitro and in vivo

approaches. We provide evidence for a progressive pathway of NK "cluster transitions" in vitro and in vivo, which suggest that Ly49 activating receptor acquisition is directed. Even though no known MHC-I ligand for Ly49G2, Ly49H and Ly49D is known in B6 mice, NK cell cluster distribution is altered in MHC-I deficient mice. Taken together, our data support the idea that NK cell clusters develop in a non-random manner and provide additional evidence that the regulatory system that controls the expression of both Ly49 activating and inhibitory receptors is non-stochastic. Our findings lead to an expanded model of NK cell receptor acquisition during NK development and maturation.

MATERIALS AND METHODS

Mice

C57B6/J, B6.SJL-Ptprca Pepcb/BoyJ, and B6.129P2-B2mtm1Unc/J β-2 microglobulin knockout ($\beta_2m^{-/-}$ KO) mice were obtained from The Jackson Laboratory and bred at the University of California, Merced. Mice of both sexes between the ages of 10 and 28 weeks were used for each experiment. We observed no significant differences between mice of both sexes or different ages, except for one specific study on cell proliferation (please see Results). Mice were housed in specific pathogen-free cages with autoclaved feed. Mice were euthanized by carbon dioxide asphyxiation followed by cervical dislocation. All animal procedures were approved by the UC Merced Institutional Animal Care and Use Committee.

Flow cytometry (FACS)

Splenic cells were harvested, processed and stained for flow cytometric analysis (FACS) as described (18). Cells were stained with the following antibodies, purchased from eBioscience, Biolegend, Miltenyi Biotec, and BD Biosciences: PE/Cy5-CD3 (145-2C11), PE/Cy5-CD4 (RM4-5), PE/Cy5-CD8a (53-67), PE/Cy5-Gr1 (RB6-8C5), PE/Cy5-CD19 (6D5), PE-CD27 (LG3A10), BV421-NK 1.1 (PK136), BV510-CD11b (M1/70), biotinylated or APC-Ly49D (4E5), APC-Cy7-Ly49G2 (4D11), FITC- or APC-Ly49H (3D10), APC-VID770-Ly49I (YLI-90), and APC-Ki67 (SolA15), CD45.1 (A20), CD45.2 (104). BUV395-streptavidin was used to develop biotinylated antibodies. Staining of all cells included a preincubation step with unconjugated anti-CD16/32 (clone 2.4G2 or clone 93) mAb to prevent nonspecific binding of mAbs to FcγR. Extracellular staining was performed as described (18). Intracellular staining was performed using the True-Nuclear™ Transcription Factor Buffer Set (BioLegend) per manufacturer's instructions. Single-color stains were used for setting compensations, and gates were determined by historical data in addition to fluorescent-minus-one control stains.

Flow cytometric data were acquired on the BD LSR II flow analyzer or FACS Aria II flow sorter (Becton Dickinson). The experimental data were analyzed using FlowJo™ Software version 10.6.0 and 10.6.3 (Becton, Dickinson and Company).

Identification of NK cell Ly49 cluster heterogeneity

NK cell clusters (C1-C16) were determined by t-stochastic neighbor embedding (tSNE) using FlowJo™ Software version 10.6.0 and analyzed with 3000 iterations, 50 perplexity, 2800 learning rate (eta), and vantage point tree KNN algorithm (19, 20). The cluster frequencies were determined by manual gating on live, lineage-negative, NK1.1+ cells and further divided by gating on populations based on Ly49I, Ly49G2, Ly49H, and Ly49D expression (please see **Figure 1E**).

Assessment of NK cell Ly49 receptor interdependencies by the product rule

Ly49I, Ly49G2, Ly49H, and Ly49D receptors were assessed for independent expression by the product rule. The product rule predicts the frequencies of NK cells that express single or a combination of Ly49 receptors. Assuming a model of independent expression of Ly49 receptors, the frequencies of NK cells expressing individual Ly49 receptors were used to calculate expected frequencies for NK cells expressing zero, one and more receptors (8, 14, 15). For example, the expected frequency for NK cells that co-express Ly49H and Ly49D, but do not express Ly49G2, equals the probability (P) of expressing Ly49H (e.g. frequency of NK cells expressing Ly49H) multiplied by the probability of expressing Ly49D, multiplied by the difference of 1 minus the probability of expressing Ly49G2 (to account for its exclusion), such that P(H,D) = P(H)*P(D)*(1-P(G2)) (please see Figure 2A). We calculated the "product rule error" between the observed and predicted frequencies as the $\log_2$(observed frequencies/predicted frequencies). If the observed frequencies were greater than the predicted frequencies (product rule error > 0), this indicated the model underestimated the observed frequencies. Alternatively, if the observed frequencies were less than predicted frequencies (product rule error < 0), this indicated the model overestimated the observed frequencies. If the error equaled zero, then we concluded that the expression of the pattern of receptors were independent. To calculate the total error, we summed the absolute value of the product rule errors amongst clusters.

In vitro NK cell cluster development assay

Splenic NK cells from C57B6/J mice were harvested and processed to a single-cell suspension in media (RPMI1640 media supplemented with 10% FBS, 0.09 mM nonessential amino acids, 2 mM L-glutamine, 1 mM sodium pyruvate, 100 U/ml penicillin, 100 mg of streptomycin, 0.025 mM beta-mercaptoethanol, and 0.01

M HEPES) and cell counts determined using a hemocytometer. Splenic cells were enriched for NK cells as described in the EasySep Positive Selection Kit (STEMCELL Technologies) manufacturer's suggested protocol by selecting with an anti-"lineage" cocktail (anti-CD3,-CD4,-CD8,-CD19,-Gr1, and -Ter119). NK cell clusters were then sorted on the FACS Aria II by gating on propidium iodide (PI)-negative (live), "lineage"-negative and NK1.1-positive cells. 90-95% post-sort purity was achieved, as measured by FACS. Approximately 20,000 cells per NK cell cluster were cultured in 96-flat bottom tissue culture plates with the addition of 100,000 lethally-irradiated (30.0 Gy) splenic feeder cells and recombinant-mouse (rm) IL-15 (75 ng/ml). NK cell cluster frequencies were quantified by FACS after 4 days of culture.

In vivo NK cell cluster adoptive transfer assay

B6.SJL mice were used as a source of donor splenic NK cells. Spleens were aseptically harvested and processed to a single-cell suspension. NK cells were enriched as described above, and then sorted for each of the 16 NK cell clusters. B6 recipient mice were sublethally irradiated (5.5 Gy) with a cesium irradiator four hours before receiving a range of 50,000 to 200,000 donor NK cluster cells by retroorbital intravenous injection. Donor-derived CD45.1+ NK cell cluster frequencies were analyzed by FACS four days after transfer.

Statistical analysis

Student's t-test with a two-tailed distribution and with two-sample equal variance (homoscedastic test) was used to determine differences in means between groups using GraphPad Prism software version 8.4.2. A p-value of 0.05 was considered to be statistically significant. Asterisks indicate statistically significant differences *$p < 0.05$, **$p < 0.01$, ***$p < 0.001$, ****$p < 0.0001$.

RESULTS

Identification of NK cell phenotypic heterogeneity amongst the combination of Ly49 receptors

NK cells express diverse frequencies and combinations of Ly49 activating and inhibitory surface receptors, but few studies have examined the relationship between expression of the activating receptor repertoire to that of the inhibitory receptor repertoire, and whether the activating receptors are subject to similar stochasticity in expression as previously described for inhibitory receptors (8, 14). We decided to focus on inhibitory receptors Ly49I and Ly49G2 and activating receptors Ly49H and Ly49D on splenic NK cells in C57B6/J (B6) mice, which express MHC-I ligands H-2K^{b} and H-2D^{b}. Ly49I's inhibitory ligand is H-2K^{b}, Ly49H binds to the m157 viral antigen, and Ly49G2 and Ly49D's known ligand is H-2D^{d} (not expressed in B6 mice) (9). Previous work (10, 17) in which analyses of Ly49H and Ly49D were performed, provided a source of historical controls to which our data could be compared. Although other Ly49 family members exist, we were limited to these 4 receptors due to the availability of fluorochrome-conjugated specific antibodies and the number of fluorochromes available on our flow cytometers. Expression of each Ly49 receptor was observed (**Figure 1A-B**). We defined sixteen NK cell "clusters" (C) by the number and type of activating receptors and inhibitory receptors expressed. That is, Cluster 1 (C1) expresses both Ly49H and Ly49D activating receptors and neither Ly49I nor Ly49G2 inhibitory receptors, whereas Cluster 16 (C16) expresses both Ly49I and Ly49G2 inhibitory receptors but neither Ly49H nor Ly49D activating receptors (**Figure 1C**). By using these four receptors, sixteen possible combinations of Ly49 activating and inhibitory receptor expression were identified by t-distributed stochastic neighbor embedding (t-SNE) analysis of flow cytometric data **(Figure 1F**), and further examination of the expression of individual Ly49 receptors allowed us to confirm each cluster phenotype **(Figure 1D)** (19). Furthermore, we developed an NK cell cluster gating strategy that identified the sixteen unique subpopulations (clusters) and their frequencies **(Figure 1E)**. Similar to previous studies which analyzed inhibitory Ly49 receptors only (8, 14), we observed Cluster 8 (C8), which expresses none of the four receptors, to be one of the most prevalent populations (**Figure 1G)**. By analyzing Ly49 activating receptor frequency, we observed that clusters co-expressing Ly49H and Ly49D activating receptors were most represented, i.e. C1 (I-G2-H+D+), C4 (I-G2+H+D+), C5 (I+G2-H+D+), and C9 (I+G2+H+D+) **(Figure 1G)**. Conversely, frequencies were lowest for clusters that express both Ly49 inhibitory receptors, such as C16 (I+G2+H-D-), C13 (I+G2+H-

D+), and C12 (I+G2+H+D-) (**Figure 1G**). These data suggest a possible selective (non-random) pressure controlling the frequencies of these clusters in mice.

High interdependencies of NK cell cluster frequencies within the immature NK stage

Next, to explore the possibility of independent (random) expression of our Ly49 receptors of interest, we utilized the product rule model for independent expression assuming the stochastic nature of Ly49 receptors. The model states that if Ly49I, Ly49G2, Ly49H, and Ly49D expression is independent of one another, then the observed frequencies of NK cells that express zero, one, two or more receptors can be predicted by the measurement of individual Ly49 receptor frequencies (8, 15) (**Figure 2A**). Thus, if the predicted frequencies match the observed biological frequencies, then we conclude no interdependencies between expression of those Ly49 receptors. Alternatively, if the observed frequencies do not match the predicted frequencies, the expression of these receptors are interdependent (non-random) for reasons including, but not limited to, linked receptor expression, gene regulation, and biased receptor selection (8, 10, 21). Our comparison of the observed versus predicted NK cluster frequencies demonstrate independent expression in some clusters (C1, C5, C6, C9, C11, C12, C15 and C16), but dependencies in others (C2, C3, C4, C7, C8, C10, C13 and C14) (**Figure 2B**). We next calculated the product rule error (e.g. $\log_2$(observed/predicted)) for each cluster to identify if the model underestimated (observed > predicted), overestimated (observed < predicted), or matched the observed frequencies (observed = predicted). An example of the product rule errors in clusters arranged by their patterns of Ly49H and Ly49D expression is shown in **Figure 2C**. We show that NK clusters C14, C8 (which are H-D-), and C4 (H+D+) frequencies were underestimated by the model, whereas clusters C10, C3 (both H+D-) and, C7, C13, and C2 (H-D+), were overestimated by the model (**Figure 2C**). We noted that the product rule underestimated the frequencies of five out of the eight clusters that express only one of the Ly49 activating receptors (C10, C3, C7, C13, and C2). These data suggest interdependencies between Ly49H and Ly49D expression.

We hypothesized that a source of NK cell Ly49 expression dependencies was the stage of maturation. To test our hypothesis, we utilized the NK cell maturation markers CD27 and CD11b to examine the frequencies of each cluster amongst immature NK (iNK; $CD27^+CD11b^-$), transitional NK (tNK; $CD27^+CD11b^+$), and mature NK (mNK; $CD27^-CD11b^+$) cells (1, 18, 22, 23) (**Figure 2D)**. We calculated the total error by summing the absolute values of the product rule errors

for each NK cell maturation stage (**Figures 2E, 2H-J**). The total error was significantly higher at the iNK cell stage relative to the tNK and mNK cell stages, suggesting more Ly49 receptor dependencies at the iNK stage (**Figure 2E**). iNK total error was significantly higher in clusters which at least one activating receptor (**Figure 2F**). Examination of the inhibitory receptors showed very similar patterns (**Figure 2G**). The exceptions were H-D- clusters which displayed similar error between iNK, tNK, and mNKs, and I-G2+ clusters, in which error was high in the iNK and mNK cells (**Figure 2F-G**). Moreover, C8, C14, C15, and C16, all of which are H-D-, showed more independent expression (lower total error) in the iNK (1.99 ± 0.21) and tNK (2.20 ± 0.18) cells relative to I-G2- clusters C1, C2, C3, C8 in the iNK (5.48 ± 0.45) and tNK (3.1 ± 0.10) cells (**Figure 2F-G**). No difference between the total error for tNK and mNK cells within the H-D- and I-G2- groups were observed (**Figure 2F-G**). Additionally, we observed the majority of clusters were either overestimated or underestimated consistently throughout NK cell maturation (**Figure 2H-J**). There were some exceptions: C14 (I+G2-H-D-) was overestimated by the model at the iNK stage and then underestimated at the tNK and mNK maturation stage, and C6 (I-G2+H-D+) was overestimated at the iNK stage and then slightly underestimated at the mNK cell stage (**Figure 2H-J**). Taken together, the product rule model provided evidence for a tightly regulated expression system for Ly49 receptors especially at the iNK maturation stage, with the highest interdependencies in clusters that express at least one Ly49H and Ly49D activating receptor.

Dominant expression of Ly49I in all clusters at the mature NK cell stage

Further analysis revealed Ly49 cluster frequencies were unique at each NK cell maturation stage (**Figure 3A-D**). We identified Ly49I receptor expression frequency to significantly increase from iNK to tNK to mNK stages (**Figure 3E**). Ly49G2, Ly49H, and Ly49D frequencies significantly increased between iNK to tNK stages, and then decreased (Ly49G2 and Ly49D) or stabilized (Ly49H) moving from the tNK to mNK stages (**Figure 3E**). The frequencies of clusters with zero or one receptor were found to decrease; conversely, clusters expressing two, three, or four receptors increased from iNK to tNK stages (**Figure 3F**).

To determine if specific clusters were predominantly grouped at the iNK, tNK or mNK cell stages of maturation, we quantified the cluster frequencies at each NK maturation stage and visualized the similarities between clusters with principal component analysis (PCA) (24). NK cell cluster percentages were quantified by normalizing each cluster frequency relative to each NK maturation stage, such that a cluster's frequency was divided by the sum of that cluster's frequencies found at

each maturation stage and then multiplied by 100 (**Supplemental Figure 1**). We computed the PCA from the average normalized frequencies of clusters at each NK stage and determined similarities between clusters with respect to NK maturation (**Figure 3G-J**). We grouped clusters found predominantly at the iNK, tNK, and mNK cell stage in our PCA, which were confirmed by observing the plotted percentages (**Figure 3H-J**). That is, we identified C8, C15, C3, and C10 to predominate the iNK cell stage (**Figure 3H**), C1, C2, C4, C6 to predominate at the tNK cell stage (**Figure 3I**), and C9, C5, C13, C16, C7, C11, C14 to predominate at the mNK cell stage (**Figure 3J**). C10, C1 and C2 assembled close together in the PCA, but we decided to group C10 into the "iNK-predominant" group because the changes in the % of C10 at the iNK, tNK and mNK were more similar to to C8, C3 and C15 (**Supplemental Figure 1**). Notably, the predominant clusters within each stage were represented at different proportions as maturation progressed. For example, C8, which expresses none of the four receptors, decreased in a sequential manner throughout NK cell maturation from 80.7% $\pm$ 1.8 in the iNK stage to 6.6% $\pm$ 1.5 at the mNK cell stage (**Figures 3H and 3J**). In contrast, tNK-predominant clusters were lower at the iNK and mNK stages, and mNK predominant clusters were lowest at the iNK and tNK stages (**Figures 3H, 3I, 3J).** Furthermore, all mNK-predominant clusters expressed the inhibitory self-Ly49I receptor, but iNK- and tNK-predominant clusters did not (**Figures 1C, 3H, 3I and 3J**) Thus, these findings suggest that the frequency and phenotype of the NK cell clusters are regulated throughout NK cell maturation to increase the types of receptors expressed, and positively select for self-Ly49I at the mNK cell stage.

Evidence for progressive NK cell Ly49 developmental pathways in mice

The observed distribution of clusters within the iNK, tNK and mNK stages (**Figure 3 and Supplemental Figure 1**) led us to hypothesize that the iNK-predominant clusters may be precursors to clusters that predominate at the tNK to mNK stages. To test this, we sorted each of the 16 NK cell clusters and cultured them with 75 ng/ml recombinant-mouse-interleukin-15 (rmIL-15) and lethally irradiated splenic feeder cells for 4 days (**Figure 4A**). We observed that iNK-predominant clusters C8, C15, C3, C10, and tNK-predominant clusters C1, C2, C4, C6, all upregulated Ly49I receptor after culture (**Figure 4B, 4C and 4D**), which would re-categorize them into clusters found predominantly in the mNK cell stage (C5, C7, C9 and C13, respectively, **Figures 1C and 3J**). Cultures initiated with mNK-predominant clusters maintained their Ly49 receptor phenotypes (data not shown). To verify our findings in vivo, we adoptively transferred sorted C8, C15, C3, C10, C1, C2, and C14 cells from B6.SJL (CD45.1+) mice into sublethally

irradiated B6 (CD45.2+) hosts and analyzed their differentiation after 4 days (**Figure 4E**). Similar to our in vitro results, we observed C8, C15, C3, C10, C1, and C2 to upregulate Ly49I **(Figure 4F-I**), and that Ly49H and Ly49D maintained stable expression (data not shown). However, in vivo, C8, C1, C2 upregulated a small frequency of inhibitory Ly49G2 receptor after 4 days (**Figure 4F and 4G**). Ly49 receptor expression on C14, a mNK-predominant cluster, was unchanged after adoptive transfer (**Figure 4H).** Altogether, these results strongly support the existence of progressive pathways of NK cell maturation from precursor NK cell clusters, and that Ly49I upregulation is a key step for mature NK cells (**Figure 4J and 4K**).

Immature NK cells display similar proliferation characteristics, regardless of cluster type

Given our discovery of progressive pathways of NK cluster development, we further analyzed the clusters for differences in their proliferative state. We hypothesized that the proliferation rates of specific NK cell clusters would be distinct. Furthermore, we expected proliferation rates to correlate with maturation stage. To test our hypotheses, we sorted and cultured bulk iNKs, tNKs, and mNKs (**Figure 5A**) on lethally irradiated splenic feeder cells in media containing 75 ng/ml of rm-IL-15, and measured cellularity at Day 2 and Day 6 post-culture. We observed the highest fold change in cellularity for cultures initiated with iNK cells, as compared to cultures initiated with tNK or mNK cells (**Figure 5B**). We disaggregated the fold changes in proliferation between iNK-predominant (C8, C15, C3, C10), tNK-predominant (C1, C2, C4, C6), and mNK-predominant (C9, C5, C16, C12, C13, C14, C11, C7) clusters within each sorted population **(Figure 5C, 5D, 5E)**. Our data show that iNK-initiated cultures increased the fold change in cellularity of tNK-predominant clusters relative to iNK- and mNK-predominant clusters (**Figure 5C**). In contrast, mNK-initiated cultures showed reduced proliferation in tNK predominant clusters relative to iNK- and mNK-predominant clusters (**Figure 5E**). Additionally, the frequency of C8, which expresses none of the four Ly49 receptors and is the most prevalent in the iNK stage, dramatically decreased during the culture period **(Figure 5F)**, which is consistent with our observation of decreased frequency of C8 at the tNK and mNK stages in vivo **(Figure 3I and 3J**).

To confirm these proliferation patterns, we stained NK cells for Ki-67 expression post-culture. After culture, we noticed that CD11b expression was downregulated universally on NK cells, preventing us from using CD11b to distinguish iNK, tNK and mNKs (data not shown), likely as an artifact of in vitro

culture (25). However, CD27 expression was still binary, allowing us to distinguish CD27+ (presumably iNK and tNKs) from CD27- mNKs. We found that NK1.1^{+}CD27^{+} cells expressed higher Ki-67 levels compared to NK1.1^{+}CD27^{-} cells (**Figure 5G and 5H**), regardless of Ly49 receptor expression (**Figure 5I**). This pattern persisted when the Ki-67 expression was examined in specific NK cell clusters, with the exception of cluster C15 (which only expresses Ly49G2) (**Figure 5J**). These data show that cluster designation (and hence Ly49 receptor expression) does not dictate NK cell proliferation. Rather, proliferative potential is a general characteristic of NK cell maturation stage, with highest proliferation in the iNK cells and lowest proliferation in mNK cells.

MHC-I-deficiency does not affect NK cell maturation, but results in underrepresentation of NK cell clusters which express activating Ly49 receptors

We next investigated the effects of MHC-I on NK cell cluster heterogeneity and NK cell maturation in β_2m$^{-/-}$ (MHC-I$^{-/-}$) mice. In MHC-I$^{-/-}$ spleens, the frequencies of NK cells expressing inhibitory Ly49I and Ly49G2 receptors increased, whereas the frequencies of NK cells expressing activating Ly49H and Ly49D receptors decreased (**Figure 6A**). These differences in Ly49 frequencies in MHC-I$^{-/-}$ mice did not appear to influence NK cell maturation (**Figure 6B**). MHC-I$^{-/-}$ mice displayed significantly lower frequencies of I-G2- NK cells (**Figure 6C and 6D**) and higher frequencies of H-D- NK cells (**Figure 6E and 6F**). Thus, NK cells from MHC-I$^{-/-}$ mice have decreased frequencies of activating receptors and increased frequencies of inhibitory receptors. The increased frequency of inhibitory receptor expressing NK cells is due to an increase in dual inhibitory receptor expressing I^{+}G2^{+} NK cells, as lower frequencies of I-G2+ NK cells were observed in MHC-I$^{-/-}$ mice (**Figure 6C-D**). Additionally, our activating receptor analysis showed that H+D- NK cells increased, whereas H+D+ cell frequencies decreased in MHC-I$^{-/-}$ mice (**Figure 6E-F**). Further investigation of individual Ly49 receptor frequencies as a function of iNK, tNK and mNK maturation stages revealed different behaviors of the inhibitory and activating Ly49 receptor behaviors in MHC-I$^{-/-}$ mice (**Figure 6G and 6H**). The frequencies of Ly49I+ and Ly49G2+ NK cells were significantly higher in MHC-I$^{-/-}$ mice compared to MHC-I$^{+/+}$ (wild-type) controls at each stage of NK maturation (**Figure 6G**). In contrast, the frequencies of Ly49H+ and Ly49D+ NK cells were significantly decreased only at the tNK and mNK stages, but similar at the iNK stage (**Figure 6H**). Overall, these data suggest MHC-I molecules play a differential role in the expression of inhibitory and activating Ly49 receptors, and that MHC-I is not essential for progression from iNK, tNK, and mNK stages during maturation.

We next compared NK cell cluster Ly49 receptor expression dependencies amongst WT and MHC-I$^{-/-}$ mice using the product rule. Any deviations between the two conditions (WT and MHC-I$^{-/-}$) would indicate dependencies which are influenced by MHC-I expression. We compared the product rule errors for each cluster in WT and MHC-I$^{-/-}$ mice, and observed significantly different errors in nine of the sixteen clusters in MHC-I$^{-/-}$ mice (**Figure 6I**). C1, C2, C5, C6, and C9 were found to increased error (e.g. more dependencies) in MHC-I$^{-/-}$ mice, and these clusters commonly express the activating Ly49D receptor (**Figure 6I**). In contrast, C10 (I-G2+H+D-), C12 (I+G2+H+D-), and C14 (I+G2-H-D-) in MHC-I$^{-/-}$ mice decreased dependencies (error) relative to WT, and do not express Ly49D. Furthermore, C15 (I-G2+H-D-) was the only cluster that flipped directionality of the error from being overestimated in WT to underestimated in MHC-I$^{-/-}$ mice. This suggest that Ly49G2 is negatively regulated in MHC-I sufficient microenvironments.

Next, we wanted to determine MHC-I's influence on NK cell cluster distributions. First, we examined NK cell frequencies based on the number of Ly49 receptors expressed, regardless of receptor type. Collectively, clusters that expressed only one receptor were increased at the iNK cell stage (**Supplemental Figure 2A**), but this increase was attributed to an increase in C15 only (**Figure 6J**). The frequencies of clusters which express two receptors were collectively lower at all stages of NK cell maturation in MHC-I$^{-/-}$ mice (**Supplemental Figure 2B)**, which was attributed to decreases in C1, C6, C7, and C11 clusters. C10 and C16, which also expressed 2 receptors, were increased in MHC-I$^{-/-}$ mice (**Figure 6J**). The overall increase in NK cells that express 3 receptors in MHC-I$^{-/-}$ mice was attributed to C12 (**Supplemental Figure 2C, Figure 6J**). All of the clusters that were increased (C15, C10, C16, and C12) express Ly49G2 (**Figure 6J**). Furthermore, C3, C1, C2, C5, C7, and C11, which lack Ly49G2 expression, were significantly decreased in NK cell frequencies (**Figure 6J**). These data suggest that MHC-I is a major regulator of Ly49G2 expression, despite the fact that no known MHC-I ligand for Ly49G2 in B6 mice has been described (3). In addition, Ly49G2-positive clusters C15, C10, C16, and C12 all lack Ly49D expression and were increased. In contrast, the Ly49G2-negative clusters C1, C2, C5, and C7, which express Ly49D, were decreased (**Figure 6J**). This suggests that there is a reciprocal dependency between Ly49D and Ly49G2 expression and MHC-I in the distribution of cluster frequencies. No common relationship between MHC-I deficiency and Ly49I or Ly49H on cluster distributions could be determined with our cluster frequency data set (**Figure 6J**).

We continued to investigate the influence of MHC-I on NK cell cluster frequencies found predominantly within the iNK, tNK, and mNK cell stage of maturation. Similar to the previous analysis in which we determined the predominant clusters within NK maturation stages (**Figure 3**), we compared MHC-$I^{-/-}$ and WT (MHC-$I^{+/+}$) clusters using PCA. We observed that most clusters in MHC-$I^{-/-}$ matched the same trends in cluster maturation found in WT mice (**Supplemental Figure 2D)**; however, C1, C2, and C16 maintained steady frequencies throughout maturation in MHC-$I^{-/-}$ mice (**Supplemental Figure 2F and 2G**). In WT mice, C15, C10, and C3 iNK-predominant clusters transition into C16, C12, and C11 (**Figure 4**). In MHC-$I^{-/-}$ mice, we observed increased C15 and C10 frequencies, matching the observed frequencies for C16 and C12. Furthermore, we observed decreased C3 and C11 frequencies (**Supplemental Figure 2E and 2G**). Additionally, tNK-predominant clusters C2 and C1 were both decreased in MHC-$I^{-/-}$ mice and their subsequent mNK clusters C7 and C5 were also both decreased (**Figure 6J**). Although tNK C4 was decreased, its subsequent cluster, C9, was found in normal frequencies at the mNK stage. C6 to C13 frequencies were also unaffected. Notably, C4, C9, C6 and C13 all co-express Ly49G2 and Ly49D. Overall, these data lend further support to the progressive pathways of NK cluster differentiation and suggest that MHC-I influences the cluster frequencies via regulation of Ly49G2 and Ly49D expression.

DISCUSSION

Previously, the product rule has been used to determine the interdependencies of inhibitory Ly49 receptors and their respective MHC-I ligand (8, 15). In this study, we extended this analysis to include the Ly49I inhibitory receptor in combination with activating receptors Ly49H and Ly49D, as well as a careful study of Ly49 receptor "clusters" based on NK cell maturation. Here, we show for the first time that the majority of the interdependencies in Ly49 receptor expression originate at the iNK cell maturation stage (8, 14), and that specific clusters predominate at each stage. Our results demonstrate strong interdependencies of the activating Ly49H and Ly49D receptors, which we propose can explain the altered cluster frequencies observed in MHC-$I^{-/-}$ mice. Moreover, our results further resolve a role for Ly49I as an important selective marker of completion of NK cell development in B6 mice (22).

Ly49I's known ligand in B6 mice is MHC-I K^b (3, 9, 26). Our NK cluster development studies suggest a process in which Ly49I-negative iNK and tNK clusters develop with high proliferative potential. We propose that when Ly49I is upregulated, transition into the mNK cell stage occurs, and proliferation is then inhibited by interactions between Ly49I and K^b. These observations are most

consistent with the “sequential expression model”, which proposes splenic NK cells sequentially accumulate inhibitory Ly49 receptors until receptors specific for self MHC-I molecules are expressed (14, 27, 28). We observed that Ly49I+ clusters become more prevalent overall at the mNK cell stage, indicating that NK cells also sequentially accumulate activating and non-self-binding Ly49 receptors before expressing Ly49I. Consistent with previous findings, we observed decreased mNK cell proliferation relative to iNK and tNK cells (**2**), which may suggest that self-inhibitory Ly49I completes the maturation process and maintains mNK cells in a quiescent state ready to be triggered in an immune response.

Our data expand the sequential expression model and suggest an updated working model in which MHC-I affects NK cell Ly49 activating and inhibitory receptor expression and alters the progressive pathways of NK cluster differentiation, but via distinct mechanisms. Our model distinguishes between the differentiation of clusters expressing only inhibitory (**Figure 6L-M**), or only activating receptors at an early maturation stage (**Figure 6N-6O**). In this working model, we focus on the Ly49 receptor interactions at the iNK and tNK stages of maturation that result in upregulation of Ly49I to complete NK cell maturation. In **Figure 6L**, in the predominant iNK cluster that expresses inhibitory Ly49G2 but no activating receptors (C15), Ly49G2 inhibitory signals are not initiated (because there is no Ly49G2 ligand in B6 mice). Due to this lack of inhibitory signal, developing NK cells then upregulate inhibitory receptor Ly49I (differentiating to C16). Ly49I binds to its H-2K^{b} ligand, and in turn, C16 NK cell development is completed and then sustained (**Figure 6L**). The increased frequencies of C15 and C16 observed in MHC-I$^{-/-}$ mice (**Figure 6I**) can be explained by this model (**Figure 6M**). In MHC-I$^{-/-}$ mice, the C15 cluster upregulates Ly49I in the same fashion as in WT mice. However, Ly49I inhibitory signals are not generated (because H-2K^{b} is not present) and the developing C15 cluster continues to expand (**Figure 6M**). Extending this working model to clusters that co-express a single activating Ly49 receptor with Ly49G2 suggests that Ly49H and Ly49D regulate cluster frequencies differently, as C10 (G2+H+D-I-) and its mature counterpart C12 (G2+H+D-I+) are both increased in MHC-I$^{-/-}$ mice, whereas frequencies of C6 (G2+D+H-I-) and its counterpart C13 (G2+D+H-I+) are unaffected. This suggests that the Ly49H+ clusters are controlled by presence of MHC-I. However, C4, which expresses both activating receptors (G2+H+D+I-), was lower in frequency in MHC-I$^{-/-}$ mice, but frequencies of its counterpart C9 (G2+H+D+I+) were normal. This indicates that the roles of Ly49H and Ly49D during NK cell development are complex, and MHC-I is not essential for some of these roles.

Our accompanying working model of NK cell development starting with clusters expressing only activating receptors at the iNK and tNK stages is shown in **Figure 6N**. The known ligand for Ly49H is m157, a mouse cytomegalovirus MHC-like protein (2, 29), while the known ligand for Ly49D is H-2D^{d}. No known self-MHC-I ligand has been identified for Ly49H and Ly49D in B6 mice (30), but it is possible weak binding to self-MHC-I or non-MHC-I ligands exist (31, 32). Freund et al. reported that activation signals via SLP-76 upregulates inhibitory Ly49A, Ly49G2, and Ly49I receptor expression (10). Similarly, we presume that in B6 mice, an activating ligand exists for Ly49H and Ly49D. NK clusters with one activating receptor (e.g. C2, C3) will generate a signal in response to this activating ligand, which promotes its differentiation and expansion. The activating signal also results in upregulation of inhibitory Ly49I at the mNK stage (**Figure 6N**). We interpret the clear effects of MHC-I deficiency on Ly49H and Ly49D frequencies to demonstrate a relationship between MHC-I and the activating receptors, but that this is not a direct ligand-receptor interaction. NK cell development and NK cell survival in MHC-I-deficient mice may be impaired by dysfunctional dendritic cell expression of IL-12 and IL-15 transpresentation **(**33, 34). In MHC-I$^{-/-}$ mice, we assume the activating ligand is absent or signaling is impaired. In the absence of these signals, low expansion and impaired differentiation to the corresponding mNK cluster in MHC-I$^{-/-}$ mice results. Lack of activating signals in MHC-I$^{-/-}$ also dysregulates the expression of Ly49I at the mNK stage (**Figure 6O**). We observed an enhanced decrease in cluster frequencies in MHC-I$^{-/-}$ mice when two activating receptors were expressed (C1 and C5), which we posit could result from lower expansion of dual H+D+ clusters (**Figure 6I**). However, C9, which is H+D+ and also co-expresses both inhibitory receptors, is unaffected in the MHC-I$^{-/-}$, suggesting a “canceling out” or “balancing” of activating and inhibitory signals in this case. This balancing is further supported by the similar frequencies of C6 and its mNK counterpart C13, which express one inhibitory and activating receptor, in B6 and MHC-I$^{-/-}$ mice (**Figure 6I)**.

In our study, we focused on the role of Ly49 receptors on NK cell development. However, given that NK cytotoxicity is governed by balance of signals between Ly49 activating and inhibitory receptors **(3)**, it is also possible that our evidence of progressive NK cell developmental pathways can be applied to the identification of NK cell clusters with high cytotoxic potential. Transcription of cytotoxicity genes increases with NK maturation with the highest cytotoxic gene expression at the mNK stage (22, 23). NK cell licensing via the expression of Ly49I and its binding to K^{b} is consistent with our observations that mNK cells acquire Ly49I expression in a manner that correlates to NK cell maturation.

Although we have focused on splenic NK cells in our work, it is also noteworthy that mice and human NK cell maturation are could be tissue-specific, which may change the NK cell Ly49 cluster pathways we observed in the spleen (22, 35). Although NK cells originate in the bone marrow, they continue to mature in peripheral tissues. However, these tissues have been shown to express different frequencies of iNK, tNK, and mNK cells (22, 36). The bone marrow and lymph node tend to express high frequencies of iNK and tNK cells, whereas the lung compartment expresses mostly mNK cells. The spleen, liver and blood tend to express all three stages of NK cell maturation (22). Additional studies are necessary to determine if the progressive pathways of NK development we observed in the spleen are conserved in other tissues.

ACKNOWLEDGMENTS

We thank the staff of the Department of Animal Research Services and the Flow Cytometry Core of the Stem Cell Instrumentation Foundry at the University of California Merced for excellent animal care and technical support. We thank Dr. Kirk Jensen with the gift of rm-IL-15 and Dr. Anna Beaudin for sharing flow cytometry reagents. We are also grateful to Drs. Marcos E. García-Ojeda and Katrina K. Hoyer, as well as the UC Merced Immunology Journal Club for their comments on the manuscript.

REFERENCES

1. Chiossone, L., J. Chaix, N. Fuseri, C. Roth, E. Vivier, and T. Walzer. 2009. Maturation of mouse NK cells is a 4-stage developmental program. *Blood* 113: 5488-5496.
2. Nabekura, T., and L. L. Lanier. 2016. Activating Receptors for Self-MHC Class I Enhance Effector Functions and Memory Differentiation of NK Cells during Mouse Cytomegalovirus Infection. *Immunity* 45: 74-82.
3. Meza Guzman, L. G., N. Keating, and S. E. Nicholson. 2020. Natural Killer Cells: Tumor Surveillance and Signaling. *Cancers (Basel)* 12.
4. Lanier, L. L. 2003. Natural killer cell receptor signaling. *Current Opinion in Immunology* 15: 308-314.
5. He, Y., and Z. Tian. 2017. NK cell education via nonclassical MHC and non-MHC ligands. *Cell Mol Immunol* 14: 321-330.
6. Joncker, N. T., N. C. Fernandez, E. Treiner, E. Vivier, and D. H. Raulet. 2009. NK cell responsiveness is tuned commensurate with the number of inhibitory receptors for self-MHC class I: the rheostat model. *J Immunol* 182: 4572-4580.
7. Jaeger, B. N., and E. Vivier. 2012. Natural killer cell tolerance: control by self or self-control? *Cold Spring Harb Perspect Biol* 4.
8. Sternberg-Simon, M., P. Brodin, Y. Pickman, B. Onfelt, K. Karre, K. J. Malmberg, P. Hoglund, and R. Mehr. 2013. Natural killer cell inhibitory receptor expression in humans and mice: a closer look. *Front Immunol* 4: 65.
9. Schenkel, A. R., L. C. Kingry, and R. A. Slayden. 2013. The ly49 gene family. A brief guide to the nomenclature, genetics, and role in intracellular infection. *Front Immunol* 4: 90.
10. Freund, J., R. M. May, E. Yang, H. Li, M. McCullen, B. Zhang, T. Lenvik, F. Cichocki, S. K. Anderson, and T. Kambayashi. 2016. Activating Receptor Signals Drive Receptor Diversity in Developing Natural Killer Cells. *PLoS Biol* 14: e1002526.
11. McCullen, M. V., H. Li, M. Cam, S. K. Sen, D. W. McVicar, and S. K. Anderson. 2016. Analysis of Ly49 gene transcripts in mature NK cells supports a role for the Pro1 element in gene activation, not gene expression. *Genes Immun* 17: 349-357.
12. Olsson-Alheim, Y. M., M. Salcedo, G. H. Ljunggren, K. Kärre, and L. C. Sentman. 1997. NK cell receptor calibration: effects of MHC class I induction on killing by Ly49Ahigh and Ly49Alow NK cells. *J Immunol* 159: 3189-3194.

13. Salcedo, M., D. A. Diehl, Y. M. Olsson-Alheim, J. Sundbäck, L. Van Kaer, K. Kärre, and G. H. Ljunggren. 1997. Altered expression of Ly49 inhibitory receptors on natural killer cells from MHC class I-deficient mice. *J Immunol* 158: 3174-3180.
14. Raulet, H. D., W. Held, I. Correa, J. R. Dorfman, M. Wu, and L. Corral. 1997. Specificity, tolerance and developmental regulation of natural killer cells defined by expression of class I-specific Ly49 receptors. *Immunological Reviews* 155: 41-52.
15. Watzl, C., M. Sternberg-Simon, D. Urlaub, and R. Mehr. 2012. Understanding natural killer cell regulation by mathematical approaches. *Front Immunol* 3: 359.
16. Forbes, C. A., A. A. Scalzo, M. A. Degli-Esposti, and J. D. Coudert. 2016. Ly49C Impairs NK Cell Memory in Mouse Cytomegalovirus Infection. *J Immunol* 197: 128-140.
17. Smith, H. R., H. H. Chuang, L. L. Wang, M. Salcedo, W. J. Heusel, and W. M. Yokoyama. 2000. Nonstochastic Coexpression of Activating Receptors on Murine Natural Killer Cells. *J. Exp. Med.* 191: 1341-1354.
18. Millan, A. J., S. R. Elizaldi, E. M. Lee, J. O. Aceves, D. Murugesh, G. G. Loots, and J. O. Manilay. 2019. Sostdc1 Regulates NK Cell Maturation and Cytotoxicity. *J Immunol*.
19. Mair, F., F. J. Hartmann, D. Mrdjen, V. Tosevski, C. Krieg, and B. Becher. 2016. The end of gating? An introduction to automated analysis of high dimensional cytometry data. *Eur J Immunol* 46: 34-43.
20. Van der Maaten, L., and G. Hinton. 2008. Visualizing Data using t-SNE. *Journal of Machine Learning Research* 9: 2579-2605.
21. Held, W., J. R. Dorfman, M. Wu, and D. H. Raulet. 1996. Major histocompatibility complex class I- dependent skewing of the natural killer cell Ly49 receptor reportoire. *Eur. J. Immunol.* 26: 2286-2292.
22. Hayakawa, Y., and M. J. Smyth. 2006. CD27 dissects mature NK cells into two subsets with distinct responsiveness and migratory capacity. *J Immunol* 176: 1517-1524.
23. Kim, S., K. Iizuka, H. S. Kang, A. Dokun, A. R. French, S. Greco, and W. M. Yokoyama. 2002. In vivo developmental stages in murine natural killer cell maturation. *Nat Immunol* 3: 523-528.
24. Pedregosa, F., G. Varoquaux, A. Gramfort, V. Michel, and B. Thirion. 2011. Scikit-learn: Machine Learning in Python. *Journal of Machine Learning Research* 12.

25. Zhang, T., S. Liu, P. Yang, C. Han, J. Wang, J. Liu, Y. Han, Y. Yu, and X. Cao. 2009. Fibronectin maintains survival of mouse natural killer (NK) cells via CD11b/Src/beta-catenin pathway. *Blood* 114: 4081-4088.
26. Dimasi, N., M. W. Sawicki, L. A. Reineck, Y. Li, K. Natarajan, D. H. Margulies, and R. A. Mariuzza. 2002. Crystal Structure of the Ly49I Natural Killer Cell Receptor Reveals Variability in Dimerization Mode Within the Ly49 Family. *Journal of Molecular Biology* 320: 573-585.
27. Roth, C., R. J. Carlyle, H. Takizawa, and H. D. Raulet. 2000. Clonal Acquisition of Inhibitory Ly49 Receptors on Developing NK Cells Is Successively Restricted and Regulated by Stromal Class I MHC. *Immunity* 13: 143-153.
28. Fahlen, L., U. Lendahl, and C. L. Sentman. 2001. MHC class I-Ly49 interactions shape the Ly49 repertoire on murine NK cells. *J Immunol* 166: 6585-6592.
29. Tripathy, S. K., H. R. Smith, E. A. Holroyd, J. T. Pingel, and W. M. Yokoyama. 2006. Expression of m157, a murine cytomegalovirus-encoded putative major histocompatibility class I (MHC-I)-like protein, is independent of viral regulation of host MHC-I. *J Virol* 80: 545-550.
30. Pegram, H. J., D. M. Andrews, M. J. Smyth, P. K. Darcy, and M. H. Kershaw. 2011. Activating and inhibitory receptors of natural killer cells. *Immunol Cell Biol* 89: 216-224.
31. Berry, R., N. Ng, P. M. Saunders, J. P. Vivian, J. Lin, F. A. Deuss, A. J. Corbett, C. A. Forbes, J. M. Widjaja, L. C. Sullivan, A. D. McAlister, M. A. Perugini, M. J. Call, A. A. Scalzo, M. A. Degli-Esposti, J. D. Coudert, T. Beddoe, A. G. Brooks, and J. Rossjohn. 2013. Targeting of a natural killer cell receptor family by a viral immunoevasin. *Nat Immunol* 14: 699-705.
32. Idris, H. A., H. R. Smith, M. H. L., R. J. Ortaldo, A. A. Scalzo, and W. M. Yokoyama. 1999. The natural killer gene complex genetic locus Chok encodes Ly-49D, a target recognition receptor that activates natural killing. *Proceedings of the National Academy of Sciences of the United States of America* 96: 6330-6335.
33. Zitvogel, L., E. Maraskovsky, T. Tursz, M. Perricaudet, M. Suter, D. Bellet, P. Ricciardi-Castagnoli, C. Flament, A. Lozier, and N. C. Fernandez. 1999. Dendritic cells directly trigger NK cell functions: Cross-talk relevant in innate anti-tumor immune responses *in vivo*. *Nature Medicine* 5.
34. Lee, G. A., Y. H. Liou, S. W. Wang, K. L. Ko, S. T. Jiang, and N. S. Liao. 2011. Different NK cell developmental events require different levels of IL-15 trans-presentation. *J Immunol* 187: 1212-1221.

35. Dogra, P., C. Rancan, W. Ma, M. Toth, T. Senda, D. J. Carpenter, M. Kubota, R. Matsumoto, P. Thapa, P. A. Szabo, M. M. Li Poon, J. Li, J. Arakawa-Hoyt, Y. Shen, L. Fong, L. L. Lanier, and D. L. Farber. 2020. Tissue Determinants of Human NK Cell Development, Function, and Residence. *Cell* 180: 749-763 e713.
36. Orr, M. T., W. J. Murphy, and L. L. Lanier. 2010. 'Unlicensed' natural killer cells dominate the response to cytomegalovirus infection. *Nat Immunol* 11: 321-327.

FOOTNOTES

[1] This work was supported by University of California (UC) Merced faculty research funding and UC graduate student fellowships (to A.J.M.).

Abbreviations: β_2m: beta-2-microglobulin; C: cluster; iNK: immature NK; Lin: Lineage; MHC-I: MHC class I; mNK: most mature NK; PCA: principal component analysis; tNK: transitional NK; tSNE: t-stochastic neighbor embedding

FIGURE LEGENDS

Figure 1. Identification of NK cell cluster phenotypic heterogeneity in B6 mice. (**A**) Frequencies of Ly49I, Ly49G2, Ly49H, and Ly49D receptors on Lin- (negative for CD3, CD4, CD8, CD19, Gr1, and Ter119), NK1.1+ gated cells. Asterisks indicate statistically significant differences between means as determined by the Student's *t*-test. ****p < 0.0001 ; (**B**) Representative flow cytometry histogram plots of Ly49 receptor expression shown in A; (**C**) Table of NK cell clusters defined by expression of Ly49 receptors, ordered from most activating (C1) to most inhibitory (C16) based on the number of activating or inhibitory receptors expressed; (**D**) tSNE color mapping plots in red for clusters with Ly49I, Ly49G2, Ly49H, and Ly49D receptor expression; (**E**) Manual gating of 16 NK cell Ly49 clusters gated on live, Lin-NK1.1+ cells; (**F**) Representative unbiased clustering of the 16 clusters visualized by tSNE; (**G**) Frequencies of each cluster in the Lin^- $NK1.1^+$ population. Each point of the graph represents an individual mouse of two separate experiments.

Figure 2. Higher interdependence of NK cell Ly49 cluster frequencies at the iNK stage. (**A**) Example of the product rule calculations of independent probability for NK cells that express Ly49H and Ly49D (H,D) out of three receptors observed. **(B)** Summary graph of experimental (observed) cluster frequencies and cluster frequencies predicted by the product rule (predicted); (**C**) Graph of NK cell log_2(observed/predicted) error grouped by activating Ly49 receptors; (**D**) Representative flow cytometry plot of CD27 and CD11b staining to distinguish stages of NK cell maturation; (**E**) Total error was calculated by the sum of the absolute values of log_2(observed/predicted) from all clusters found at each NK maturation stage determined by the product rule and observed frequencies (iNK, white bars, tNK, gray bars and mNK, black bars); (**F-G**) Total product rule for NK cells organized by expression of (**F**) activating receptors or (**G**) inhibitory receptors; (**H-J**) Log_2(observed/predicted) error plots for each cluster found in (**H**) iNK, (**I**) tNK, and (**J**) mNK cell stages of maturation. Positive error values indicate underestimation while negative values indicate overestimation. Each point on the graph represents an individual mouse. Asterisks indicate statistically significant differences between means as determined by the Student *t* test. **p < 0.01, ***p < 0.001, ****p < 0.0001.

Figure 3. Certain NK clusters predominate at each stage of NK cell maturation. (**A**) Map of cluster location via tSNE plot; (**B-D**) Representative tSNE

plots of (**B**) iNK, (**C**) tNK, and (**D**) mNK cells visualized by density; (**E**) Summary graph of Ly49I, Ly49G2, Ly49H, and Ly49D receptor frequencies gated on iNK (white bars), tNK (gray bars), or mNK cells (black bars); (**F**) Summary graph of each NK cell maturation stage expressing 0, 1, 2, 3, or 4 Ly49 receptors; (**G**) PCA plots were generated from 4 biological replicates of average percentage for clusters with respect to NK cell maturation stage; (**H-J**) Summary graph of each calculated cluster percentage for each cluster at (**H**) iNK, (**I**) tNK, (**J**) and mNK cell stage. Each point of the graph represents an individual mouse. Asterisks indicate statistically significant differences between means as determined by the Student *t* test. *$p < 0.05$.

Figure 4. Evidence for progressive pathways of NK cell cluster differentiation in vitro and in vivo. (**A**) Scheme of experimental design for sorting clusters and in vitro culture; (**B-C**) Representative Ly49I vs. Ly49G2 flow cytometry plots of sorted clusters showing post-sort purity on Day 0 (top row) and 4-days after culture (bottom row) of gated NK1.1+ cells; (**B**) Differentiation of clusters predominantly found at the iNK stage, (**C**) differentiation of clusters predominantly found at the tNK stages: (**D**) Summary graph of cluster Ly49I receptor expression after Day 4 of culture, calculated by subtracting Day 4 Ly49I frequency from Day 0 Ly49I frequency; (**E**) Scheme of experimental design of in vivo adoptive transfer of selected NK clusters; (**F-H**) Representative Ly49I vs. Ly49G2 flow cytometry plots of sorted clusters for post-sort purity of gated NK cells on Day 0 (top row) and Day 4 after adoptive transfer into recipient mice (bottom row); (**F**) In vivo differentiation of clusters predominantly found at the iNK stage; (**G**) In vivo differentiation of clusters predominantly found at the tNK stage, and (**H**) in vivo differentiation of C14, found predominantly in mNK; (**I**) Summary graph of cluster Ly49I receptor expression 4 days after adoptive transfer, calculated as in D. Each point of the graph represents an experimental replicate; (**J**) Schematic summary of progressive pathways from iNK-predominant clusters; (K) Summary of progressive pathways from tNK-predominant clusters.

Figure 5. Immature NK cells display in vitro characteristics of proliferation, regardless of cluster type. (A) Scheme of experimental design to sort and culture iNK ($CD27^+CD11b^-$), tNK ($CD27^+CD11b^+$), and mNK ($CD27^-CD11b^+$) cells; (**B-E**) NK cell proliferation as determined by flow cytometry and calculating the fold change in cellularity between Day 2 and Day 6 of culture (e.g. # of cells at Day 6 divided by # of cells at Day 2) for (**B**) overall cell proliferation, proliferation in

cultures initiated with sorted (**C**) iNKs, (**D**) tNKs, and (**E**) mNKs, further categorized into predominant iNK, tNK, and mNK clusters (n=3 experimental replicates; (**F**) Fold change in proliferation for clusters that originated from sorted iNK cells; (**G**) Intracellular Ki-67 expression of Lin^- $NK1.1^+$ $CD27^+$ (iNK and tNK stages) and Lin^- $NK1.1^+$ $CD27^-$ (mNK stage) cells post-culture (n=2 female mice (triangles; 24 weeks old), n=2 male mice (circles; 19 weeks old); (**H**) Summary plots of Ki-67 expression between $CD27^+$ or $CD27^-$ NK cells: (**I**) Ki-67 expression on $CD27^+$ and $CD27^-$ NK cells disaggregated by Ly49 receptor type, and (**J**) Ki-67 expression on NK cells disaggregated by cluster type. Asterisks indicate statistically significant differences between means as determined by the Student*'s t* test. *p < 0.05, **p < 0.01, ****p < 0.0001.

Figure 6. Altered NK cell cluster distribution in MHC-$I^{-/-}$ mice. (**A**) Summary graph of Ly49I, Ly49G2, Ly49H, and Ly49D frequencies gated on $NK1.1^+$ cells in $\beta_2m^{-/-}$ (MHC-$I^{-/-}$) and B6 (MHC-$I^{+/+}$) spleens; (**B**) Graph of frequencies of iNK ($CD27^+CD11b^-$), tNK ($CD27^+CD11b^+$), and mNK ($CD27^-CD11b^+$) cells; (**C,E**) Representative plots of $Lin^-NK1.1^+$ cells examining (**C**) Ly49I and Ly49G2 and (**E**) Ly49H and Ly49D in MHC-$I^{+/+}$ (left) and MHC-$I^{-/-}$ mice; (**D,F**) Summary plots for data shown C and E; (**G**) Graphs gated on parent iNK, tNK or mNK gate for Ly49I and Ly49G2; (**H**) Graph gated on parent iNK, tNK or mNK gate for Ly49H and Ly49D; (**I**) Log2(observed/expected) values for MHC-$I^{-/-}$ and MHC-$I^{+/+}$ NK cell clusters; (**J**) Graph of NK cell cluster frequencies in MHC-$I^{+/+}$ and MHC-$I^{-/-}$ mice; (**K-N**) Working model illustrating MHC-I's influence on NK cell pathways for clusters expressing only inhibitory receptors (**K-L)** or activating receptors (**M-N**); (**K and M**) model of cluster pathways in MHC-$I^{+/+}$ mice; (**L and N**) model of cluster pathways in MHC-$I^{-/-}$ mice. Each point of the graph represents an individual mouse. Asterisks indicate statistically significant differences between means as determined by the Student *t* test. *p < 0.05, **p < 0.01, ***p < 0.001, ****p < 0.0001.

FIGURES AND FIGURE LEGENDS

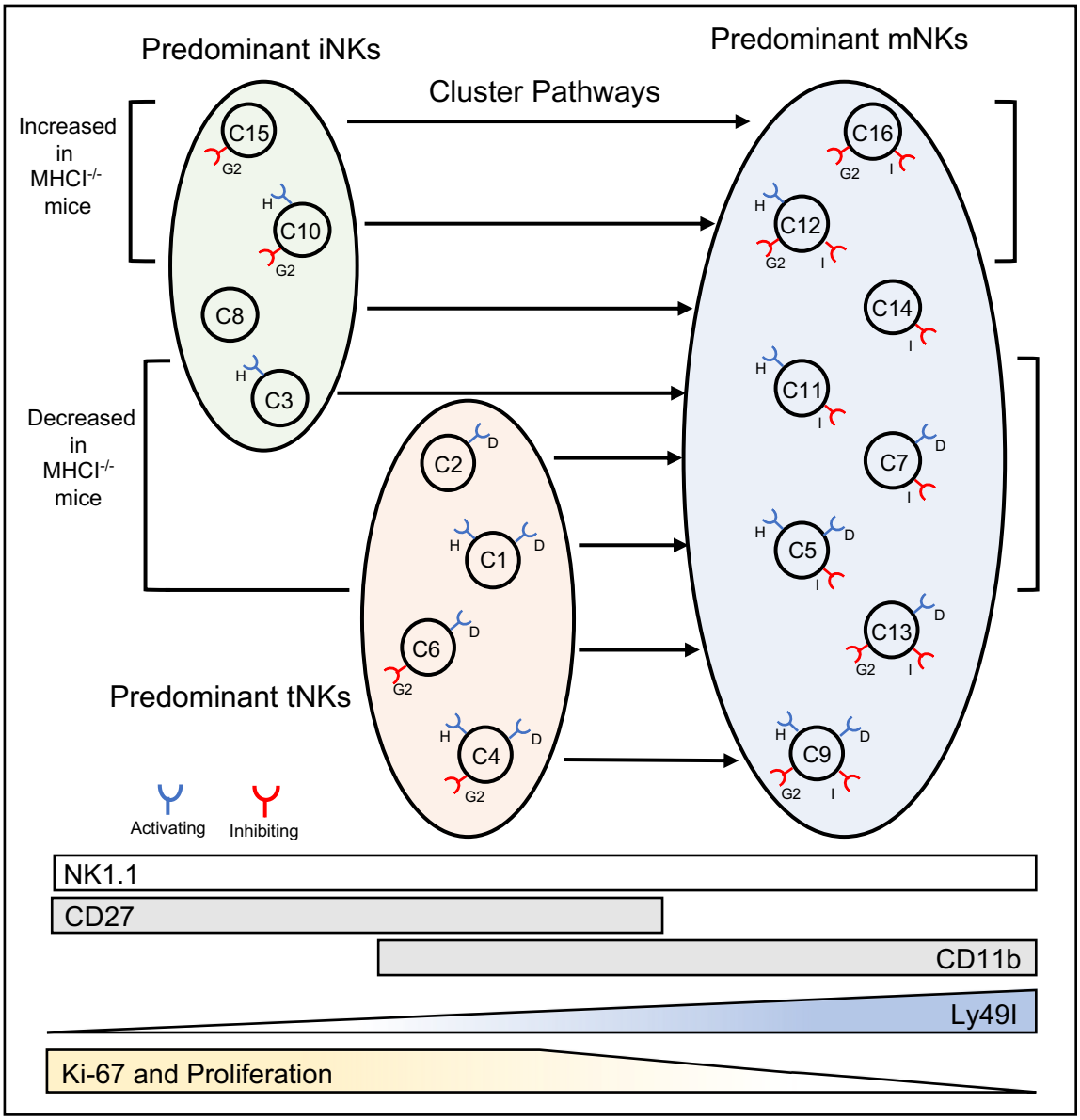

Figure 3: Graphical Abstract for Chapter 3. Representative image from the conclusions discovered in chapter 3 of this dissertation.

Millan et al. 2020. Figure 1

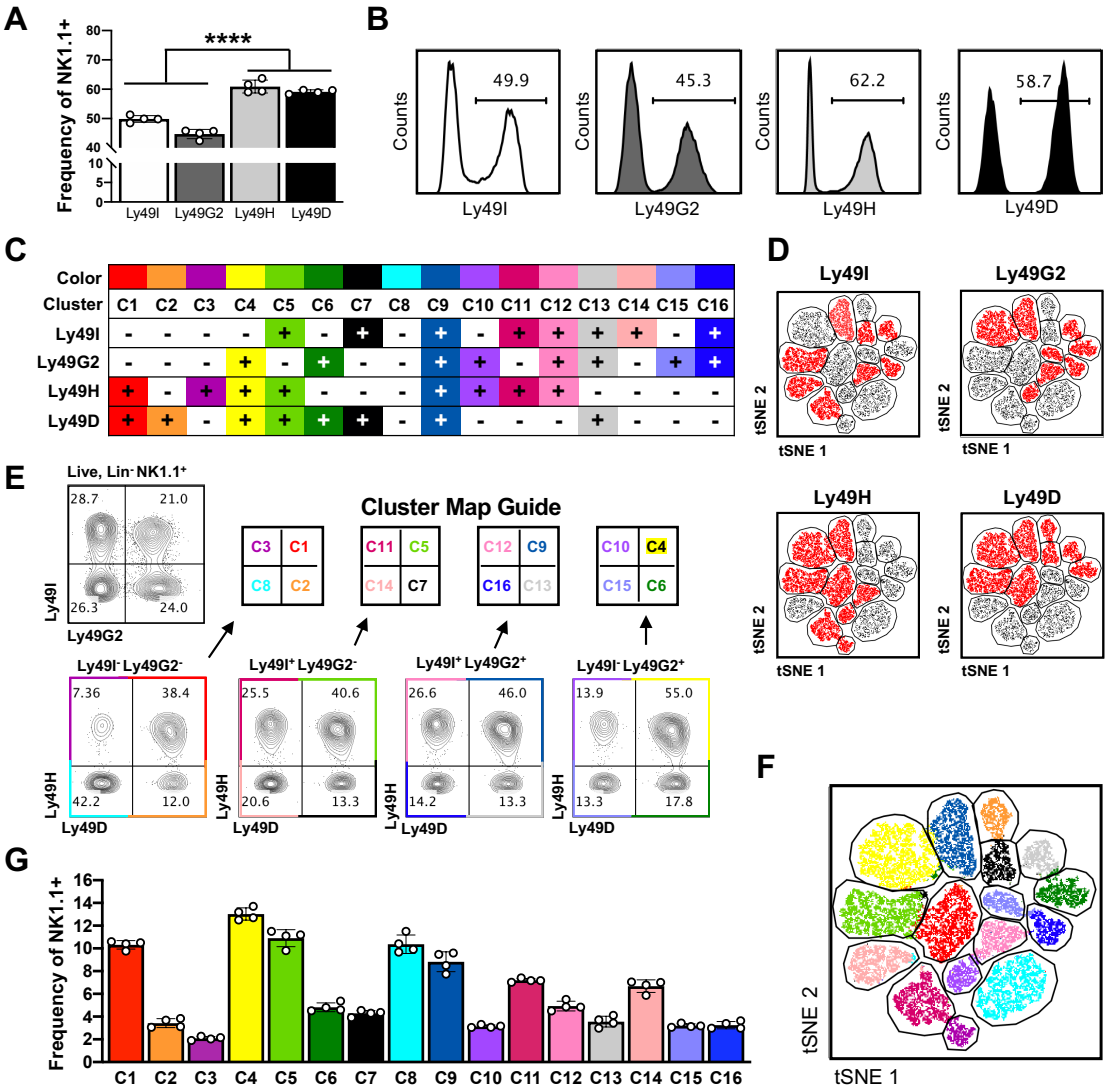

Millan et al. 2020. Figure 2

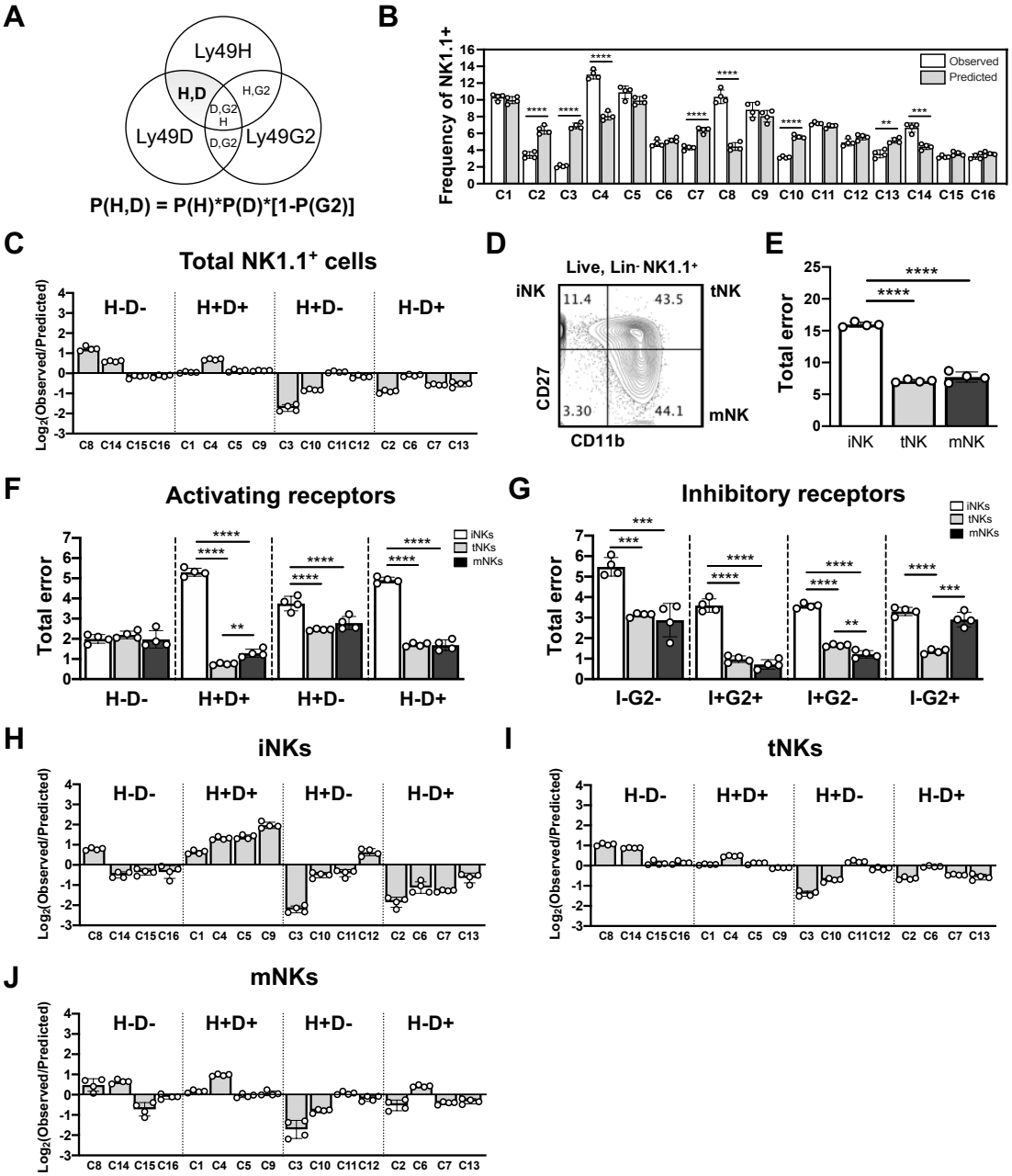

Millan et al. 2020. Figure 3

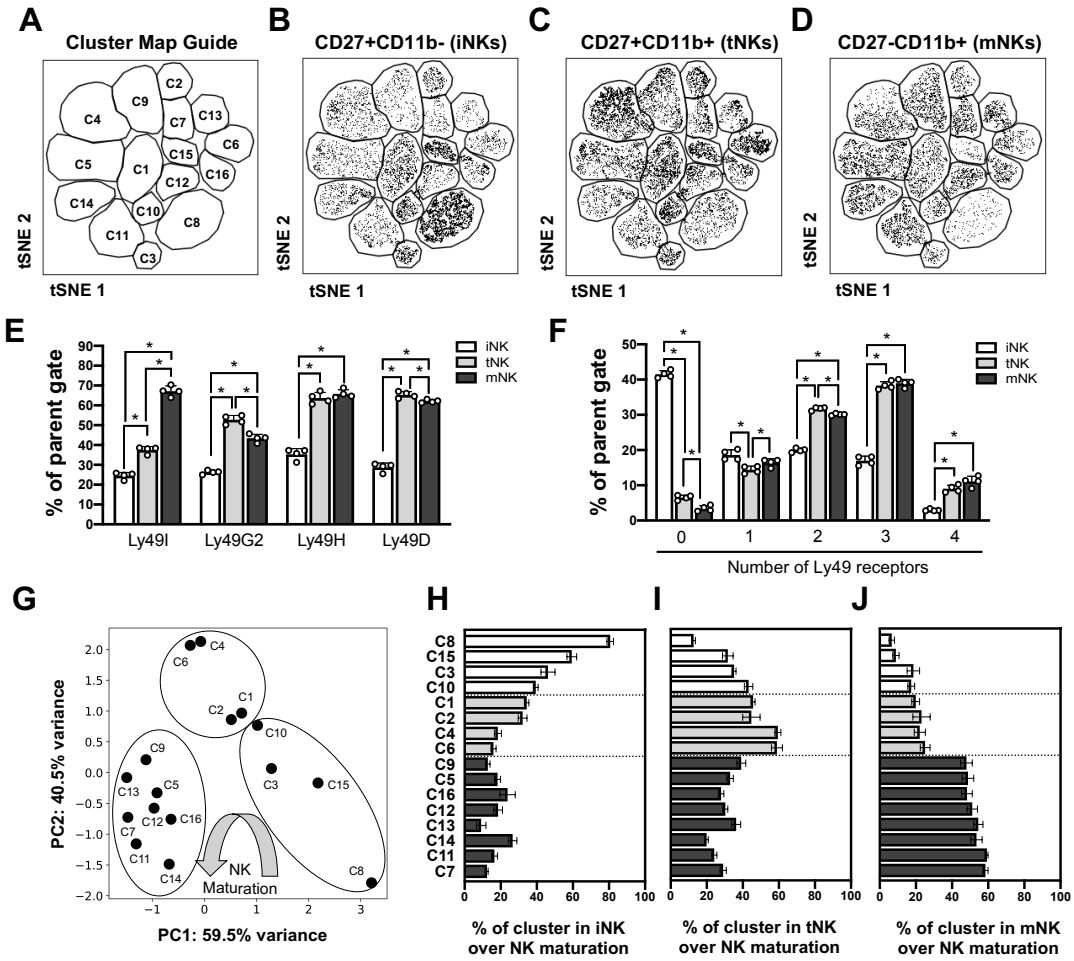

Millan et al. 2020. Figure 4

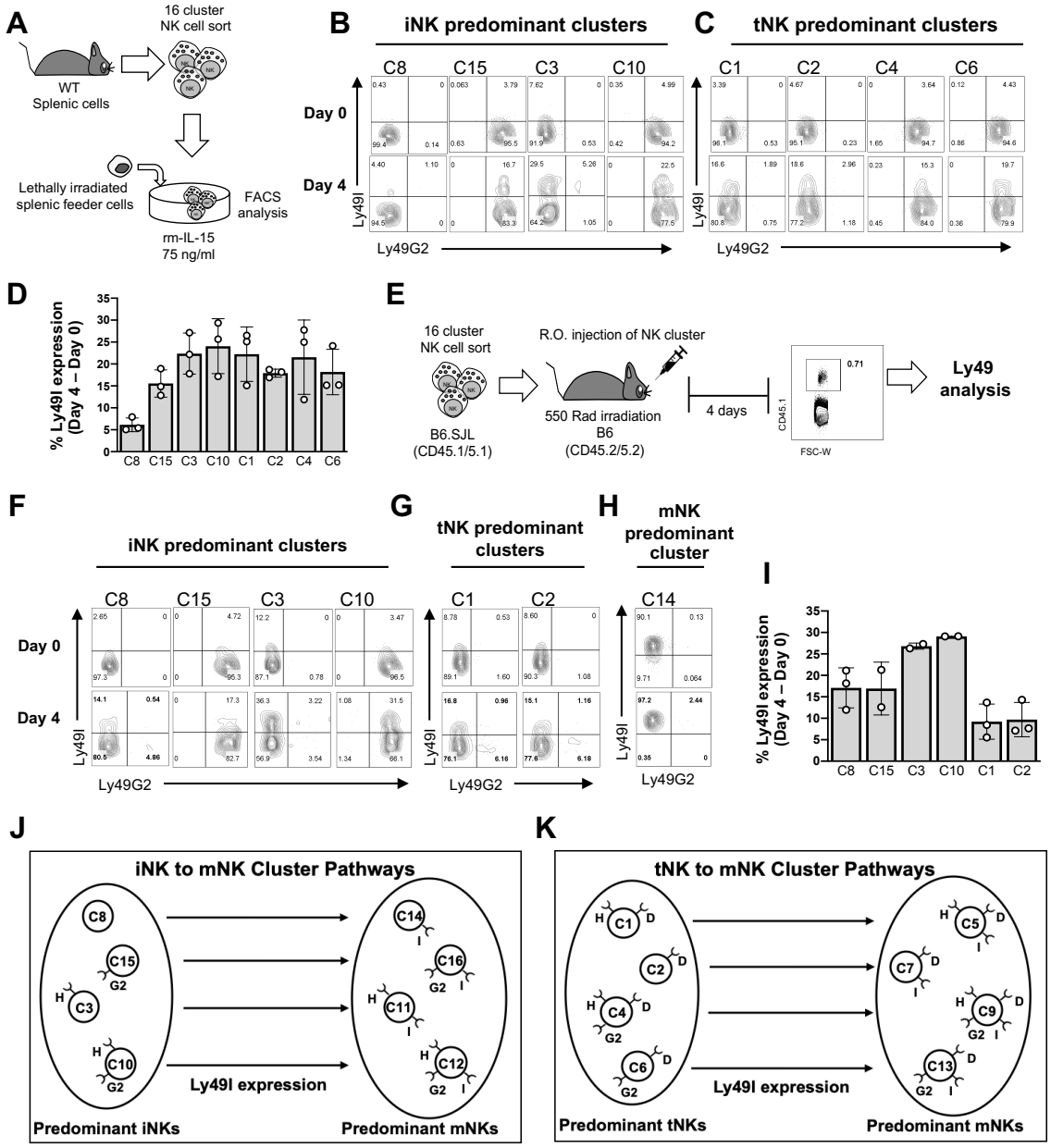

Millan et al. 2020. Figure 5

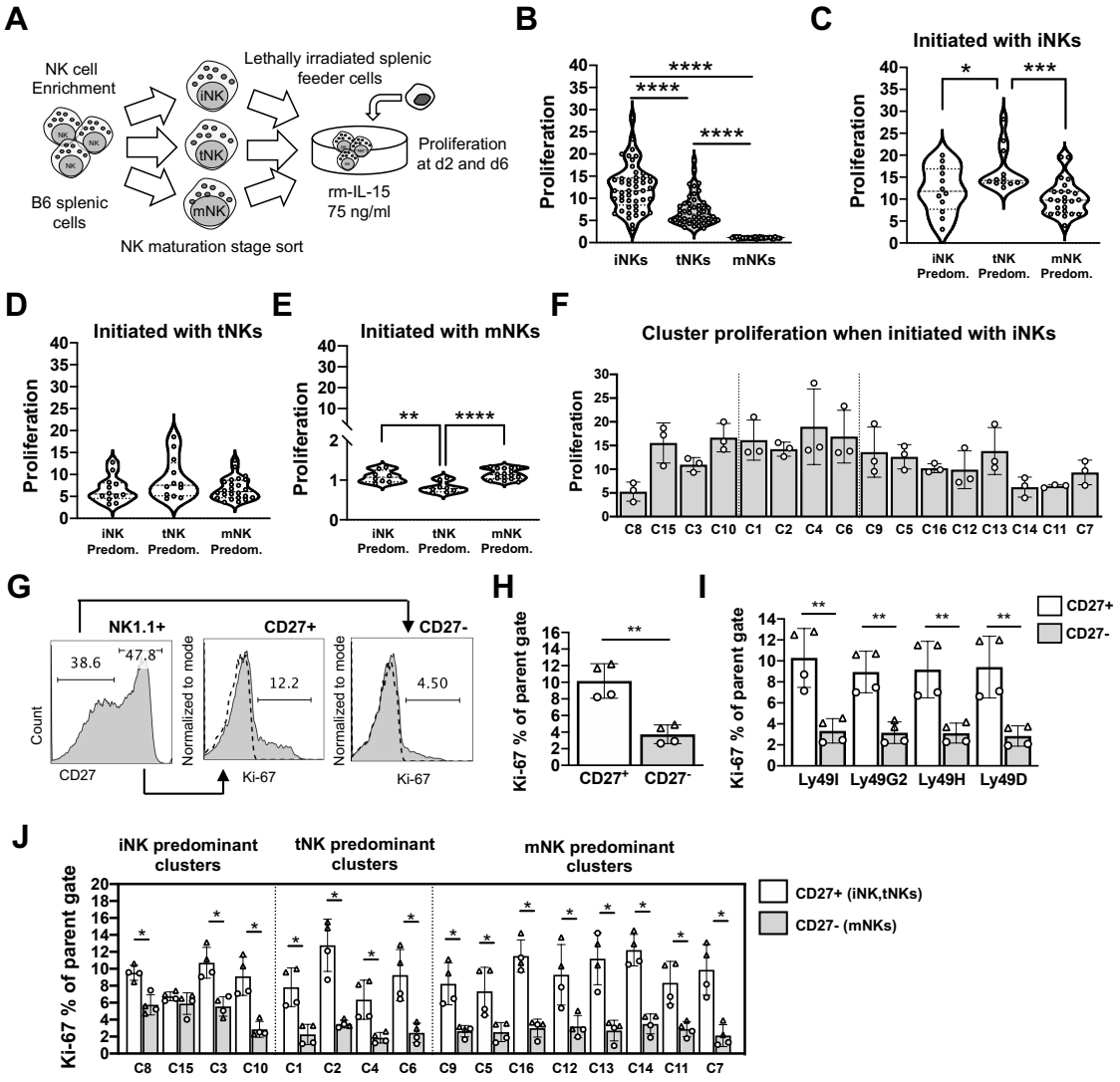

Millan et al. 2020. Figure 6

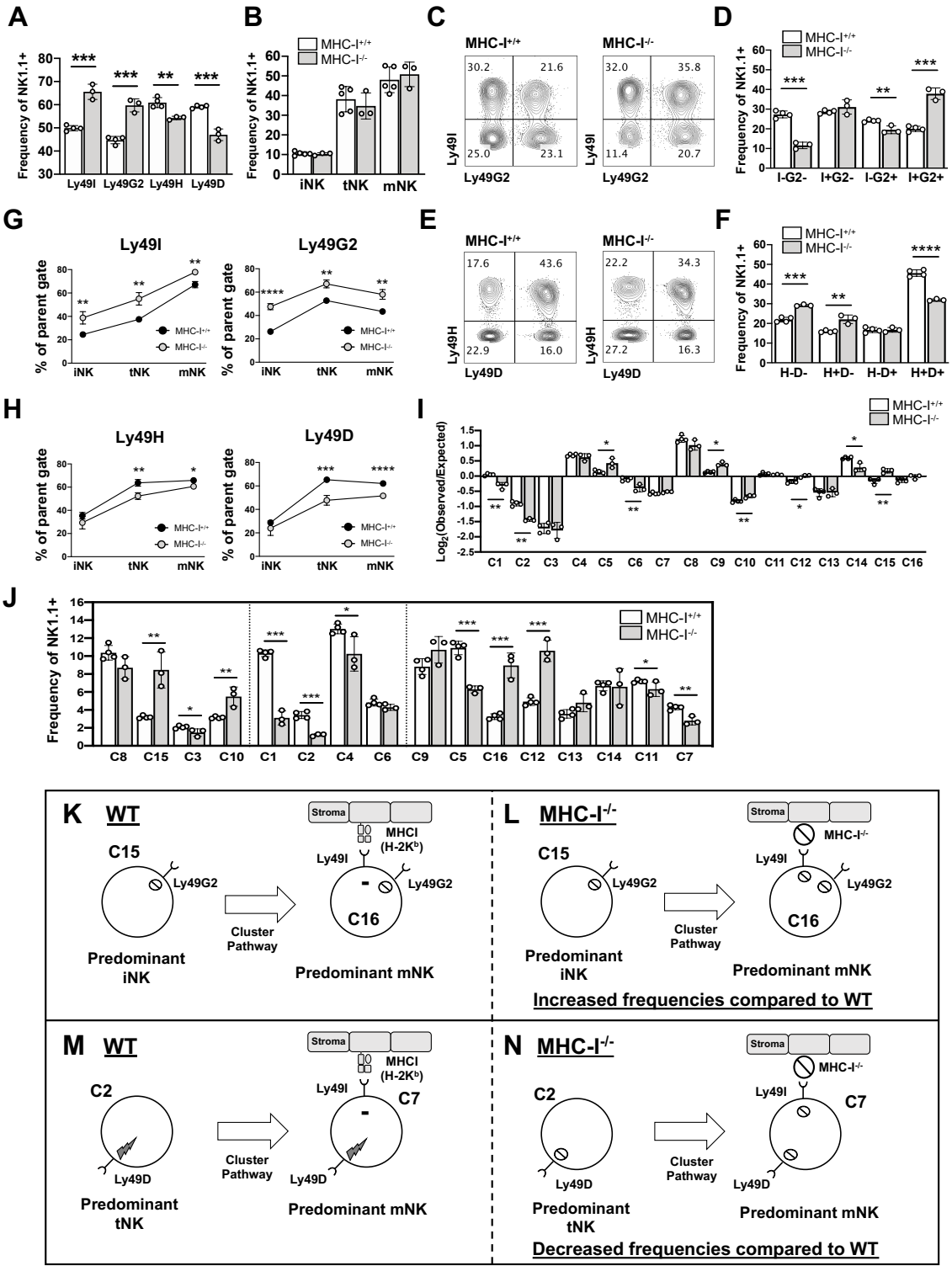

Millan et al. 2020. Supplemental Figure 1

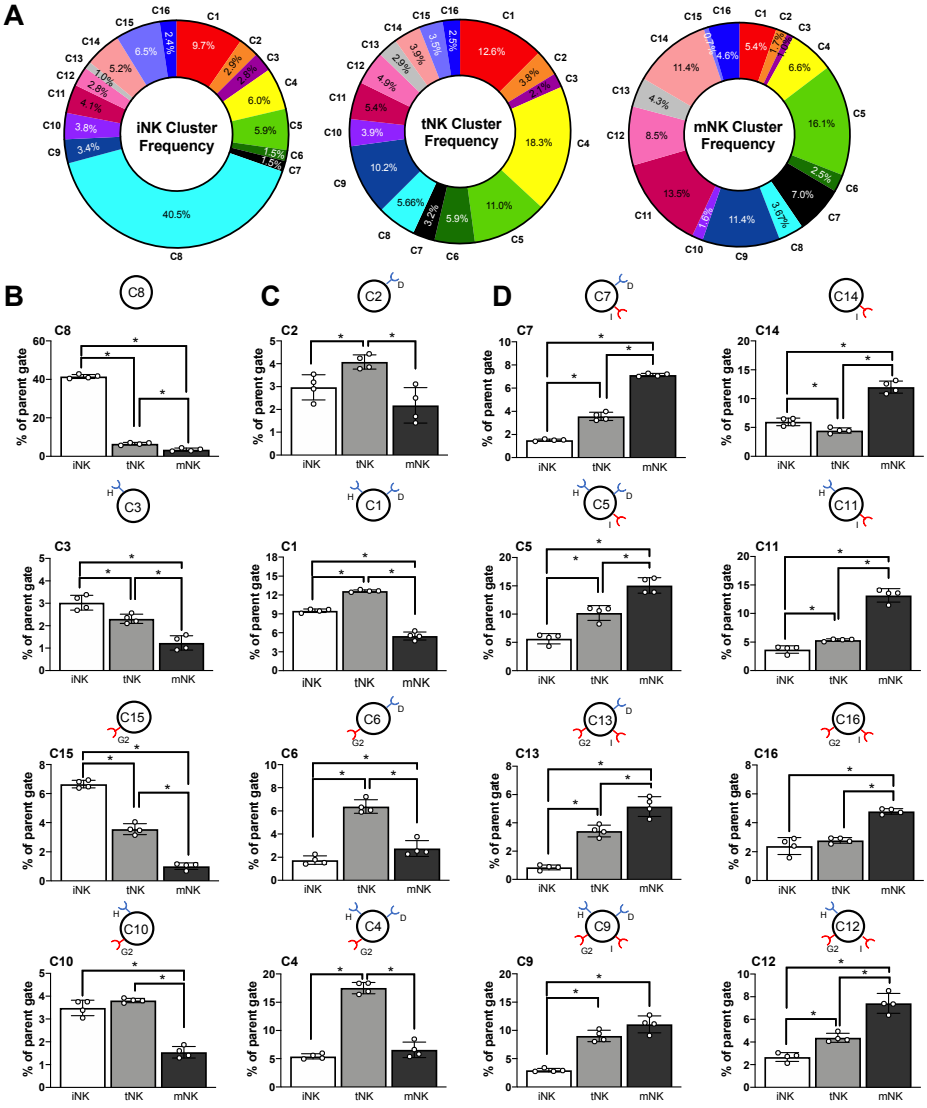

Supplemental Figure 1. NK cell Ly49 cluster frequencies predominantly found at iNK, tNK and mNK cell stage. (A) Summarized NK cell cluster mean frequencies gated on iNK (CD27+CD11b-), tNK (CD27+CD11b+) and mNK (CD27-CD11b+) cells and plotted on as part of a whole; (**B-C**) NK cell frequencies gated on parent maturation stage and grouped in clusters found predominantly in the (**B**) iNK, (**C**) tNK, (**D**) and mNK compartments. Asterisks indicate statistically significant differences between means as determined by the Student *t* test. *p < 0.05.

Millan et al. 2020. Supplemental Figure 2

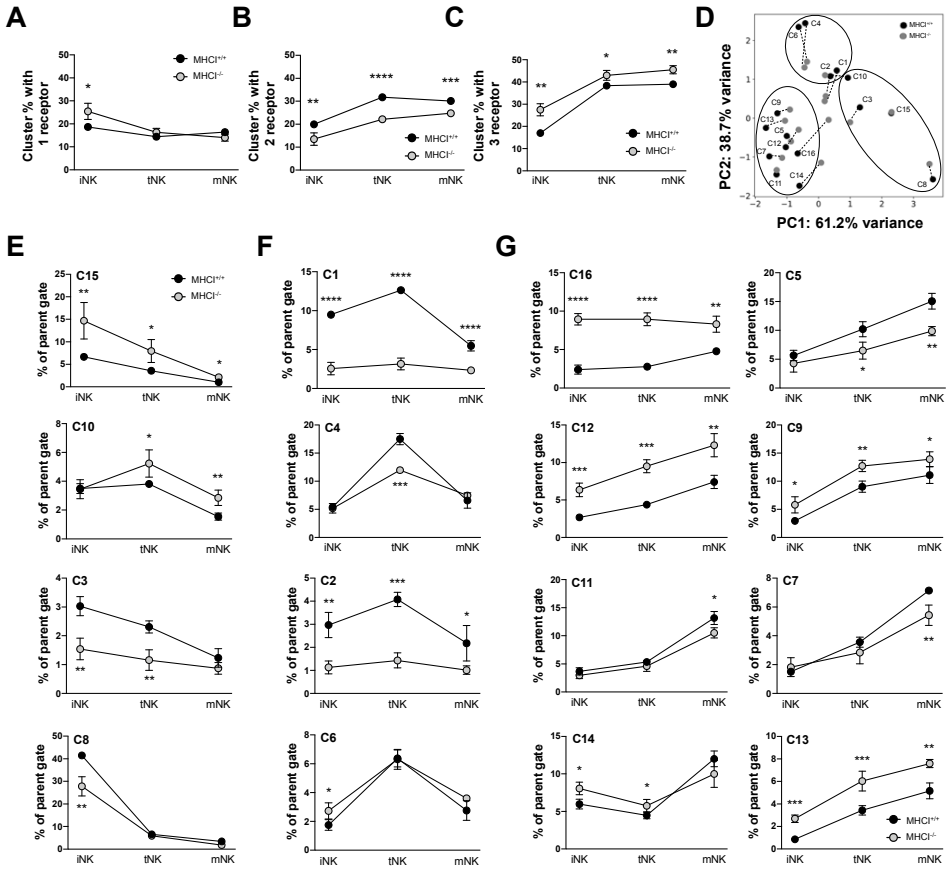

Supplemental Figure 2. MHC-I$^{-/-}$ mice display altered frequencies of NK cell clusters at each maturation stage. (**A**) Sum of frequencies of MHC-I$^{-/-}$ and MHC-I$^{+/+}$ NK cell clusters gated on iNK, tNK, and mNKs that express one, (**B**) two, and (**C**) three Ly49 surface receptors; (**D**) PCA analysis of calculated percent of NK cell clusters from a given iNK, tNK, or mNK stage of maturation between MHC$^{-/-}$ (grey dots) and MHC$^{+/+}$ (black dots) with a dotted line between the clusters to show changes between the two groups; (**E-G**) NK cell frequencies gated on parent maturation stage and grouped in clusters found predominantly in the (**E**) iNK, (**F**) tNK, (**G**) and mNK compartments for MHC-I$^{-/-}$ and MHC-I$^{+/+}$ mice. Asterisks indicate statistically significant differences between means as determined by the Student *t* test. *p < 0.05, **p < 0.01, ***p < 0.001, ****p < 0.0001.

CHAPTER 4

CONCLUSION

CHAPTER 4: CONCLUSIONS AND FUTURE DIRECTIONS

CONTRIBUTIONS TO THE FIELD

Natural Killer Cell Biology

The first half of my work described in this dissertation defines a novel role between the microenvironmental factor, Sostdc1, and NK cells. Sostdc1 is a secreted protein which has been previously identified in the context of bone regulatory protein, kidney disease, hair follicle formation, early digit formation, and bone fractures (1-3). Previously, NK cells have been extensively studied in terms of transcriptional regulation and receptor surface expression in development, maturation, and cytotoxicity (4). We have learned through hematopoietic stem cell (HSC) studies that microenvironmental influences are essential for HSC quiescent, maintenance, and hematopoiesis (5). However, only limited number of studies have addressed the influence of microenvironment on NK cell behavior. The work described in Chapter 2 demonstrated Sostdc1 as an important factor in NK cell maturation and function through two distinct mechanisms. Our findings support that Sostdc1 from two distinct sources, nonhematopoietic stromal cells and hematopoietic cells (in particular, $CD4^+$ and $CD8^+$ T cells), regulate NK cell maturation versus Ly49 receptor expression and frequencies in somewhat an independent manner. These dependencies were found to be controlled by Wnt signaling activation. Additionally, we show that developmental and functional NK cytotoxicity are regulated by niche cell populations for healthy NK cell repertoire that can distinguish between self and non-self-cells. Understanding the details of the basic biology underlying the development and regulation of NK cell cytotoxicity and how these processes are integrated could be an applied method for the production of specific numbers of NK cells with enhanced killing ability (4, 6).

The second half of my dissertation work extends the current knowledge on NK cell Ly49 receptors expression combined with maturation, which together can enhance our current understanding of NK cell cytotoxicity models. Ly49 receptors have been identified on multiple immune cell subsets, such as uterine NK, memory NK cells, NKT cells, dendritic cells, plasmacytoid dendritic cells, macrophages, neutrophils, activated T cells, and regulatory $CD8^+$ T cells (7). The Ly49 receptors in mice and killer cell immunoglobulin-like receptors (KIR) in humans, consist of both highly polymorphic activating and inhibitory surface receptors which serve as key players in NK cell killing (7, 8). The inhibitory Ly49 receptors are involved in NK cell education, a process in which NK cells acquire function and tolerance toward cells that express self-MHC-I, while the activating Ly49 receptors recognize

altered cells expressing activating ligands. The NK cell field has effectively been working on understanding the regulatory mechanisms which control Ly49 receptor expression and how these receptors mediate killing (7). In Chapter 3 of this dissertation, we extended the current knowledge of Ly49 receptors by studying interdependencies between inhibitory Ly49I, Ly49G2 and activating Ly49H, Ly49D receptors and maturation. We showed for the first time that the majority of the interdependencies in Ly49 receptor expression originate at the iNK cell stage, and that specific clusters predominate at each stage of maturation. My study expands the current models of NK cell education and suggest an updated model in which MHC-I and maturation affects NK cell Ly49 activating and inhibitory receptor expression in a progressive pathway.

FUTURE DIRECTIONS

Microenvironmental factors

The studies in this dissertation have focused on BM and splenic conventional NK cells. However, understanding what drives NK cell maturation and effector function in different tissues would enhance our current understanding of NK cell biology and potential avenues for NK cell immunotherapies. One possible outcome to consider is the influence of NK cell specific cytokines, which have been shown to regulate NK cell function. In particular, how the abundance of microenvironmental cytokines drive tissue-specific NK maturation and function. For example, IL-15 cytokine has been well studied in the context of development, homeostasis, and activation, whereas IL-2, IL-4, IL-7, IL-10, IL-12, IL-18, and IL-21 have been shown to enhance activating and effector function (9). We show that NK cells from Sostdc1$^{-/-}$ mice exhibit hyporesponsive response towards β_2m$^{-/-}$ targets, which was not mediated by IL-12-producing dendritic cells in the spleen (10). However, our analysis was limited in the microenvironmental cytokines that may influence NK cell maturation and function, in particular IL-15. To fully determine the role of Sostdc1 from the microenvironment, it would be necessary to also measure cytokine production from surrounding cells.

We have shown that CD4$^+$ and CD8$^+$ splenic T cells expressing levels of the *Sostdc1* gene may influence NK cell Ly49 receptor expression. Previous studies have identified some T cell subsets as *Sostdc1*-expressing T follicular helper (T_{FH}) and T follicular regulatory (T_{FR}) cells in the peripheral lymph node (pLN) and Peyer's patches (11). Additionally, CD4 PD-1 T cells in the spleen were found to express a memory phenotype (CD44^{high}CD62L^{low}) and high levels of Sostdc1 of aged mice (12). Furthermore, In vitro stimulation with anti-CD3 and

anti-CD28 results in an increase of *Sostdc1* (12). Together, these results may provide some evidence for T cell and NK cell regulation by Sostdc1. To test the hypothesis that T cells regulate NK cell Ly49 receptor expression by Sostdc1, one could perform a series of mixed BM transplantation experiments. BM from T cell-deficient ($CD3^{-/-}$ or $RAG^{-/-}$) and $Sostdc1^{-/-}$ could be simultaneously transplanted into fully irradiated congenic WT mice. In the recipient mice, the only cells lacking expression of *Sostdc1* are the T cells. When mice are reconstituted, one could determine the interplay between T cells and NK cell Ly49 receptor expression by flow cytometric analysis. These experiments may provide further evidence of interplay between T cells and NK cell Ly49 receptor expression.

NK cell Ly49 variegated expression patterns

The variegated pattern of Ly49 expression for each NK cell subset suggest a stochastic mechanism for each receptor. The association between MHC-I-specific inhibitory Ly49 receptors and NK cell development has been shown previously with sequential expression in vivo and in vitro (13-15). Furthermore, we have shown that NK maturation by CD27 and CD11b express a variegated pattern of Ly49 expression with increasing self-inhibitory Ly49I receptor at the mNK ($CD27^{-}CD11b^{+}$) cell stage. Perhaps, this tight regulation of self-inhibitory Ly49 receptors are involved in the acquisition of NK cell self-tolerance by MHC-I molecules (15). Furthermore, our results from Chapter 3 were limited in the number of self-inhibitory Ly49 and NKG2A receptors we analyzed for self-MHC-I molecules. To fully determine the influence of self-inhibitory receptors in NK cell maturation, we would need to observe additional self-MHC-I-specific Ly49 and NKG2 family receptors, such as Ly49C and NKG2A, expression patterns of the receptors throughout maturation. Sternberg-Simon et al. analysis of inhibitory receptors in mice show that Ly49C was over-represented and Ly49I was under-represented under the product rule (16). The study further show that NKG2A-single positive NK cell frequencies were found more frequent than expected in MHC-I-KO mice. Notably, Ly49C is known to have strong binding to $H2\text{-}K^{b}$ and bind MHC-I in a *cis* manner, whereas Ly49I has been shown to bind weakly to $H2\text{-}K^{b}$ (14). Binding of these self-inhibitory receptors to MHC-I ligand may contribute to the variegated pattern of expression in NK cells. Moreover, more experiments are required with multiple activating and inhibitory receptors throughout NK cell maturation to further determine the patterns of variegated receptor expression to fully determine interdependencies between Ly49 receptor expression.

NK cell Immunotherapies

Immunotherapies are innovative approaches for the treatment of cancers and disease with the idea of harnessing the immune system. Similar to mouse NK cell Ly49s, human inhibitory KIRs recognize HLA class-I alleles (8) and lack killing of autologous cells expressing self-HLA. Within an environment where tumors downregulate self-HLA, NK cells mediate killing. Conversely, the KIR activating receptors are activated by a series of non-HLA-specific receptors and co-receptors that are commonly expressed on tumor cells (17). Thus, NK cells make for a great source for cancer immunotherapies. One focus of NK cell cancer immunotherapies are therapeutic monoclonal antibodies against inhibitory KIR receptors, such as anti-pan-KIR2D (lirilumab) (https://www.innate-pharma.com/en/pipeline/ lirilumab-first-class-anti-kir-mab-licensed-bristol-myers-squibb). Blocking KIR2D on the NK cells would mimic “missing-self” response and killing by disrupting the interaction between the inhibitory receptor and its ligand.

Chapter 3 of this dissertation identifies diverse Ly49 expression in NK cell subsets and their predominate stages in maturation. However, given that NK killing can be governed by the balance of signals between Ly49 activating and inhibitory receptors (18), it is possible that our progressive NK cell cluster pathways can be applied to the identification of NK cell clusters with high cytotoxic potential. It has been shown that cytotoxicity increases with NK maturation with the highest cytotoxic gene expression at the mNK stage (19). Furthermore, we show that the self-inhibitory Ly49I receptor is expressed on all predominate mNK ($CD27^{+}CD11b^{+}$) cells in K^{b} expressing C57BL/6 mice. Thus, our studies suggest that NK killing may be evidence of proper maturation and upregulation of self-inhibitory Ly49 receptors. In parallel to the human NK cell immunotherapies, I believe it would be essential to promote NK cell maturation before treatment of monoclonal inhibitory KIR antibodies for optimal NK cell killing. Together, NK cell Ly49 receptors play an important role in governing NK cell killing and further analyzing cluster progression could enhance current NK cell immunotherapies.

More recently, chimeric antigen receptor (CAR)-NK cell immunotherapies have proven to kill hematological and solid tumor cells in preclinical and clinical trials (20) with improved safety and effectiveness compared to CAR-T cells immunotherapy (21). CAR-NK which express the transmembrane surface receptor NKG2D and ligated CD3ζ induce down-stream signal transduction of phosphorylated DAP10 have been shown to have strong antitumor effects on acute lymphocytic leukemia (ALL), osteosarcoma, and prostate tumors (22). The DAP10 signals active adaptor proteins that produce perforin and granzyme mediate NK cell killing (23). Moreover, regulating the tumor microenvironmental may increase the efficacy of CAR-NK cell immunotherapy. Mohammed et al. have

engineered an inverted cytokine receptor in which IL-4 receptor exodomain fused to the IL-7 receptor endodomain (4/7 ICR) (24). IL-4 in the tumor microenvironment acts as an immunosuppressant for T cell function, thus utilizing the IL-7 downstream signaling domains when IL-4 binds would promote T cell activating and evade immunosuppression. This is an example of how the microenvironmental influence can be optimize for enhanced NK cell immunotherapies.

SUMMARY

NK cells play an important role in the elimination of cancerous and virally infected cells. Understanding the role of the microenvironment factors and the diversity of surface Ly49 receptors provides information which can be translated to develop NK cells with high effector function in vitro or in vivo. Furthermore, the complexity observed in the regulation of maturation and Ly49 expression in this dissertation can be potentially applied towards the improvement of current NK cell immunotherapies. Moreover, we have demonstrated a novel role for Sostdc1/Wnt signaling in the regulation of maturation and cytotoxicity. Altogether, this research promotes the further understanding of NK cell behavior.

REFERENCES

1. Laurikkala, J., M. L. Mikkola, M. James, M. Tummers, A. A. Mills, and I. Thesleff. 2006. p63 regulates multiple signalling pathways required for ectodermal organogenesis and differentiation. *Development* 133: 1553-1563.
2. Shigetani, Y., and N. Itasaki. 2007. Expression of Wise in chick embryos. *Dev Dyn* 236: 2277-2284.
3. Chen, G., H. Gong, T. Wang, J. Wang, Z. Han, G. Bai, S. Han, X. Yang, W. Zhou, T. Liu, and J. Xiao. 2018. SOSTDC1 inhibits bone metastasis in non-small cell lung cancer and may serve as a clinical therapeutic target. *INTERNATIONAL JOURNAL OF MOLEcULAR MEdIcINE* 42.
4. Wang, D., and S. Malarkannan. 2020. Transcriptional Regulation of Natural Killer Cell Development and Functions. *Cancers* 12.
5. Richter, J., D. Traver, and K. Willert. 2017. The role of Wnt signaling in hematopoietic stem cell development. *Crit Rev Biochem Mol Biol* 52: 414-424.
6. Cifaldi, L., F. Locatelli, L. Marasco, L. Moretta, and V. Pistoia. 2017. Boosting natural killer cell-based immunotherapy with anticancer drugs: a perspective. *Trends Mol. Med.* 23: 1156–1175.
7. Rahim, M. M., M. M. Tu, A. B. Mahmoud, A. Wight, E. Abou-Samra, P. D. Lima, and A. P. Makrigiannis. 2014. Ly49 receptors: innate and adaptive immune paradigms. *Front Immunol* 5: 145.
8. Minetto, P., F. Guolo, S. Pesce, M. Greppi, V. Obino, E. Ferretti, S. Sivori, C. Genova, R. M. Lemoli, and E. Marcenaro. 2019. Harnessing NK Cells for Cancer Treatment. *Front Immunol* 10: 2836.
9. Marcais, A., S. Viel, M. Grau, T. Henry, J. Marvel, and T. Walzer. 2013. Regulation of mouse NK cell development and function by cytokines. *Front Immunol* 4: 450.
10. Millan, A. J., S. R. Elizaldi, E. M. Lee, J. O. Aceves, D. Murugesh, G. G. Loots, and J. O. Manilay. 2019. Sostdc1 Regulates NK Cell Maturation and Cytotoxicity. *J Immunol* 202: 2296-2306.
11. Chicana, B., C. Donham, A. J. Millan, and J. O. Manilay. 2019. Wnt Antagonists in Hematopoietic and Immune Cell Fate: Implications for Osteoporosis Therapies. *Curr Osteoporos Rep* 17: 49-58.
12. Shimatani, K., Y. Nakashima, M. Hattori, Y. Hamazaki, and N. Minato. 2009. PD-1+ memory phenotype CD4+ T cells expressing C/EBPalpha underlie T cell immunodepression in senescence and leukemia. *Proc Natl Acad Sci U S A* 106: 15807-15812.
13. Dorfman, R. J., and D. H. Raulet. 1998. Acquisition of Ly49 Receptor Expression by Developing Natural Killer Cells. *J. Exp. Med* 187: 609-618.
14. Hanke, T., H. Takizawa, C. McMahon, D. Busch, E. Pamer, F. Lemonnier, P. Bjorkman, and D. H. Raulet. 1999. Direct assess- ment of MHC class I binding by seven Ly49 inhibitory NK cell receptors. *Immunity* 11: 67-77.

15. Raulet, D. H., E. Vance, R.,, and C. McMahon. 2001. Regulation of the Natural Killer Cell Receptor Repertoire. *Annu. Rev. Immunol.* 19: 291-330.
16. Sternberg-Simon, M., P. Brodin, Y. Pickman, B. Onfelt, K. Karre, K. J. Malmberg, P. Hoglund, and R. Mehr. 2013. Natural killer cell inhibitory receptor expression in humans and mice: a closer look. *Front Immunol* 4: 65.
17. Sivori, S., S. Carlomagno, S. Pesce, A. Moretta, M. Vitale, and E. Marcenaro. 2014. TLR/NCR/KIR: Which One to Use and When? *Front Immunol* 5: 105.
18. Guzman, M., N. Keating, and S. E. Nicholson. 2020. Natural Killer Cells: Tumor Surveillance and Signaling. *Cancers (Basel)* 12.
19. Hayakawa, Y., and M. J. Smyth. 2006. CD27 dissects mature NK cells into two subsets with distinct responsiveness and migratory capacity. *J Immunol* 176: 1517-1524.
20. Siegler, E. L., Y. Zhu, P. Wang, and L. Yang. 2018. Off-the-Shelf CAR-NK Cells for Cancer Immunotherapy. *Cell Stem Cell* 23: 160-161.
21. Wang, W., J. Jiang, and C. Wu. 2020. CAR-NK for tumor immunotherapy: Clinical transformation and future prospects. *Cancer Lett* 472: 175-180.
22. Chang, Y. H., J. Connolly, N. Shimasaki, K. Mimura, K. Kono, and D. Campana. 2013. A chimeric receptor with NKG2D specificity enhances natural killer cell activation and killing of tumor cells. *Cancer Res* 73: 1777-1786.
23. Voskoboinik, I., M. J. Smyth, and J. A. Trapani. 2006. Perforin-mediated target-cell death and immune homeostasis. *Nat Rev Immunol* 6: 940-952.
24. Mohammed, S., S. Sukumaran, P. Bajgain, N. Watanabe, H. E. Heslop, C. M. Rooney, M. K. Brenner, W. E. Fisher, A. M. Leen, and J. F. Vera. 2017. Improving Chimeric Antigen Receptor-Modified T Cell Function by Reversing the Immunosuppressive Tumor Microenvironment of Pancreatic Cancer. *Mol Ther* 25: 249-258.